



<https://theses.gla.ac.uk/>

Theses Digitisation:

<https://www.gla.ac.uk/myglasgow/research/enlighten/theses/digitisation/>

This is a digitised version of the original print thesis.

Copyright and moral rights for this work are retained by the author

A copy can be downloaded for personal non-commercial research or study,
without prior permission or charge

This work cannot be reproduced or quoted extensively from without first
obtaining permission in writing from the author

The content must not be changed in any way or sold commercially in any
format or medium without the formal permission of the author

When referring to this work, full bibliographic details including the author,
title, awarding institution and date of the thesis must be given

Enlighten: Theses

<https://theses.gla.ac.uk/>
research-enlighten@glasgow.ac.uk

**Nucleus-Electron Interactions
in Chemistry.**

by Robert Wallace.

A thesis submitted in part fulfilment of the
requirements for the Degree of Doctor of
Philosophy at the University of Glasgow.
September 1964.

ProQuest Number: 10984192

All rights reserved

INFORMATION TO ALL USERS

The quality of this reproduction is dependent upon the quality of the copy submitted.

In the unlikely event that the author did not send a complete manuscript and there are missing pages, these will be noted. Also, if material had to be removed, a note will indicate the deletion.



ProQuest 10984192

Published by ProQuest LLC (2018). Copyright of the Dissertation is held by the Author.

All rights reserved.

This work is protected against unauthorized copying under Title 17, United States Code
Microform Edition © ProQuest LLC.

ProQuest LLC.
789 East Eisenhower Parkway
P.O. Box 1346
Ann Arbor, MI 48106 – 1346

Preface.

Several aspects of the two related fields of Nuclear Magnetic Resonance Spectroscopy and Nuclear Quadrupole Resonance Spectroscopy are discussed in this thesis. The principle controlling much of my research has been an interest in correlating experimentally observed quantities with the conceptual framework of chemistry. For this reason, I have not interested myself in particular groups of chemical compounds. Instead, I have been concerned with methods for obtaining spectra, for extracting the relevant parameters from these spectra, and for interpreting these parameters in terms of molecular and electronic structure.

In N.M.R. spectroscopy, my main research topic has involved methods for extracting molecular parameters from complex high resolution spectra. To a lesser extent I have also studied the interpretation of these parameters in terms of molecular electronic structure.

My work in the field of N.Q.R. spectroscopy has been entirely centred around putting the subject "on its feet" in the department. This has involved constructing a Nuclear Quadrupole Zeeman Resonance Spectrometer and developing methods for evaluating quantum mechanical "matrix elements" necessary for the interpretation of nuclear quadrupole coupling constants in terms of electronic structure.

I would like to thank The Royal Society for granting funds enabling the spectrometer to be built, Professor J.M. Robertson for obtaining the grant, and Dr. A.L. Porte for supporting my interest in the field. For helping with the construction of the spectrometer, I would like to acknowledge the assistance of all members of the departmental workshops. In particular, I wish to thank Mr. M. Riggans and Mr. J. Mulhinch for their contributions. For enabling me to speed the construction of the spectrometer, the willing co-operation of Mr. G. Kerr, Mr. A. Hislop, and Mr. M. Riggans is appreciated. The enthusiasm, expert advice, and practical help in electronics due to Mr. J. Lumsden has been invaluable.

In my computing work, I am indebted to the staff of the University Computing Department for assistance in correcting programmes.

For suggesting the "Isotope Shift Effect" problem, for providing introductory notes concerning "A Least Squares Method for Refining Chemical Shifts and Spin-Spin Coupling Constants", and for his interest and supervision I wish to thank Dr. A.L. Porte.

Finally, I would like to express my gratitude to The Carnegie Trust for the Universities of Scotland for financial support during the entire period in which this research has been carried out.

The arrangement of the material is quite straightforward. There are two main sections, each of which is divided into chapters and sub-chapters. Diagrams and tables are indexed according to the chapter and sub-chapter in which they occur. I have assumed that the reader is familiar with quantum mechanics, theoretical chemistry, and is acquainted with magnetic resonance spectroscopy.

R. Wallace.

(1964)

Contents.

| Chapter | Page. |
|---|-------|
| Preface | i |
| General Introduction | 1 |
| SECTION A: NUCLEAR MAGNETIC RESONANCE SPECTROSCOPY. | 2 |
| <u>1.</u> Introductory Theory | 3 |
| <u>2.</u> Some Chemical Aspects of High Resolution N.M.R. Spectroscopy. | 7 |
| <u>3.</u> <u>Chemical Shifts of Protons in Some Substituted Benzenes</u> | 8 |
| <u>4.</u> <u>A Method of Analysis of Complex Proton Magnetic Resonance Spectra.</u> | 17 |
| 4.1 Introduction. | 18 |
| 4.2 The Refinement Method. | 22 |
| 4.3 Formulation of the Matrix T. | 25 |
| 4.4 ----- | |
| 4.5 The Refinement Method for a system of Three Protons. | 27 |
| 4.6 Program RWLA : T Matrix Programme for a Three Spin System. | 30 |
| 4.7 Program LWLB : The Three Spin Refinement Programme. | 32 |
| 4.8 Summary of the Refinement Process. | 35 |
| 4.9 An Example of the Refinement Method Applied to a Three Spin Spectrum. | 36 |
| 4.10 Programmes for the Analysis of Four Spin Spectra | 42 |
| 4.11 The Analysis of Four Spin Proton Magnetic Resonance Spectra. | 43 |
| 4.12 Research Applications of the Spectral Analysis Method | 58 |
| <u>5</u> <u>The Interpretation of Chemical Shift and Spin-spin Coupling Constant Parameters in Terms of Molecular Electronic Structure.</u> | 60 |
| 5.1 Introduction. | 61 |
| 5.2 Calculation of the Chemical Shift. | 62 |
| 5.3 Theory of the Spin-spin Coupling Constant. | 68 |
| 5.4 Calculation of Chemical Shifts and Spin-spin Coupling Constants. | 69 |
| <u>6</u> <u>Effects of Isotopic Substitution on the Magnetic Shielding Constants of Nuclei.</u> | 70 |
| 6.1 Introduction. | 71 |
| 6.2 Differences in Magnetic Shielding Constants of the Protons in H ₂ and HD. | 72 |
| 6.3 Effect of a Small Variation in R upon $(\varphi \quad 1/r \quad \varphi)$. | 75 |
| 6.4 Effect of a Small Variation in k upon $(\varphi \quad 1/r \quad \varphi)$. | 76 |
| 6.5 Perturbation of the Electronic Energy Caused by Nuclear Quadrupole Coupling. | 77 |
| 6.6 The Vibrational Ground State Energy Levels of H ₂ and HD. | 78 |
| <u>7</u> <u>The Transition from N.M.R. to N.Q.R. Spectroscopy.</u> | 79 |

General Introduction

Many atomic nuclei in their ground state possess non-zero spin angular momentum. Such nuclei possess a magnetic dipole moment and several of them exhibit also an electric quadrupole moment. These nuclear moments interact with magnetic and electric fields in such a way as to produce a series of nonequivalent sub-levels of the ground state nuclear energy level. It is possible to observe transitions between these sub-levels by radiofrequency spectroscopy. In addition to interacting with externally applied magnetic and electric fields, these moments also interact with internal fields generated primarily by the electrons of the molecule or crystal in which the nuclei are situated. The subjects of Nuclear Magnetic Resonance Spectroscopy and Nuclear Quadrupole Resonance Spectroscopy are concerned with the observation of these nuclear splittings and chemical interest in these subjects is largely concerned with the nature of these internally produced magnetic and electric fields. It is with such investigations that we shall be concerned in this thesis.

Nuclear Magnetic Resonance Spectroscopy

Section A.

Introductory Theory 1.

As we have already mentioned, many nuclei in their ground state possess non-zero angular momentum, which we shall represent by J . If this angular momentum is regarded as a vector property of the nucleus, then its magnetic moment can be regarded as a parallel vector. Hence we can write:-

$$\mu = \gamma J \quad (1.1)$$

where γ is a scalar quantity known as the magnetogyric ratio.

In quantum theory, μ and J are treated as vector operators. The meaning of the concept of two operators being "parallel" is found by considering the matrix elements of the operators. Suppose we define a dimensionless angular momentum operator, I , by $J = \hbar I$, I^2 then has eigenvalues I which are either integral or half-integral. Any component of I , for example I_z , if the nucleus is described in a Cartesian reference frame, commutes with I^2 , so that we may specify simultaneously eigenvalues of both I^2 and I_z . Let us call the eigenvalues I and m respectively. Then m may take any of the $2I + 1$ values $I, I - 1, \dots, -I$. The meaning of (1.1) is then that

$$(I\ m|\mu_{x'}|I\ m') = \gamma \hbar (I\ m|I_{x'}|I\ m') \quad (1.2)$$

where $\mu_{x'}$ and $I_{x'}$ are components of the operators μ and I along the arbitrarily chosen x' direction. The validity of this expression is based upon the Wigner - Eckart Theorem.¹

If a nucleus of magnetic moment μ is subjected to a magnetic field H , the energy of interaction is given by the expectation value of the operator:-

$$\mathcal{H} = -\mu \cdot H \quad (1.3)$$

If we choose the direction of the applied field to be along the z - axis, the coupling Hamiltonian takes the simple form:-

$$\mathcal{H} = -\gamma\hbar H_0 I_z \quad (1.4)$$

The eigenvalues of this Hamiltonian are given by

$$\begin{aligned} E_m &= -\gamma\hbar H_0 \langle I_z | I_z | I m \rangle \\ &= -\gamma\hbar H_0 m \quad m = I, I-1, \dots, -I \end{aligned} \quad (1.5)$$

These magnetic energy levels are equally spaced, differing in energy by $\gamma\hbar H_0$.

We can detect the presence of such a set of energy levels by radiofrequency spectroscopy. What is required is to have an interaction which can cause transitions between levels. The interaction must be time dependent and of such an angular frequency that

$$\hbar\omega = \Delta E \quad (1.6)$$

where ΔE is the energy difference between initial and final nuclear energy levels. Furthermore, the interaction must have a nonvanishing matrix element between initial and final states.

The coupling most commonly used to produce magnetic resonances is an alternating magnetic field applied perpendicular to the static field. If we write the alternating field in terms of an amplitude H_x^0 , we get a perturbing term in the Hamiltonian of

$$\mathcal{H}_{\text{pert}} = -\gamma\hbar H_x^0 I_x \cos\omega t \quad (1.7)$$

The operator I_x has matrix elements between states m and m' which vanish unless $m' = m \pm 1$. Consequently the allowed transitions are between levels which are adjacent in energy, giving

$$\hbar\omega = \Delta E = \gamma\hbar H_0 \quad (1.8)$$

If we have a sample containing an assembly of nuclei of the same species, we can, by suitable experiment, detect the frequency at which resonance takes place. By way of an example, the magnetic moment of the proton is 1.42×10^{-23} ergs/gauss, which means that

at a field strength of about 14,000 gauss, the resonance frequency of the proton magnetic moment is in the vicinity of 60 Mc/s. which can be fairly simply produced by radiofrequency techniques.

The information which one can obtain from a nuclear magnetic resonance spectrum depends very much upon whether the sample under study is in the solid or liquid state. With solids one obtains what are called broad-line spectra, the line width of the resonance depending largely upon the magnitude of nuclear magnetic dipole-dipole interactions in the solid. In liquids in which the molecules are tumbling rapidly, these dipolar interactions average to zero and line width is then limited primarily by the homogeneity of the applied magnetic field. Spectra which are obtained with liquid samples under conditions of high magnetic field homogeneity are referred to as "High Resolution Nuclear Magnetic Resonance Spectra". Such spectra exhibit small splittings of the resonance lines due to nucleus-electron interactions. It is the observation of these splittings which makes the subject of nuclear magnetic resonance (N.M.R.) spectroscopy so interesting to the chemist and it is with this subject that we shall be concerned in this section of the thesis.

There are two distinct mechanisms causing these splittings. The first is due to the fact that the applied magnetic field induces a small magnetic field in the electrons of the molecule. As this induced field depends upon the nature of the electron distribution, nuclei in electronically different environments experience different induced fields. If the induced field at the nucleus is H , then the resonance frequency of the nucleus becomes:-

$$\omega = \gamma(H_0 + \Delta H) \quad (1.9)$$

where ΔH is proportional to H_0 . If we define a quantity σ which is independent of the applied field by

$$\Delta H = -\sigma H_0$$

the resonance frequency becomes

$$= \gamma H_0 (1 - \sigma) \quad (1.10)$$

σ is usually referred to as the "magnetic shielding constant" of the nucleus. This dependence of the resonance frequency upon the field induced in the electrons has become known as the "chemical shift". There is another mechanism responsible for the splitting of N.M.R. spectra which is independent of the strength of the applied magnetic field and which does depend only upon the electronic environment of the nuclei in the molecule. This splitting mechanism arises because of magnetic polarization of the electrons by the nuclear magnetic moment, this polarization being transferred to other nuclei by electron spin-spin interaction. This indirect coupling of nuclear spins is referred to as "spin-spin coupling. We shall examine the theory of both chemical shift and spin-spin coupling phenomena in greater detail in chapter 5.

Some Chemical Aspects of
High Resolution N.M.R. Spectroscopy

2.

To the chemist there are essentially two aspects of high resolution N.M.R. spectroscopy, the first being experimental in nature and being concerned with the detection of spectra, and the second, theoretical, involving the interpretation of these spectra.

Because the perturbation of the nuclear spin energy levels due to nucleus-electron interactions is small compared to the splitting of these levels by the applied magnetic field, nuclei of the same species resonate at only slightly different field strength at constant frequency, (eqn. 1.10). As a result of this, and because of the importance of the technique to organic chemistry, there has been a tendency to design N.M.R. spectrometers with a view to the detection of proton magnetic resonance spectra. Because the spectrometer which was available to us was being used exclusively for the detection of proton magnetic resonances, we have been concerned only with this sort of spectroscopy.

The problem of interpretation of the high resolution proton magnetic resonance spectrum of a complex organic molecule resolves into two related parts, the first being concerned with the extraction from the spectrum of all sets of chemical shift and spin-spin coupling constant parameters which are consistent with the spectrum, and the second that of assigning these parameters to particular nuclei and pairs of nuclei within the molecule. In current practice, the problem of interpretation is usually aided by the use of tables of empirically determined chemical shift and spin-spin coupling constant parameters, these being listed for protons in a wide variety of chemical environments. This usage of high resolution N.M.R. spectroscopy as a means to determine molecular structure will be illustrated in the next chapter.

**Chemical Shifts of Protons in
Some Substituted Benzenes**

Chapter 3

In order to examine the possible application of high resolution proton magnetic resonance spectroscopy to the identification of aromatic molecules formed by degradation of certain natural products, High resolution spectra of a number of substituted benzenes were recorded.

The use which can be made of these spectra as "fingerprints" of molecular structure is governed very largely, as we shall subsequently show, by our ability to analyse complex spectra, and it is to this problem that we wish to draw particular attention in this chapter.

The spectra which we shall discuss were obtained using an RS 2 nuclear magnetic resonance spectrometer made by Associated Electrical Industries, operating at a frequency of 60 Mc/s. Spectrum 3.1 is a typical example of the spectra recorded.

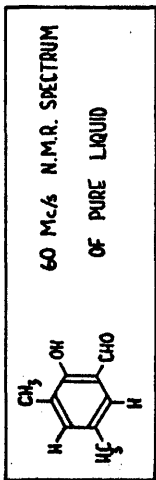
By the use of tables of chemical shifts, such as those of Tiers,² together with the observed spectral intensities, we can make the following assignment of the resonances appearing in spectrum 3.1 (chemical shifts being measured on the " τ scale" with respect to tetramethyl silane used as an internal reference²).

| τ | Assignment |
|----------|--------------------------|
| -1.25 | -OH (intramol. H bonded) |
| 0.35 | -C=O |
| ca. 3.10 | 2 x aryl-H |
| ca. 7.85 | 2 x -CH ₃ |

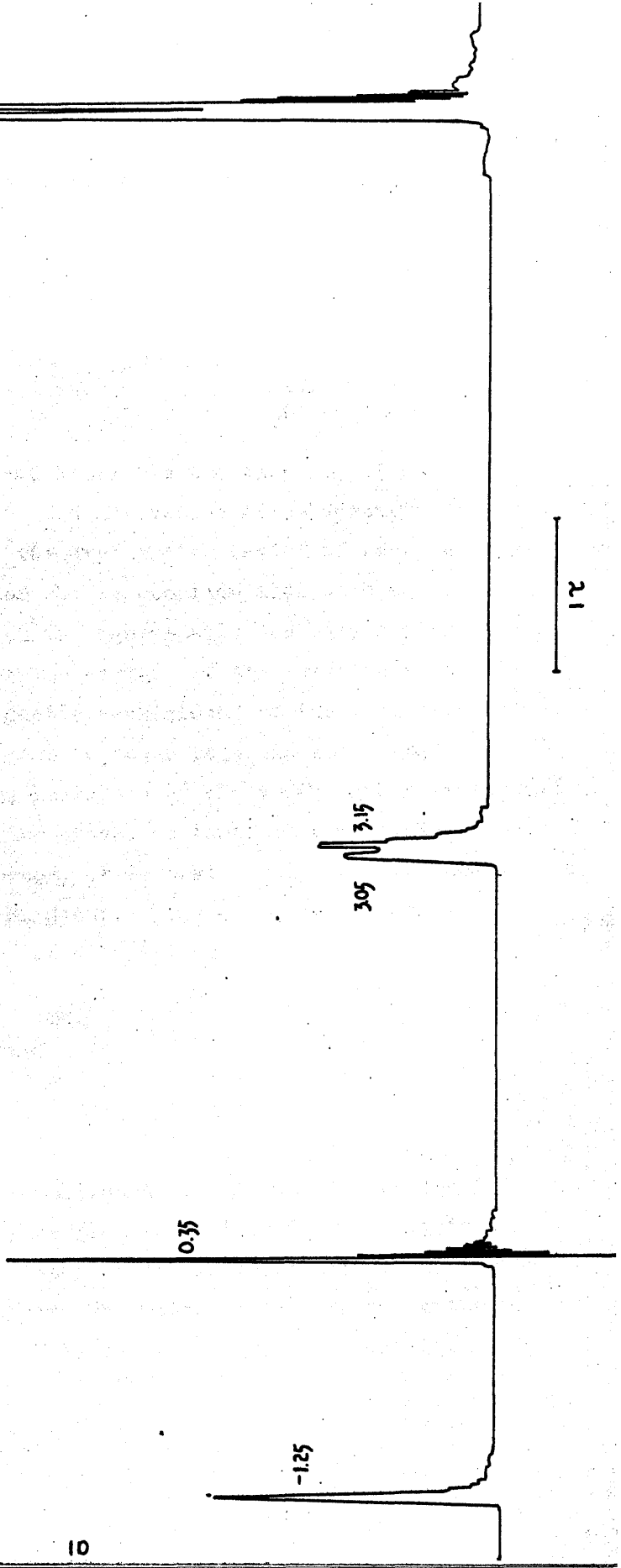
This assignment of the spectrum is consistent with the identification of the molecule as a dimethyl substituted derivative of salicaldehyde although the substitution pattern cannot be derived from the spectrum. Use of the technique in the determination of this molecular structure would therefore appear to be limited to that of providing six alternative molecular structures differing only in substitution pattern.

For many of the aromatic molecules which we have studied, this limitation may be removed if it is possible to unravel the complex

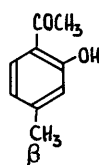
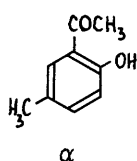
SPECTRUM 1 : CHAPTER 3



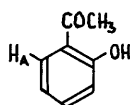
7.80
7.90



multiplet of resonances due to the strongly coupled aryl protons. The analysis of the aryl proton region of such spectra is, for instance, the key to the determination of the molecular structures of the isomeric molecules α and β :-

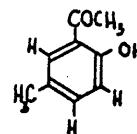
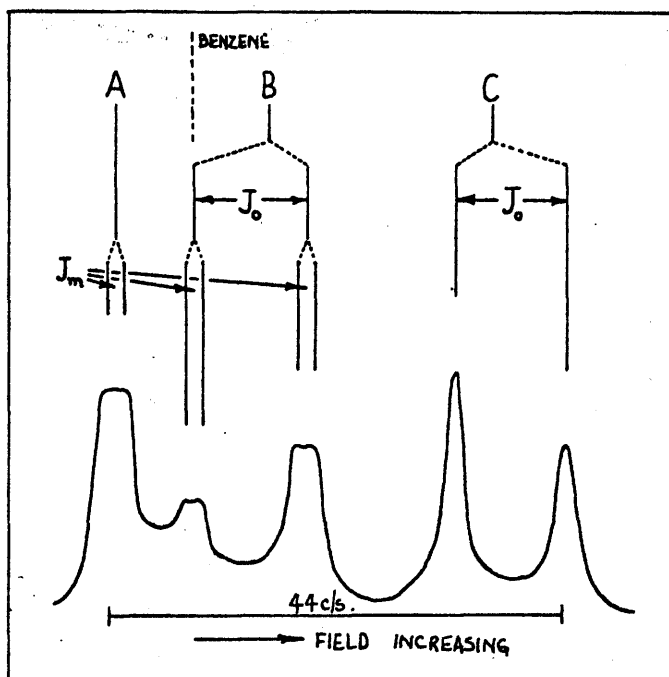


By use of Tiers tables, we can attribute the spectrum of each of these molecules to a methyl substituted derivative of o-hydroxy acetophenone. By an analysis of the aryl proton region of each spectrum, illustrated in spectra 2a and 2b, we conclude that each molecule contains one proton, A, which is magnetically deshielded with respect to the protons in the benzene molecule. Of the three substituents, $-\text{COCH}_3$ is known to cause magnetic deshielding of the ring protons,³ whereas the other two are known to cause magnetic shielding. Furthermore, The deshielding influence of the $-\text{COCH}_3$ group is strongest for those protons ortho to the group, so that, in a molecule containing two shielding groups, it is most likely that the deshielded proton is ortho to the $-\text{COCH}_3$ group. This being so, we derive the following partial structure for each molecule:-

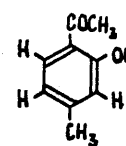
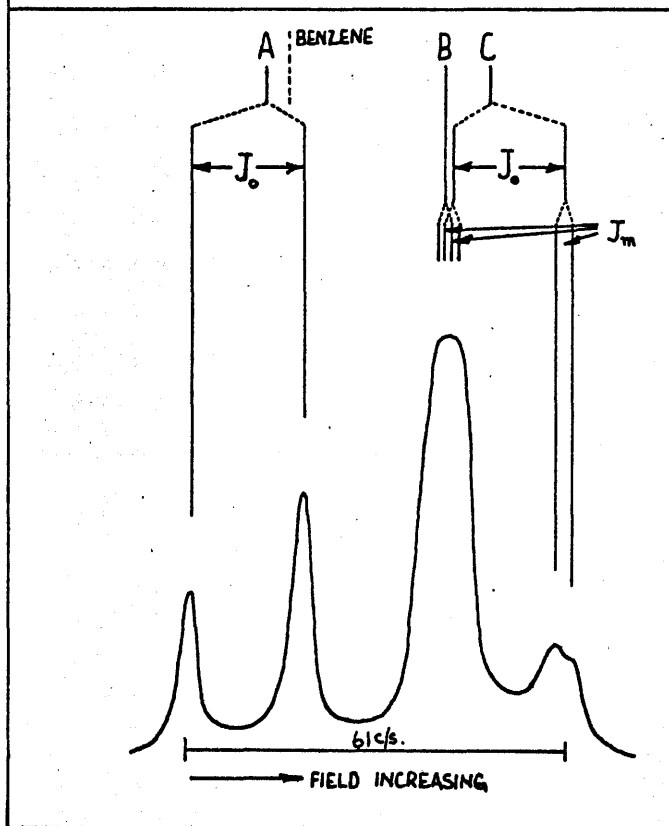


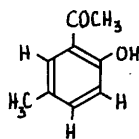
From spectrum 2a we see that nucleus A is only weakly coupled to nucleus B, which is strongly coupled to nucleus C. The magnitude of these coupling constants leads us to the conclusion that, in the molecule represented by spectrum 2a, proton A is meta to proton B, which is ortho to proton C. This is consistent with only one molecular structure:-

SPECTRUM 2a



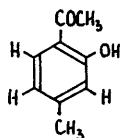
SPECTRUM 2b





which is identical to α .

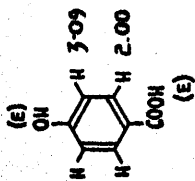
Similarly, from spectrum 2b, we conclude that proton A is ortho to proton C, which is meta to proton B, this again being sufficient to determine the following molecular structure:-



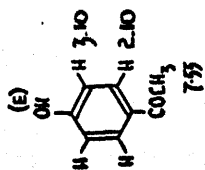
which is identical to β .

From the examples we have just described, it is obvious that the power of proton magnetic resonance spectroscopy as a molecular structure determining tool is largely dependent upon satisfactory analysis of complex spectra being possible, this analysis being by no means a simple matter. This is true, not only of the aromatic molecules which we have studied, but of organic molecules in general. In the next chapter we shall examine existing methods of spectral analysis and shall propose a method of spectral analysis for complex spectra.

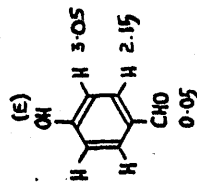
Using spectral analysis methods which we shall subsequently describe, chemical shifts for the protons in the molecules shown in tables 1, 2, and 3 were derived. The symbol E beside certain protons in these molecules signifies that the resonance due to these protons was not observed.



SAT. SOLN. DIOXANE

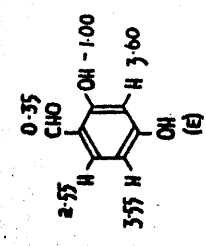


SAT. SOLN. DIOXANE

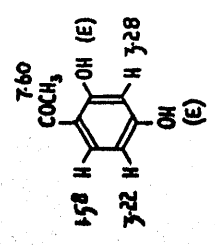


SAT. SOLN. DIOXANE.

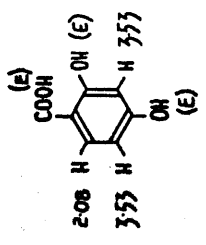
TABLE I : DI-SUBSTITUTED BENZENES.



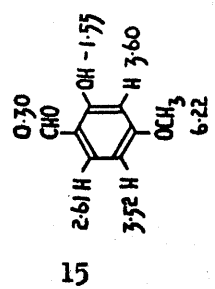
SAT. SOLN. DIOXANE.



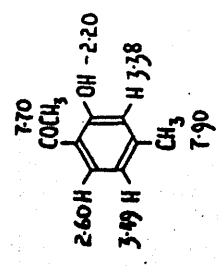
SAT. SOLN. DIOXANE



SAT. SOLN. DIOXANE



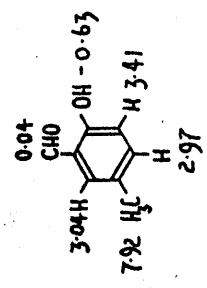
SAT SOLN CCl₄



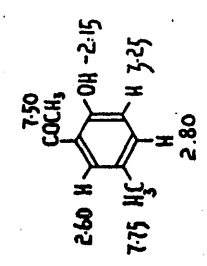
PURE LIQUID



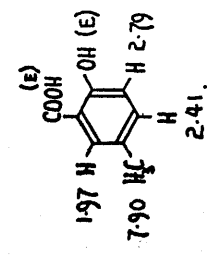
SAT. SOLN. DIOXANE.



SAT. SOLN. CCl₄

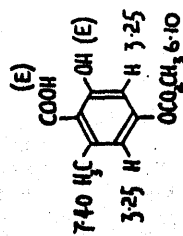


SAT. SOLN CCl₄

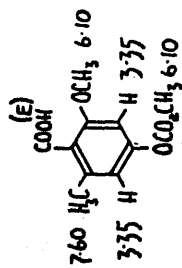


SAT SOLN. DIOXANE.

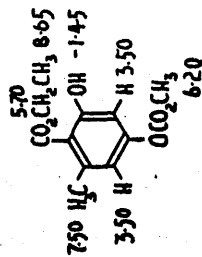
TABLE 2 : TRI-SUBSTITUTED BENZENES.



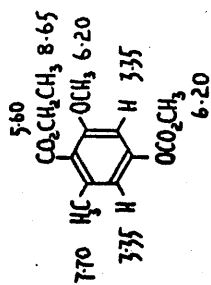
SAT. SOLN. DIOXANE



SAT. SOLN. CHCl₃



SAT. SOLN. CHCl₃



SAT. SOLN. CHCl₃

TABLE 3. TETRASUBSTITUTED
 BENZENES

**A Method of Analysis of
Complex Proton Magnetic Resonance Spectra**

Chapter 4

High resolution proton magnetic resonance spectra can be described, as we have already seen, by a set of "chemical shift" and "spin-spin coupling constant" parameters. The determination of the experimental values of these parameters by the analysis of complex P.M.R. spectra can often be a perplexing problem even though the general theory of the origin of such spectra based upon the properties of angular momentum is well known.⁴⁻⁶

In the analysis of simple spectra, first order perturbation theory is generally used.⁷⁻⁹ For such an approximate treatment to be valid, the spin-spin coupling constants must be much smaller than the differences between the chemical shifts.

In the analysis of slightly more complex spectra, the next step is to consider two of the nuclear spins to be strongly coupled. In this method, all the nuclei except the two strongly coupled ones are treated by first order perturbation theory. The Hamiltonian matrix then consists of a series of two by two sub-matrices and single elements. The two by two matrices are simply diagonalized, and all the energy levels and transition frequencies can then be written explicitly in terms of the spectral parameters. The AEX approximation of Pople, Bernstein, and Schneider^{4,10} is an example of this method of analysis. The ABK approximation¹¹ is a refinement of this method in which the off-diagonal matrix elements of the Hamiltonian are included by the use of second order perturbation theory. This type of improved approximation can be extended to larger spin systems.

Group theory is also applicable in the analysis of all N.M.R. spectra which are derived from molecules possessing symmetry. By a proper choice of spin functions, as dictated by molecular symmetry, a factoring of the Hamiltonian matrix is possible. In some cases of high symmetry, the factoring is sufficient to allow all of the spin energy levels to be written explicitly. Wilson¹³ was the first to give a detailed discussion of the application of group theory to the analysis of nuclear magnetic resonance spectra.

Pople et al.^{13,14} have shown how the approximate methods used for the analysis of spectra of some of the simpler nuclear spin systems such as ABX, AB₂X, ABX₂ can be generalized so as to be applicable to the analysis of spectra of $\begin{matrix} A & B \\ m & n \end{matrix} \text{---} \begin{matrix} R & X \\ p & q \end{matrix}$ systems.

In all the approximate methods so far mentioned, the general approach has been to reduce the Hamiltonian matrix by symmetry and by a neglect of certain off-diagonal matrix elements.

The next stage in the development of methods for the analysis of N.M.R. spectra has been the use of electronic computers for the calculation of spectra from trial parameters. The observed spectrum is then compared with those calculated. The agreement can often be improved by trial and error methods. It has been shown by Swalen and Reilly¹⁵ that it is possible to improve upon these trial and error methods by employing an iterative technique for the adjustment of calculated spectra to those observed. We have tackled the same problem as Swalen and Reilly but by a rather different approach. We shall subsequently relate the method of these workers to that which we shall develop in this chapter.

The most difficult step in the analysis of a complex proton magnetic resonance spectrum is usually that of making an assignment of the observed lines to the many possible energy transitions. A comparison of the observed and calculated spectra can be made provided that a set of trial values for the parameters is available. Naturally, the closer the trial values are to the actual values, the easier it is to assign the spectrum. This raises the question of how to choose the trial parameters judiciously. The most straightforward way would be to analyse the observed spectrum by one of the approximate treatments or possibly by the moment method.⁴ Approximate values for at least some of the parameters might thus be obtained.

The approximate treatments, however, are likely to be less useful in the analysis of the spectra of larger molecules containing many interacting spins. Complicated spectra of broad bands that do not readily yield to analysis can be expected from such molecules. As the number of interacting spins in a molecule increases, the number of possible transitions in its N.M.R. spectrum increases very rapidly.

A technique that is sometime applicable to the analysis of complex spectra is that of spin decoupling by double irradiation.¹⁶⁻¹⁹

Saturation of the lines from one nucleus while recording the spectrum of the remaining ones to which it is coupled can sometimes give a spectrum sufficiently simplified to yield to fairly simple analysis. The parameters so obtained can be used in the analysis of the complete spectrum.

Whitman¹⁹ uses frequency and intensity sum rules to obtain an assignment and the energy levels for three and four spin cases. He instructs the computer to calculate all possible energy level diagrams consistent with the sum rules and a set of experimental errors. This method has the advantage of eliminating any bias but unfortunately requires considerable computer time trying the many possibilities.

Swalen and Reilly¹⁵ use the energy level diagram to verify an assignment. They also use a partial assignment to give a complete assignment by use of frequency and intensity sum rules. Their iteration method depends upon using the approximate eigenfunctions obtained from the first order perturbation energy to calculate the second order perturbation energy and so lead to improved values of the parameters.

In this introduction we have surveyed existing methods of analysing proton magnetic resonance spectra. The Swalen-Reilly method, though the best of these, would seem to have been applied only to the analysis of fairly simple, well resolved spectra. For the analysis of spectra which are not well resolved or which are extremely complex, the derivation of the energy levels from the observed spectrum is extremely difficult, if not impossible. For such spectra the Swalen-Reilly method is scarcely applicable, as the successful operation of the frequency sum rules requires that a fairly large number of transitions be assigned.

The method which we shall develop differs from the latter in that theoretical and observed spectra are compared directly without use of the intermediate energy levels. Refinement of the spectral parameters depends upon variation of each transition energy with respect to every spectral parameter in such a way as to minimize the

discrepancy of each assigned transition.

In the method of spectral analysis which we shall adopt, we shall be concerned with the problem of bringing a theoretical spectrum, based upon guessed parameters, into coincidence with the corresponding observed spectrum. To do this, we must consider the effect of a variation in parameters, namely chemical shifts and spin-spin coupling constants, upon each transition energy of the theoretical spectrum.

Consider a system of n strongly coupled nuclei. Let the chemical shift of the i^{th} nucleus be H_i and the coupling constant between nuclei i and j be J_{ij} . A small increment ΔH_i in the chemical shift H_i will cause an increment ΔE_k in the k^{th} transition energy E_k given by

$$\Delta E_k = \frac{\delta E_k}{\delta H_i} \cdot \Delta H_i \quad (4.2.1)$$

Similarly, a small increment ΔJ_{ij} in the coupling constant J_{ij} will cause an increment ΔE_k in the transition energy E_k given by

$$\Delta E_k = \frac{\delta E_k}{\delta J_{ij}} \cdot \Delta J_{ij} \quad (4.2.2)$$

Simultaneous increments in all H_i and J_{ij} will cause an increment in E_k given by

$$\Delta E_k = \frac{\delta E_k}{\delta H_1} \cdot \Delta H_1 + \dots + \frac{\delta E_k}{\delta H_n} \cdot \Delta H_n + \frac{\delta E_k}{\delta J_{12}} \cdot \Delta J_{12} + \dots + \frac{\delta E_k}{\delta J_{(n-1)n}} \cdot \Delta J_{(n-1)n} \quad (4.2.3)$$

An equation of this type must exist for each permitted transition energy E_k .

Putting the set of equations (4.2.3) in matrix form, we have:-

$$\begin{bmatrix} \Delta E_1 \\ \Delta E_2 \\ \cdot \\ \cdot \\ \cdot \\ \Delta E_y \\ \Delta E_y \end{bmatrix} = \begin{bmatrix} \frac{\delta E_1}{\delta H_1} & \frac{\delta E_1}{\delta H_2} & \dots & \frac{\delta E_1}{\delta J_{(n-1)n}} \\ \frac{\delta E_2}{\delta H_1} & \dots & \dots & \dots \\ \cdot & \cdot & \cdot & \cdot \\ \cdot & \cdot & \cdot & \cdot \\ \frac{\delta E_y}{\delta H_1} & \dots & \dots & \frac{\delta E_y}{\delta J_{(n-1)n}} \end{bmatrix} \begin{bmatrix} \Delta H_1 \\ \Delta H_2 \\ \cdot \\ \cdot \\ \cdot \\ \Delta J_{(n-1)n} \end{bmatrix} \quad (4.2.4a)$$

which we shall subsequently refer to as

$$[E]_{y \times 1} = [T]_{y \times \frac{1}{2}n(n+1)} \cdot [H]_{\frac{1}{2}n(n+1) \times 1} \quad (4.2.4b)$$

We must now seek a possible method to apply this matrix equation to the problem.

If, on the basis of our zero order or "guessed" calculated spectrum, we can assign calculated transition energies to the corresponding observed transition energies, we could define the quantity ΔE_k by the relation

$$\Delta E_k = E_k^{obs} - E_k^{calc} \quad (4.2.5)$$

If this could be done for each transition energy we could then formulate the complete matrix $[\Delta E]$. Presuming we can formulate the matrix $[T]$, we could then solve the matrix equation to obtain the matrix $[H]$, the elements of which would be given by

$$\Delta H_i = H_i^{obs} - H_i^{calc} \quad (4.2.6)$$

As the number of transitions, y , is greater than the $\frac{1}{2}n(n+1)$ unknown parameters, the matrix $[\Delta H]$ is essentially overdetermined.

To enable use to be made of all observational data in solving for $[\Delta H]$, it is convenient to reduce the large set of equations, (4.2.3), to a set of $\frac{1}{2}n(n+1)$ simultaneous equations. This is most simply done by multiplying both sides of (4.2.4) from the left by the transpose of $[T]$,

$$[T]_{\frac{1}{2}n(n+1) \times y}' \cdot [\Delta E]_{y \times 1} = [T]_{\frac{1}{2}n(n+1) \times y}' \cdot [T]_{y \times \frac{1}{2}n(n+1)} \cdot [\Delta H]_{\frac{1}{2}n(n+1) \times 1} \quad (4.2.7a)$$

which we shall write as

$$[A]_{\frac{1}{2}n(n+1) \times 1} = [B]_{\frac{1}{2}n(n+1) \times \frac{1}{2}n(n+1)} \cdot [\Delta H]_{\frac{1}{2}n(n+1) \times 1} \quad (4.2.7b)$$

where

$$[A] = [T]' \cdot [\Delta E]$$

$$[B] = [T]' \cdot [T]$$

Assuming that we can formulate the matrix ΔE , as we have previously discussed, solution of (4.2.7) for those H_i and J_{ij} which bring the calculated spectrum into coincidence with the observed spectrum can be carried out if the matrix T can be formulated. We shall consider this problem next.

As can be seen from equation (4.2.4a), the elements of the matrix T are the partial differential coefficients of each transition energy with respect to each parameter H_i and J_{ij} . Before these partial differentials can be found, it is necessary to formulate an expression for each transition energy in terms of the H_i and J_{ij} . These expressions can be derived from the expressions for the eigenvalues of the system as we shall now show.

The time independent Schrodinger equation can be written:-

$$\mathcal{H}|\psi_a\rangle = W_a|\psi_a\rangle \quad (4.3.1)$$

where \mathcal{H} is the Hamiltonian operator for the system, W_a is the eigenvalue characteristic of the eigenvector $|\psi_a\rangle$. If the ψ 's are expressed as linear combinations of a set of orthonormal functions φ_i , we may write:-

$$|\psi_a\rangle = \sum_i A_i |\varphi_i\rangle \quad (4.3.2a)$$

$$|\psi_b\rangle = \sum_i B_i |\varphi_i\rangle \quad (4.3.2b)$$

Equation (4.3.1) then becomes:-

$$\mathcal{H} \sum_i A_i |\varphi_i\rangle = W_a \sum_i A_i |\varphi_i\rangle \quad (4.3.3)$$

thus
$$\sum_i A_i \mathcal{H} |\varphi_i\rangle = W_a \sum_i A_i |\varphi_i\rangle$$

Multiplying from the left by $\langle \varphi_j |$, we have:-

$$\sum_i A_i \langle \varphi_j | \mathcal{H} | \varphi_i \rangle = W_a \sum_i A_i \langle \varphi_j | \varphi_i \rangle \quad (4.3.4)$$

As the φ_i are orthonormal, this simplifies to:-

$$\sum_i A_i \langle \varphi_j | \mathcal{H} | \varphi_i \rangle = W_a A_j \quad (4.3.5)$$

Therefore
$$W_a = \frac{\sum_i A_i (\varphi_j | \mathcal{H} | \varphi_i)}{A_j} \quad (4.3.6a)$$

Similarly
$$W_b = \frac{\sum_i B_i (\varphi_j | \mathcal{H} | \varphi_i)}{B_j} \quad (4.3.6b)$$

It can be seen that the expression for each eigenvalue consists of a series of terms each of which involves a numerical coefficient multiplied by a matrix element. The method of evaluation of these matrix elements is well known⁴. It turns out that the diagonal matrix elements depend linearly upon the chemical shift terms, and linearly upon the coupling constant terms, whereas the off-diagonal matrix elements depend only upon the coupling constants, the dependence once more being linear. Each eigenvalue W_a can therefore be represented by an equation which is linear in the H_i and J_{ij} . Since the expression for each transition energy is formed by taking the difference between the two corresponding eigenvalues:-

$$E_{k(a \leftarrow b)} = W_a - W_b \quad (4.3.7)$$

this expression must also be linear in the chemical shift and coupling constant parameters. It follows that the partial differential coefficient of each transition energy with respect to one of these parameters is given simply by the coefficient of that term in the transition energy expression which involves the parameter considered. Thus, in order to set up the T matrix for the theoretical spectrum, all that we require is the set of eigenvector coefficients A_i, B_i, \dots . For any particular spin system, these can be obtained by diagonalization of the energy matrix.

It would seem that the refinement method which we have outlined is generally soluble. The obvious next step is to apply the method to a nuclear spin system of the type that we have discussed. As the eigenfunctions and matrix elements of an n spin system depend upon the value n, we shall find it convenient to consider systems with different numbers of nuclei separately.

The N.M.R. spectrum of a system of three coupled protons is defined by the magnitude of six spectral parameters H_i and J_{ij} , which we shall write in matrix form as follows:-

$$[H] = \begin{bmatrix} H_1 \\ H_2 \\ H_3 \\ J_{12} \\ J_{13} \\ J_{23} \end{bmatrix} \quad (4.5.1)$$

The eigenfunctions for such a system can be written:-

$$\begin{aligned} |\varphi_1\rangle &= |\alpha(1) \alpha(2) \alpha(3) \rangle \\ |\varphi_2\rangle &= |\alpha(1) \alpha(2) \beta(3) \rangle \\ |\varphi_3\rangle &= |\alpha(1) \beta(2) \alpha(3) \rangle \\ |\varphi_4\rangle &= |\beta(1) \alpha(2) \alpha(3) \rangle \\ |\varphi_5\rangle &= |\alpha(1) \beta(2) \beta(3) \rangle \\ |\varphi_6\rangle &= |\beta(1) \alpha(2) \beta(3) \rangle \\ |\varphi_7\rangle &= |\beta(1) \beta(2) \alpha(3) \rangle \\ |\varphi_8\rangle &= |\beta(1) \beta(2) \beta(3) \rangle \end{aligned} \quad (4.5.2)$$

These eigenvectors form a basis upon which the nuclear spin system can be represented. Upon this basis the eigenvalue matrix may be formulated:-

$$[W] = \left([k] + [l] \right) \cdot [H] \times 0.5 \quad (4.5.3)$$

where $[k]$ and $[l]$ are respectively matrices of diagonal and off-diagonal matrix element coefficients. These are given by:-

$$[k] = \begin{bmatrix} 1 & 1 & 1 & 0.5 & 0.5 & 0.5 \\ 1 & 1 & -1 & 0.5 & -0.5 & -0.5 \\ 1 & -1 & 1 & -0.5 & 0.5 & -0.5 \\ -1 & 1 & 1 & -0.5 & -0.5 & 0.5 \\ 1 & -1 & -1 & -0.5 & -0.5 & 0.5 \\ -1 & 1 & -1 & -0.5 & 0.5 & -0.5 \\ -1 & -1 & 1 & 0.5 & -0.5 & -0.5 \\ -1 & -1 & -1 & 0.5 & 0.5 & 0.5 \end{bmatrix}$$

$$[l] = \begin{bmatrix} 0 & 0 & 0 & 0 & 0 & 0 \\ 0 & 0 & 0 & 0 & \frac{A_{24}}{A_{22}} & \frac{A_{23}}{A_{22}} \\ 0 & 0 & 0 & \frac{A_{34}}{A_{33}} & 0 & \frac{A_{32}}{A_{33}} \\ 0 & 0 & 0 & \frac{A_{43}}{A_{44}} & \frac{A_{42}}{A_{44}} & 0 \\ 0 & 0 & 0 & \frac{A_{56}}{A_{55}} & \frac{A_{57}}{A_{55}} & 0 \\ 0 & 0 & 0 & \frac{A_{65}}{A_{66}} & 0 & \frac{A_{67}}{A_{66}} \\ 0 & 0 & 0 & 0 & \frac{A_{75}}{A_{77}} & \frac{A_{76}}{A_{77}} \\ 0 & 0 & 0 & 0 & 0 & 0 \end{bmatrix}$$

The matrix of allowed transition energies $[E_k]$ is got by multiplying the matrix $[W]$ from the left by the matrix $[m]$. This multiplication is equivalent to the step shown by equation (4.3.7). Matrix $[m]$ is given by:-

$$[m] = \begin{bmatrix} 1 & -1 & 0 & 0 & 0 & 0 & 0 & 0 \\ 1 & 0 & -1 & 0 & 0 & 0 & 0 & 0 \\ 1 & 0 & 0 & -1 & 0 & 0 & 0 & 0 \\ 0 & 1 & 0 & 0 & -1 & 0 & 0 & 0 \\ 0 & 1 & 0 & 0 & 0 & -1 & 0 & 0 \\ 0 & 1 & 0 & 0 & 0 & 0 & -1 & 0 \\ 0 & 0 & 1 & 0 & -1 & 0 & 0 & 0 \\ 0 & 0 & 1 & 0 & 0 & -1 & 0 & 0 \\ 0 & 0 & 1 & 0 & 0 & 0 & -1 & 0 \\ 0 & 0 & 0 & 1 & -1 & 0 & 0 & 0 \\ 0 & 0 & 0 & 1 & 0 & -1 & 0 & 0 \\ 0 & 0 & 0 & 1 & 0 & 0 & -1 & 0 \\ 0 & 0 & 0 & 0 & 1 & 0 & 0 & -1 \\ 0 & 0 & 0 & 0 & 0 & 1 & 0 & -1 \\ 0 & 0 & 0 & 0 & 0 & 0 & 1 & -1 \end{bmatrix}$$

As can be seen from equation (4.5.3), the $[T]$ matrix can be written:-

$$[T] = 0.5 \times [m] \cdot ([k] + [1])$$

The next step is to write a computer programme to calculate the $[T]$ matrix, given the eigenvector coefficients A_{ij} which are available from the matrix diagonalization programme.

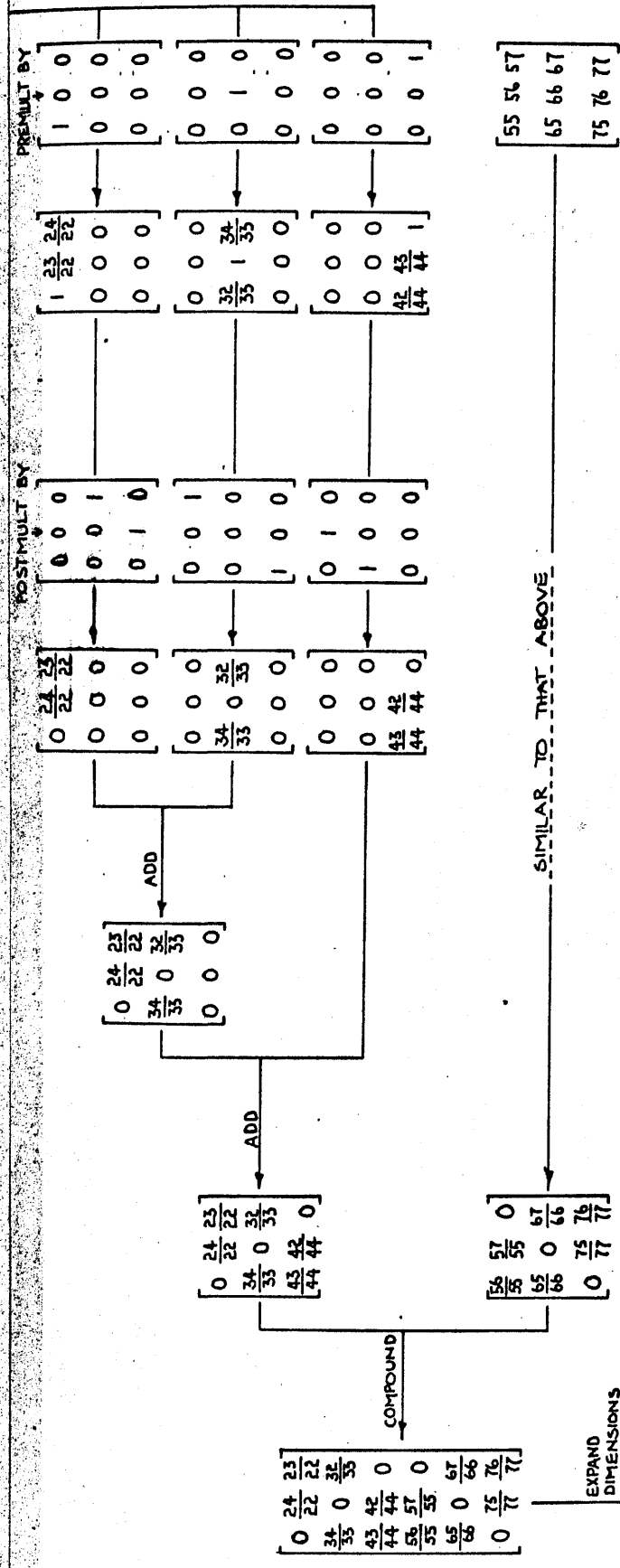
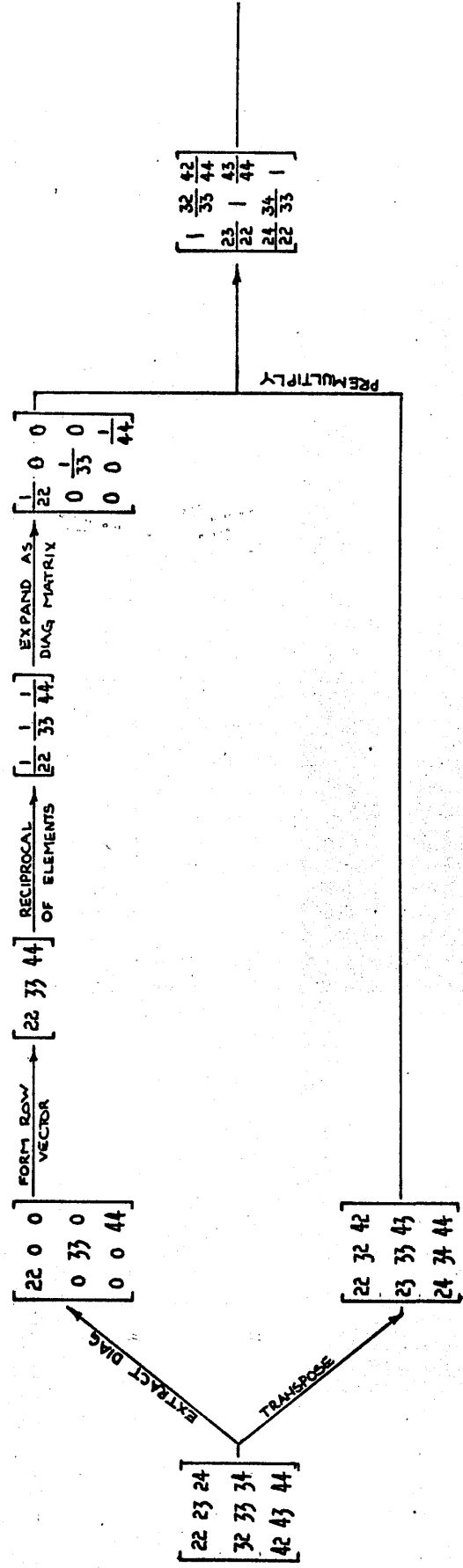
The eigenvector coefficients necessary as input for the T matrix programme can be obtained as output from existing N.M.R. computer programmes for the Deuce computer. Having specified a set of chemical shifts and coupling constants, these programmes both set up and diagonalize the energy matrix for the system. For a three spin system the eigenvector coefficients are obtained as two three by three matrices:-

$$\begin{bmatrix} A_{22} & A_{23} & A_{24} \\ A_{32} & A_{33} & A_{34} \\ A_{42} & A_{43} & A_{44} \end{bmatrix} \qquad \begin{bmatrix} A_{55} & A_{56} & A_{57} \\ A_{65} & A_{66} & A_{67} \\ A_{75} & A_{76} & A_{77} \end{bmatrix}$$

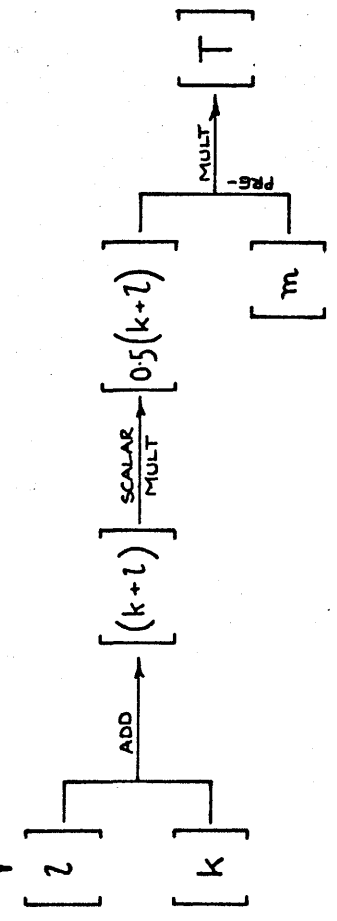
To set up the T matrix, the main part of the problem is concerned with the transformation of these matrices into matrix [1]. A flówsheet for this process and for the subsequent steps leading to the formation of the T matrix is included on the next page. Each step has been designed with a view to use of Deuce code G.I.P. Details of the operation of the program will be found in Appendix 1.

CHAPTER 4.6

T MATRIX SET-UP PROGRAMME FLOWSHEET



IN ALL MULTIPLICATION STEPS [A].[B] → [C]
 MATRIX [B] IS AUTOMATICALLY TRANSPOSED.
 BY DEUCE



We have shown in equations (4.2.1) to (4.2.7) that a solution of the matrix equation (4.2.7) for the matrix $[\Delta H]$ can be found if the matrix $[\Delta E]$ can be formulated. Equation (4.2.5) :-

$$\Delta E_k = E_k^{\text{obs}} - E_k^{\text{calc}}$$

which expresses the general element of the $[\Delta E]$ matrix, shows that a correct assignment of all calculated transition energies to observed transition energies must be made before the complete $[\Delta E]$ matrix can be written. This is not in general possible as several of the transitions may be forbidden or may have so low an intensity that they cannot be observed. Such transitions cannot be included in the refinement and it is necessary to include some mechanism of selective elimination of these ΔE_k values. This will become clearer if we consider the method of formulation of the $[\Delta E]$ matrix which we shall adopt.

The set of calculated transition energies $[E_{\text{calc}}]$ is obtained in the computer as a fifteen by one matrix by multiplication of H from the left by $[T]$. Inspection of the zero order or "guessed" calculated spectrum should enable a partial arrangement of the observed transition energies in the same order as the calculated transition energies, i.e. a partial assignment. Where no assignment is possible, we shall put E_k^{obs} equal to zero. Having calculated $[E^{\text{calc}}]$ in the computer, we can include as input the $[E^{\text{obs}}]$ matrix and use the computer to calculate $[\Delta E]$ as given by equation (4.2.5). It is obvious that many of the ΔE_k formed will be false due to the selection of the value zero for the non-assigned transition energies. These false ΔE_k values may be eliminated by inclusion of a matrix $[C]$ in the input programme, the use of this matrix being subsequently demonstrated.

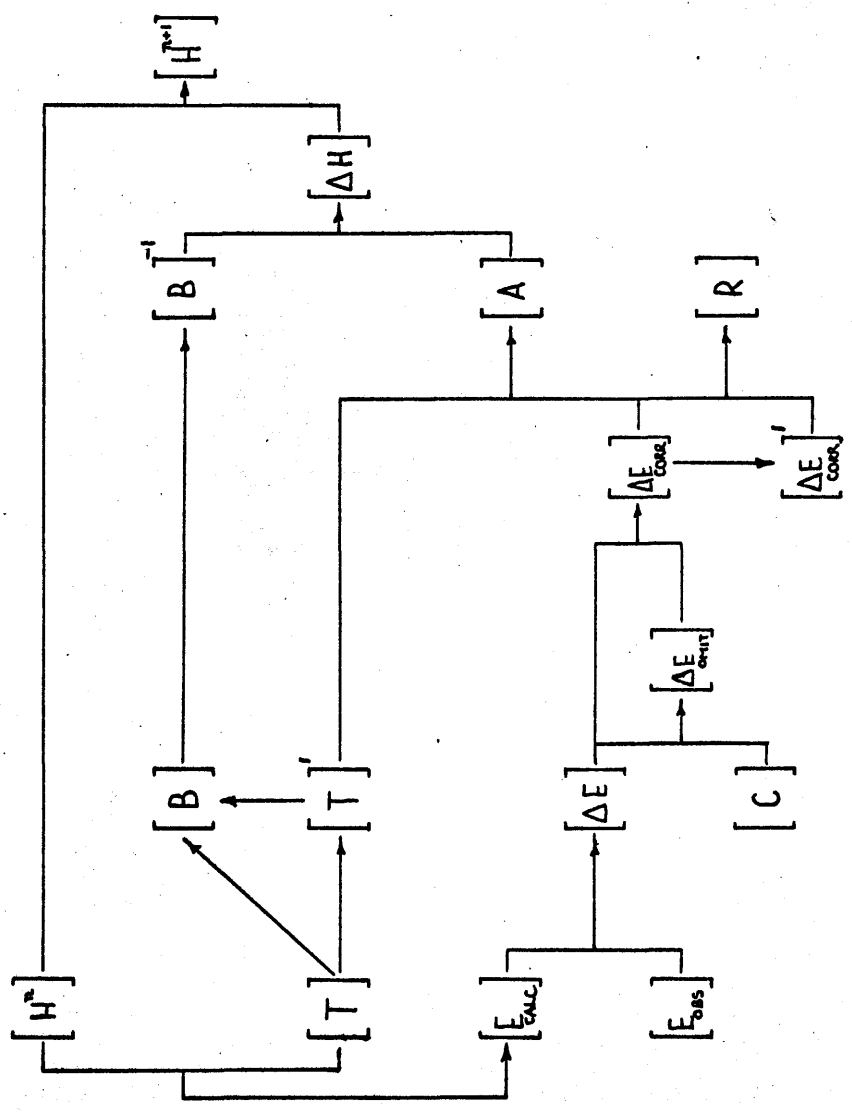
Having obtained the corrected matrix $[\Delta E_{\text{corr}}]$, the matrix equation (4.2.7) can be solved to obtain the $[\Delta H]$ matrix. An improved set of spectral parameters is obtained by the addition:-

$$[H'] = [H] + [H]$$

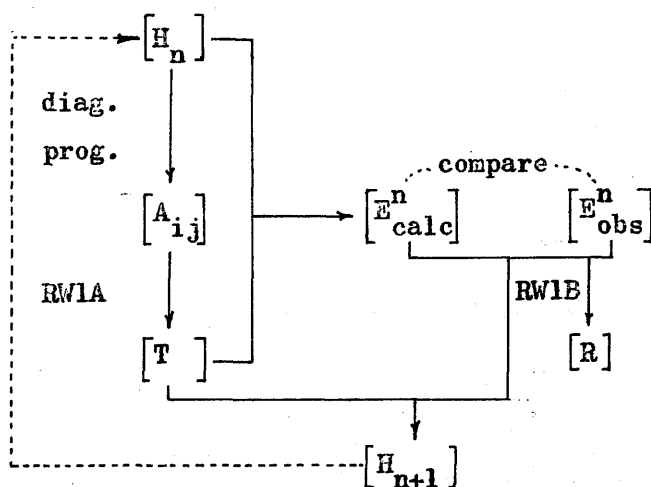
The $[H']$ matrix can then be used as input for a new iterative cycle, the refinement process being continuous.

At the end of each cycle of refinement it is desirable to have an index of the disagreement between calculated and observed spectra. This is suitably provided by the sum of the squares of the discrepancies ΔE_k . This quantity, R, can be obtained by pre-multiplication of the $[\Delta E_{\text{corr}}]$ matrix by its transpose. A flowsheet for the refinement programme is included on the next page, the actual programme having been written in Deuce code G.I.P. Details of the operation of the programme will be found in Appendix I.

CHAPTER 4.7
REFINEMENT PROGRAMME FLOWSHEET.

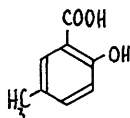


The complete cycle for the refinement of spectral parameters is represented in the following flow diagram:-



An Example of the Refinement Method
Applied to a Three Spin Spectrum. 4.9

To provide a simple test and to illustrate the operation of the refinement method, we shall describe the analysis of the aryl proton region of the spectrum of the following compound:-



The molecule of this compound contains three non-equivalent aryl protons which give rise to an ABC spectrum which is illustrated in spectrum 4.9.

This spectrum consists of three groups of resonances at 0, 30, and 55c/s respectively. The groups at 0 and 30c/s are split by about 10c/s, that at 30c/s exhibiting secondary splitting by about 2c/s. The group at 55c/s shows a similar 2c/s splitting. The intensities of these groups of transitions indicate that each group originates from resonances involving only one proton. From these observations we can derive the set of "guessed" spectral parameters shown in column H_0 of table 4.9. Using these parameters, a zero order spectrum was computed, the resulting transition energies being given by column E_0 of this table. The observed transition energies, arranged so as to correspond to the calculated transition energies are given in the E_{obs} column of the table. Agreement between calculated and observed spectra is seen to be fairly close. Of the fifteen calculated transitions, twelve can be assigned with ease to observed transitions, the remaining three being forbidden. A complete assignment of the spectrum can therefore be made.

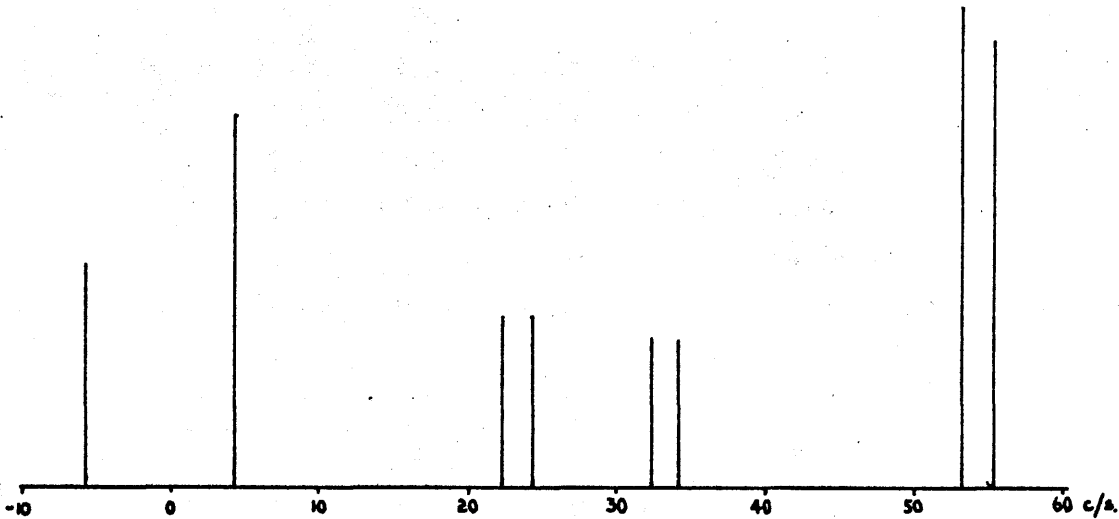
On the basis of this assignment, three cycles of iterative refinement were carried out. The following matrices were used as input for the first iterative cycle:-

- (1) The T matrix obtained in the calculation of the zero order spectrum.
- (2) The H_0 matrix (column vector formed by col. H_0 of the table).

CHAPTER 4.9

Spectrum 4.9

OBSERVED SPECTRUM.



REFINED CALCULATED SPECTRUM

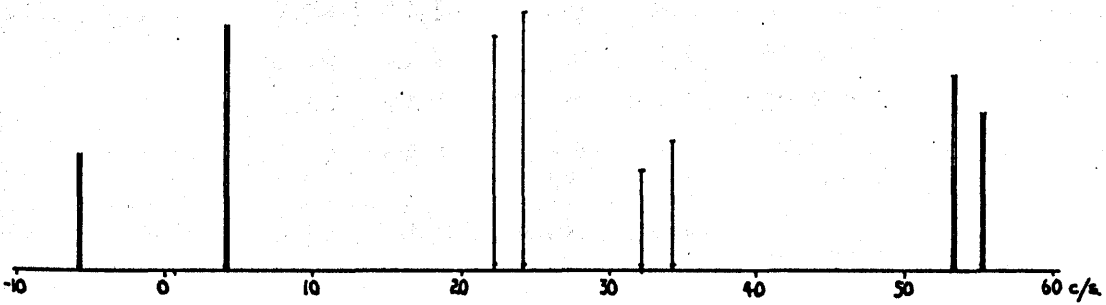


Table 4.9

Refinement of Chemical Shifts

| | H_0 | H_1 | H_2 | H_3 | H_4 |
|----------|-------|-------|-------|-------|-------|
| H_A | 54.37 | 54.37 | 54.36 | 54.36 | 54.36 |
| H_B | 27.74 | 27.66 | 27.61 | 27.58 | 27.56 |
| H_C | 00.00 | 00.14 | 00.21 | 00.25 | 00.27 |
| J_{AB} | 02.00 | 02.05 | 02.06 | 02.06 | 02.06 |
| J_{AC} | 00.00 | -0.07 | -0.08 | -0.08 | -0.08 |
| J_{BC} | 10.00 | 10.01 | 10.01 | 10.01 | 10.01 |

Refinement of Spectra

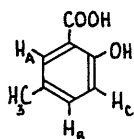
| | E_0 | E_1 | E_2 | E_3 | E_{obs} | C |
|---|--------|--------|--------|--------|-----------|---|
| | 04.15 | 04.26 | 04.32 | 04.36 | 04.4 | 0 |
| | 34.53 | 34.50 | 34.45 | 34.43 | 34.4 | 0 |
| | 55.41 | 55.41 | 55.40 | 55.40 | 55.4 | 0 |
| | 24.55 | 24.50 | 24.45 | 24.43 | 24.4 | 0 |
| | 55.34 | 55.40 | 55.40 | 55.40 | 55.4 | 0 |
| | 83.86 | 83.65 | 83.53 | 83.47 | (f'bddn) | 1 |
| | -5.83 | -5.73 | -5.67 | -5.63 | -5.6 | 0 |
| | 24.95 | 25.17 | 25.28 | 25.33 | (f'bddn) | 1 |
| | 53.47 | 53.42 | 53.41 | 53.40 | 53.4 | 0 |
| | -26.70 | -26.64 | -26.62 | -26.61 | (f'bddn) | 1 |
| | 04.07 | 04.25 | 04.32 | 04.36 | 04.4 | 0 |
| | 32.59 | 32.50 | 32.45 | 32.43 | 32.4 | 0 |
| | 53.40 | 53.41 | 53.40 | 53.40 | 53.4 | 0 |
| | 22.61 | 22.50 | 22.45 | 22.43 | 22.4 | 0 |
| | -5.90 | -5.74 | -5.67 | -5.63 | -5.6 | 0 |
| R | 0.45 | 0.12 | 0.03 | 0.01 | | |

(3) The E_{obs} matrix (column vector formed by col. E_{obs}).

(4) The C matrix, which is a fifteen by fifteen matrix whose off-diagonal elements are zero and whose diagonal elements are given by column C of table 4.9. The diagonal elements are zero for transitions which can be assigned and unity for transitions which are forbidden or which cannot be assigned.

The matrix of improved spectral parameters and the disagreement factor R , obtained from the first iterative cycle, are shown in columns E_1 and E_0 . The complete cycle of calculations was repeated three times using the set of refined parameters obtained in each cycle. The results are shown in the table, the refined set of spectral parameters being given in column E_2 . The small negative trend in the para coupling constant J_{AC} should not be regarded as significant because splitting of the spectrum due to this coupling was not observed.

From the analysis of the spectrum, we have assigned protons A, B, and C in the following manner:-



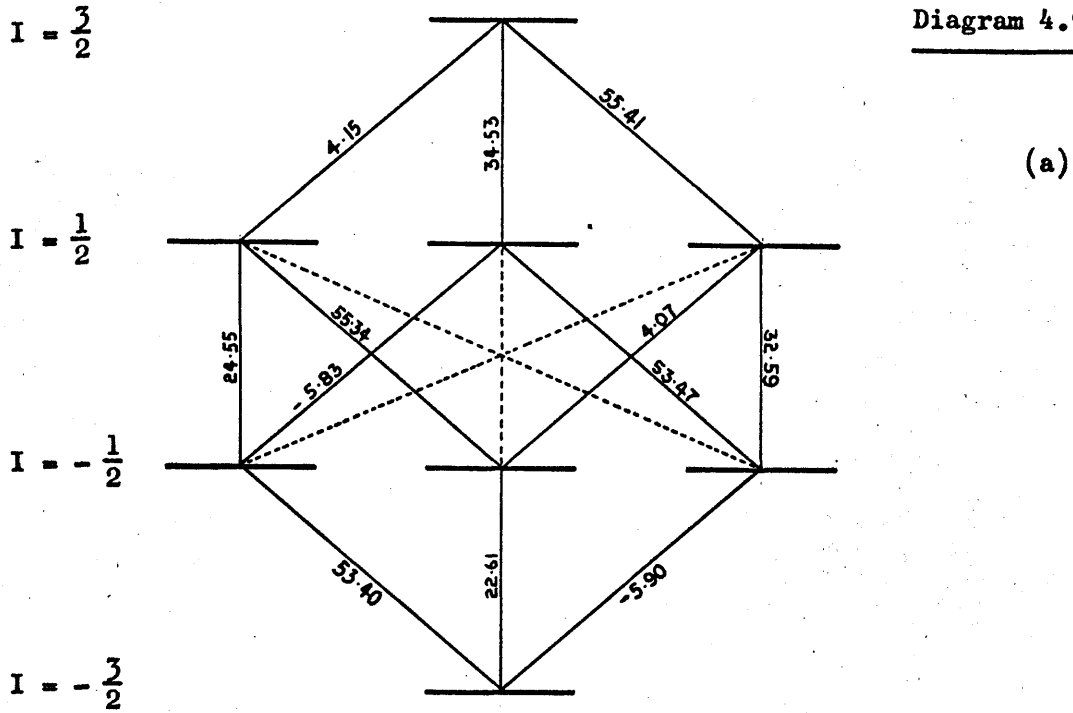
The increasingly closer agreement between refined and observed spectra which results with each iterative cycle is sufficient to show that the refinement method is quite satisfactory for the analysis of well resolved spectra.

It is of interest to compare the Reilly-Swalen method with our own. Using the same "guessed" parameters, a comparison of the zero order calculated spectrum with the observed spectrum leads to the same assignment of transitions. This enables the "observed" energy level diagram, 4.9.2b, to be drawn so as to correspond to the theoretical energy level diagram, 4.9.2a. From the "observed" energy level diagram, relative values for all the energy levels can be derived. Each of the eight energy levels can be expressed in terms of the six spectral parameters, as shown by equation (4.3.6), so that the refinement by iterative perturbation theory amounts to finding

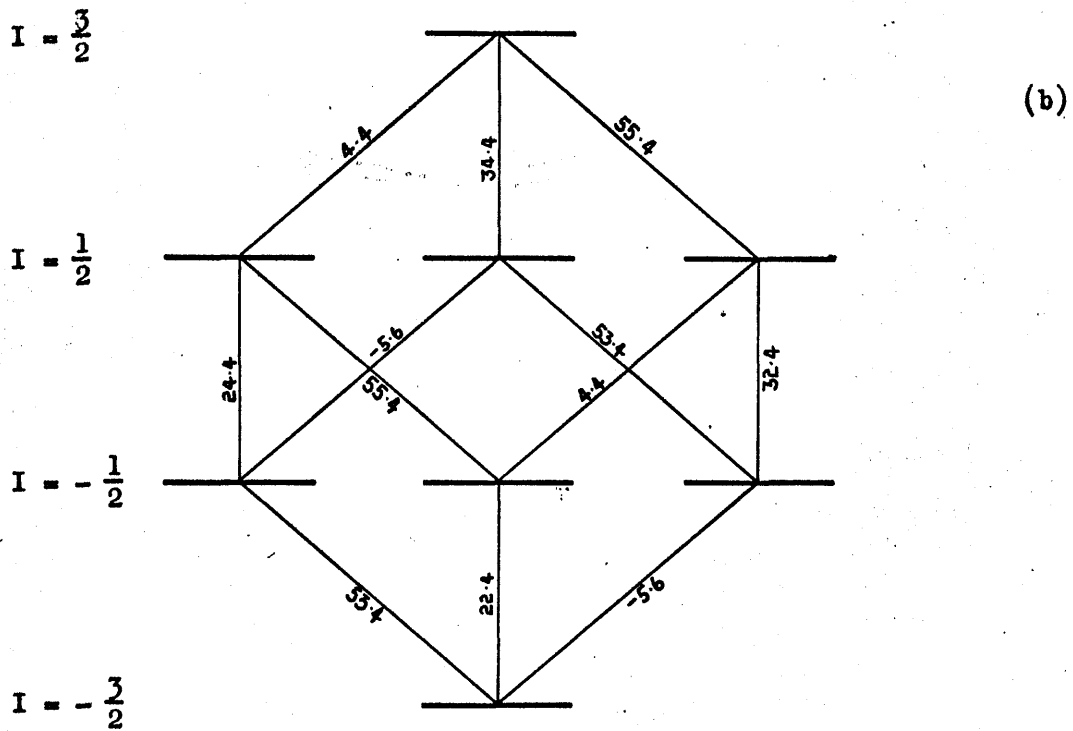
that set of parameters which leads to the "observed" set of energy levels.

In the analysis of a spectrum as simple and well resolved as that which we have discussed, there would appear to be little to choose between the Reilly-Swalen method and our own. If anything, our method has the advantage of eliminating the intermediate step of using the energy levels, theoretical and observed spectra being compared directly at all stages of refinement. The actual advantage of this approach will be seen more clearly when we come to deal with the analysis of four spin ABCD spectra.

Diagram 4.9.2



Theoretical Energy Level Diagram.



"Observed" Energy Level Diagram.

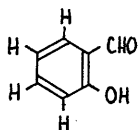
The refinement method described in general in chapters 4.2 - 4.3 and for the three spin system in particular in chapters 4.5 - 4.8 can be extended in an obvious way to the interpretation of four spin spectra. As details of the programmes would be extremely cumbersome to present, they will not be given. Programmes for the interpretation of four spin spectra, completely analogous to those for three spin spectra, were written, as before, in Deuce code G.I.P. Because of the relative complexity of four spin spectra, the four spin programmes have been used to a greater extent in research work than the three spin programmes. The use of these programmes and the development of a complete method of spectral analysis will be demonstrated in the example which follows.

The Analysis of Four Spin Proton
Magnetic Resonance Spectra 4.11

The operation of the refinement method has already been described. In this chapter we shall therefore concentrate upon the actual problem of spectral analysis.

In chapter 4.1 it was stated that the most difficult step in the analysis of a complex proton magnetic resonance spectrum was usually that of assigning the observed lines to the many possible energy transitions. Existing methods of making these assignments were also discussed. In this chapter we shall see how it is possible to obtain many of these assignments by making proper use of the refinement method. To see how this comes about, the analysis of a complex ABCD spectrum will be described in detail.

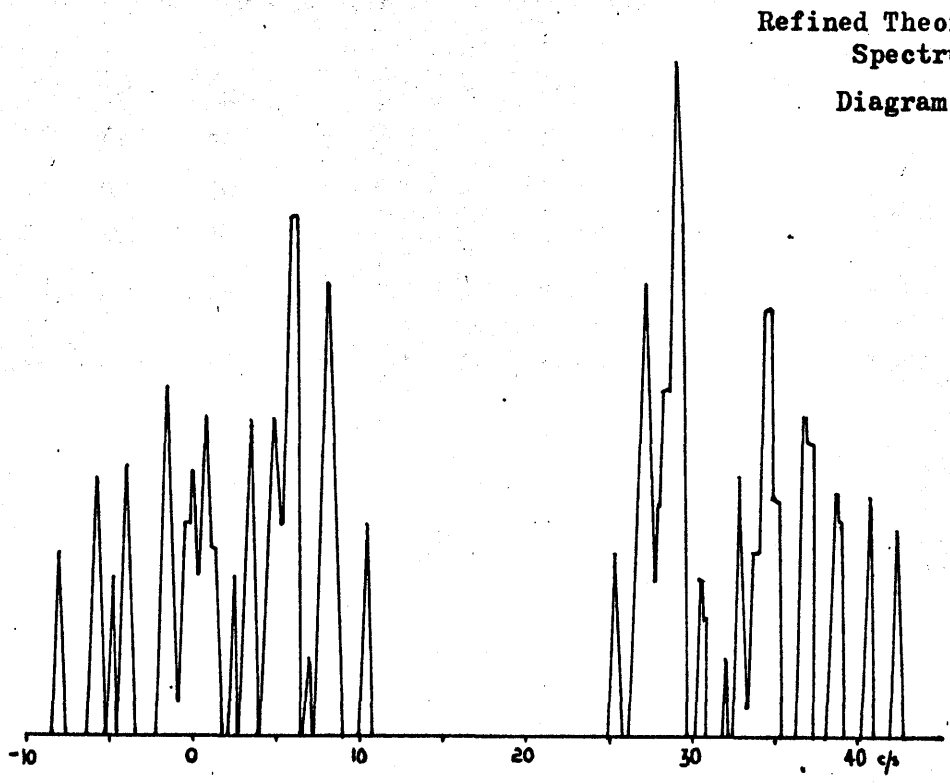
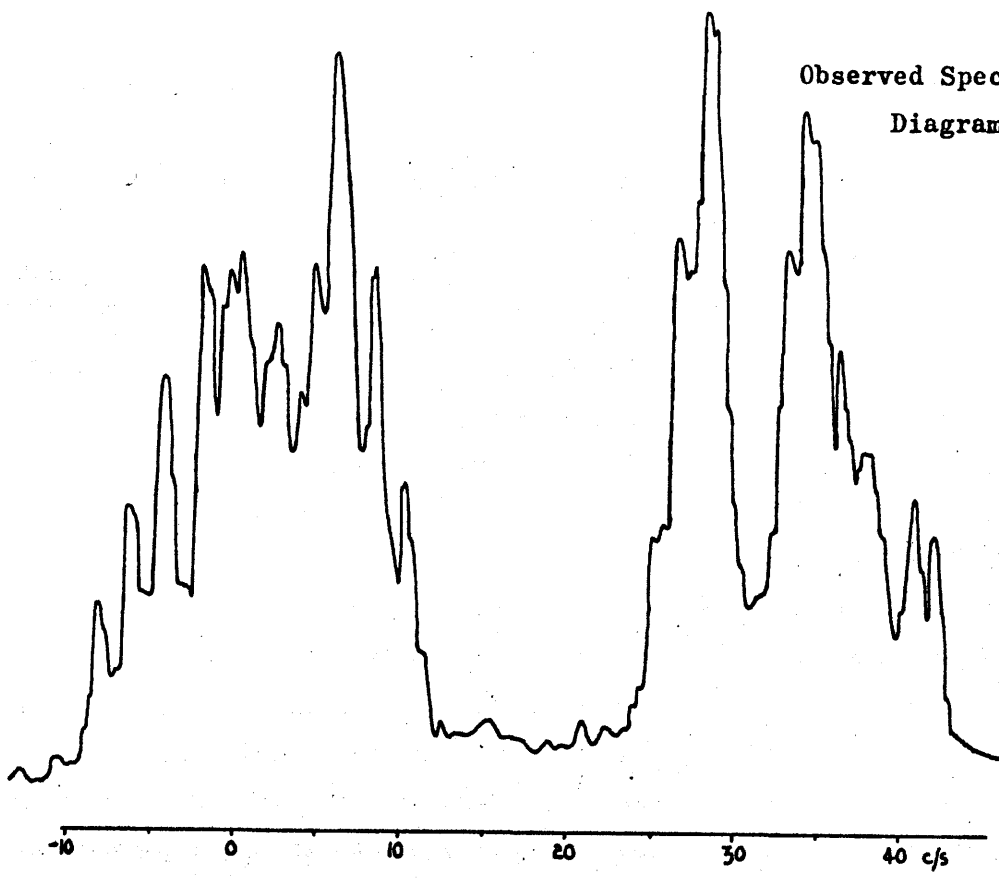
The four non-equivalent aryl protons of the salicylaldehyde molecule:-



give rise to a good example of a complex ABCD spectrum, as shown by the observed 60 Mc/s spectrum in diagram 4.11.1. The complete aryl proton spectrum occupies a bandwidth of only fifty cycles per second, there being between twenty five and thirty resolved or partially resolved transitions within the band. Apart from complexity arising from the strong coupling of the nuclear spins, the spectrum is further complicated by the near equivalence of pairs of the four chemical shifts which causes the resonances due to two of the nuclei to be superimposed upon the resonances due to the other two. In addition, many combination transitions are permitted.

Several spectra were recorded under conditions of maximum instrumental resolution. All spectra were similar, although there were small differences in position, line-width, and intensity of the resonances in different spectra. Diagram 4.11.1 illustrates a typical spectrum.

Six spectra were employed to obtain mean values of the transition



energies, these being obtained to within ± 0.3 c/s. Accuracy of measurement was limited by line-width, superimposition of the resonances, and slight non-linearity of the field sweep.

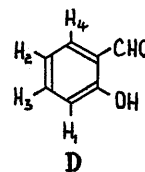
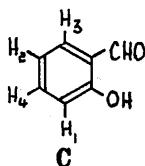
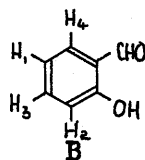
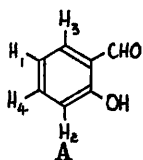
Analysis of the spectrum.

The distribution of intensities in the high and low field regions of the observed spectrum suggests that each of these regions originates from resonances involving two protons. Assuming that the ortho-para directive influence of the substituents controls the magnetic environment of the ring protons³, it seems reasonable to assume that the resonances at high field are due to protons ortho and para to the hydroxyl group, those at low field being due to protons meta to the hydroxyl group.

By examination of the observed spectrum, relative chemical shifts of 0, 3, 30, and 34 c/s were guessed. Assuming for the moment that ortho coupling constants are the only ones different from zero, these having a value of 8 c/s, there are four sets of spectral parameters consistent with our assumptions:-

| | H ₁ | H ₂ | H ₃ | H ₄ | J ₁₂ | J ₁₃ | J ₁₄ | J ₂₃ | J ₂₄ | J ₃₄ |
|---|----------------|----------------|----------------|----------------|-----------------|-----------------|-----------------|-----------------|-----------------|-----------------|
| A | 34 | 30 | 3 | 0 | 0 | 8 | 8 | 0 | 8 | 0 |
| B | 34 | 30 | 3 | 0 | 0 | 8 | 8 | 8 | 0 | 0 |
| C | 34 | 30 | 3 | 0 | 0 | 0 | 8 | 8 | 8 | 0 |
| D | 34 | 30 | 3 | 0 | 0 | 8 | 0 | 8 | 8 | 0 |

These correspond to the following arrangements of the protons:-



The conventional method for obtaining a spectrum from which assignments might be made was initiated by calculating zero order spectra for A, B, C, and D. The spectrum for arrangement C is shown in diagram IIIa, spectra for arrangements A, B, and D being similar. By trial and error methods, these guessed chemical shifts were altered until better agreement between calculated and observed spectra resulted. Diagram IIIb shows the spectrum obtained in this way for arrangement C. The improved parameters for A, B, C, and D were as follows:-

| | H_1 | H_2 | H_3 | H_4 | J_{12} | J_{13} | J_{14} | J_{23} | J_{24} | J_{34} |
|---|-------|-------|-------|-------|----------|----------|----------|----------|----------|----------|
| A | 32.5 | 30.5 | 2.0 | 1.0 | 0 | 8 | 8 | 0 | 8 | 0 |
| B | 33.0 | 31.0 | 0.5 | 0 | 0 | 8 | 8 | 8 | 0 | 0 |
| C | 34.0 | 33.0 | 2.0 | 1.0 | 0 | 0 | 8 | 8 | 8 | 0 |
| D | 34.0 | 33.0 | 1.0 | 0 | 0 | 8 | 0 | 8 | 8 | 0 |

The "improved" spectra for A, B, C, and D were much more alike than the zero order spectra due to the approaching equivalence of the pairs of chemical shifts H_1 and H_2 , and H_3 and H_4 . So alike were the spectra that refinement of any one spectrum would automatically include refinement of the others. Arrangement C was chosen for refinement, diagram IIIc showing this spectrum re-calculated with the inclusion of meta coupling constants of 1.5 c/s. The beginnings of the correct spectral structure are obvious in this spectrum. Several attempts were made to refine spectrum IIIc but with little success as a sufficient number of transitions could not be assigned with any certainty.

We have just described the usual method for calculating a spectrum from which assignments can be made and shown how this fails. The manner in which this spectrum can be obtained by use of the refinement method will now be considered.

DIAGRAM IIIa
ZERO ORDER SPECTRUM

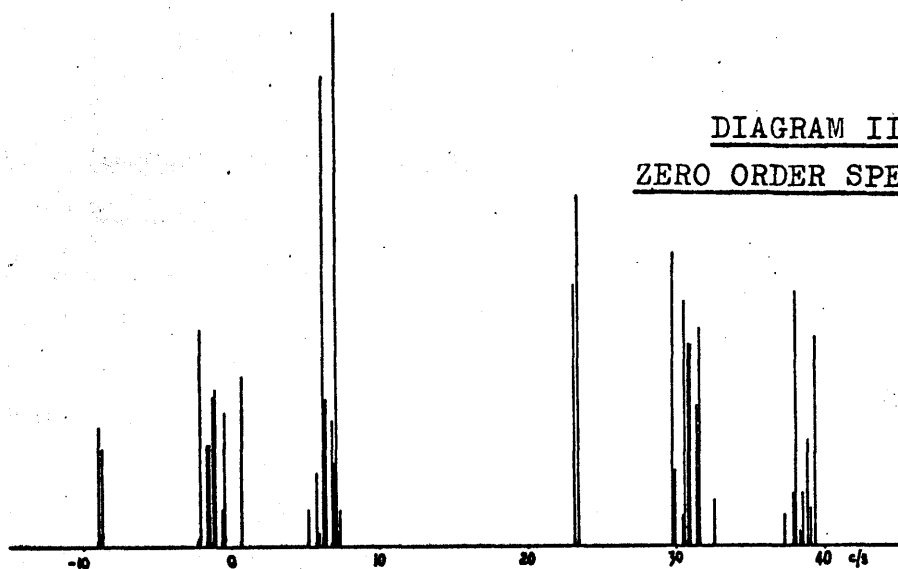


DIAGRAM IIIb
FIRST ORDER SPECTRUM

$$J_m = 0$$

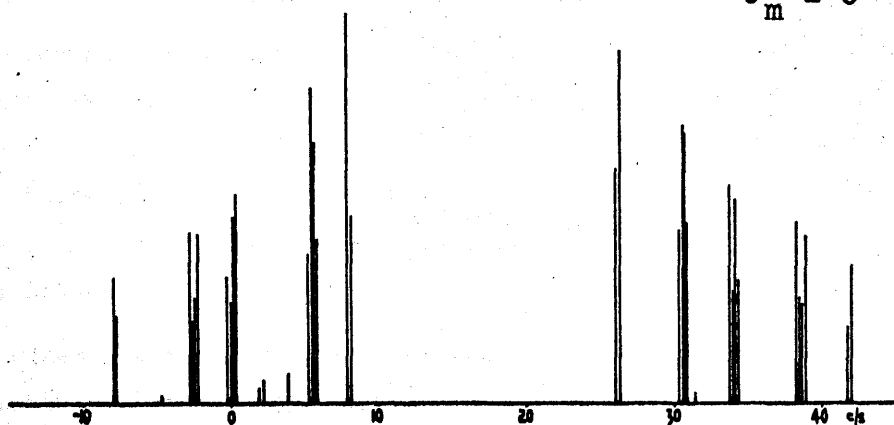
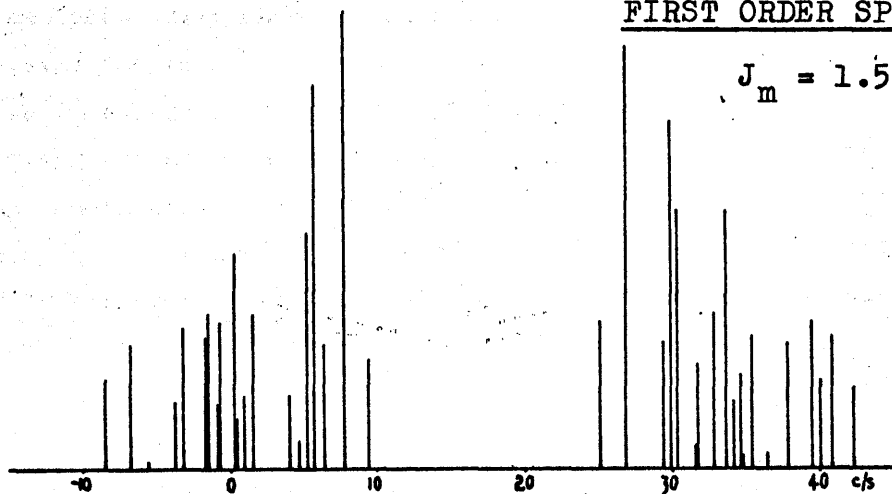


DIAGRAM IIIc
FIRST ORDER SPECTRUM

$$J_m = 1.5 \text{ c/s}$$



Use of the refinement method to calculate a spectrum from which assignments can be made.

Of the expressions for the fifty six transitions for a four spin system, thirty two involve only a single chemical shift term. These transitions can be said to belong to a particular nucleus. The expressions for the remaining twenty four transitions involve more than one chemical shift term, these transitions being referred to as combination transitions. The elements of the T matrix form an index of the parameters upon which each transition depends, the first four elements of each row describing dependence upon the chemical shift terms. By using this information it is possible to assign each transition of the theoretical spectrum to a particular nucleus or particular nuclei as the case may be. The calculated spectrum can then be decomposed into components belonging to particular nuclei as illustrated by the decomposition of the zero order spectrum (diagram IIIa) which is shown in diagram IV. Use of this form of representation in the initial stages of spectral analysis is the key to obtaining a spectrum from which assignments can be made. There are two reasons why this is so:-

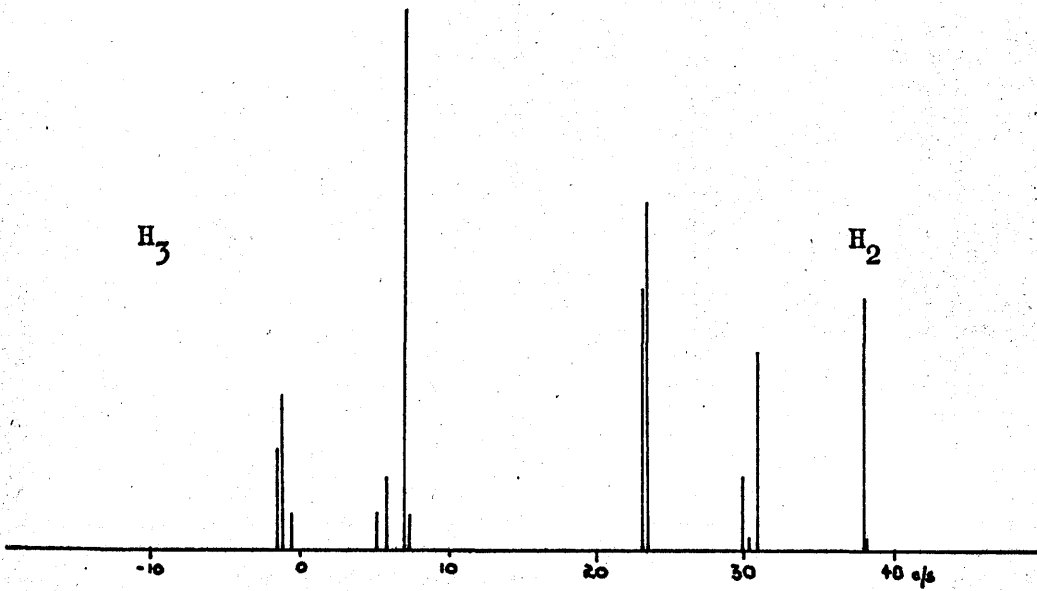
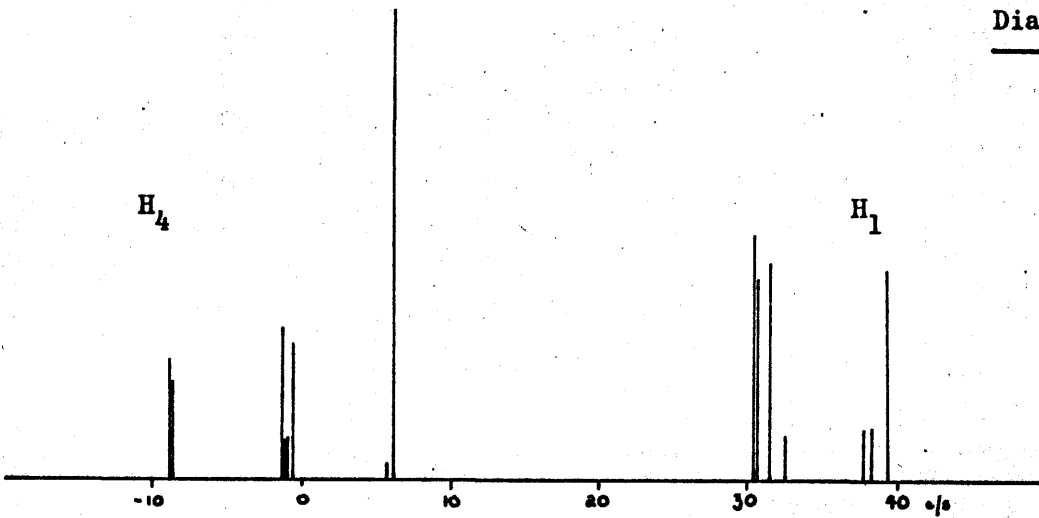
(1) Three quarters of the total intensity of the spectrum results from transitions involving only one nucleus.

(2) A small increase or decrease in a chemical shift causes a corresponding increase or decrease in the frequency of the resonances due to that particular chemical shift, resonances due to the remaining protons being unaltered. Changes in intensities resulting from small increments in the chemical shifts are relatively small.

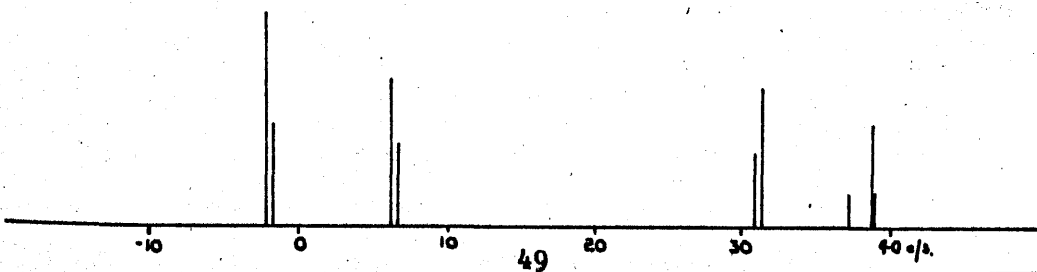
By drawing the components of the spectrum on transparent paper and examining the spectrum which results by various superpositions of the components, it is possible to proceed directly from the zero order spectrum to one which very much resembles the first order spectrum. By expressing this spectrum in terms of its components, as in diagram V, it is possible to derive assignments of the eight starred transitions of the theoretical spectrum. These eight transitions are the two lowest and two highest transitions of the low field and high

Chapter 4.11

Diagram IV

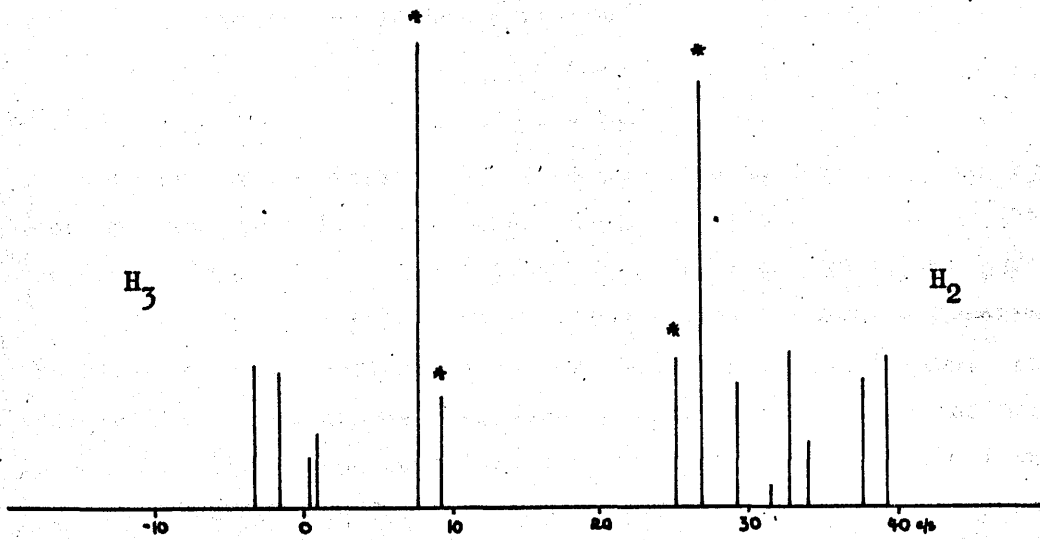
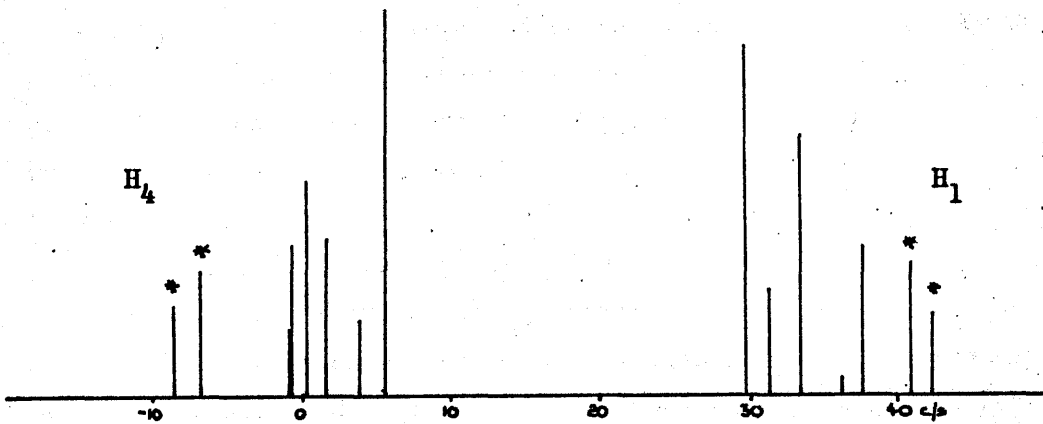


Combination Transitions

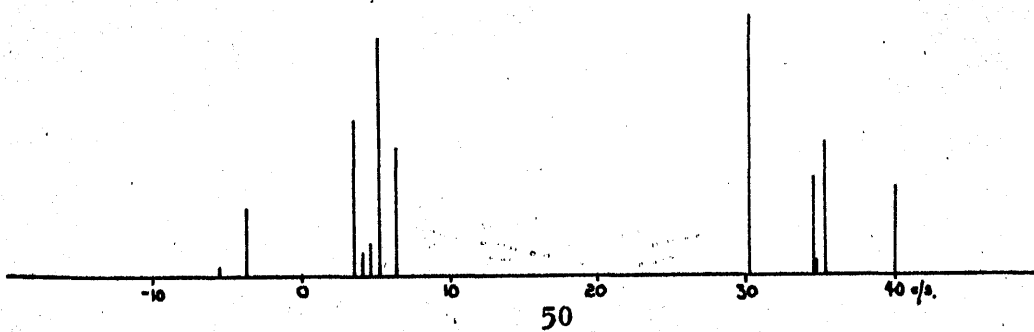


Chapter 4.11

Diagram V



Combination Transitions



field parts of the spectrum. A general rule in the analysis of complex spectra appears in making these assignments. This is that the transitions of the theoretical spectrum which can most easily be assigned are usually the outer transitions of any multiplet. From diagram V it can be seen that two transitions belonging to each nucleus have been assigned. The small splitting between each pair of lines is determined largely by the magnitude of the meta coupling constants.

By carrying out a few cycles of refinement based upon the assignment of these eight transitions, fairly accurate values for the two meta coupling constants and improved values for the four chemical shifts were obtained. Examination of the components of the refined spectrum enabled several more transitions to be assigned and so the refinement process could be initiated.

Refinement

Progress of the refinement of spectral parameters is shown by the contents of Table 1. After two iterations it became obvious that representation of the spectrum by sharp lines was no longer sufficient as many of the absorption peaks of the observed spectrum appeared to be closely spaced multiplets rather than single transitions. The theoretical spectrum was therefore recalculated with the inclusion of a suitable line-shape function, allowance being made in the final two cycles of refinement for superimposition of the resonances. The refined theoretical spectrum is shown in diagram II, theoretical and observed transition energies being compared in Table 2.

Table 1 : Chapter 4.11

 Refinement of Spectral Parameters

| | Iteration | | | | | | |
|----------|-----------|-------|--------------|-------|-------|-------|-------|
| | 0 | 1 | 2 | 3 | 4 | 5 | 6 |
| H_1 | 32.80 | 32.83 | 32.84 | 32.80 | 32.77 | 32.72 | 32.68 |
| H_2 | 32.80 | 32.83 | 32.86 | 32.90 | 32.95 | 32.98 | 33.00 |
| H_3 | 1.78 | 1.79 | 1.81 | 1.81 | 1.82 | 1.82 | 1.82 |
| H_4 | 1.78 | 1.76 | 1.74 | 1.70 | 1.67 | 1.60 | 1.56 |
| J_{12} | 1.50 | 1.47 | 1.46 | 1.46 | 1.46 | 1.47 | 1.47 |
| J_{13} | 8.20 | 8.21 | 8.25 | 8.30 | 8.33 | 8.41 | 8.48 |
| J_{14} | 0.30 | 0.29 | 0.28 | 0.34 | 0.41 | 0.38 | 0.36 |
| J_{23} | 7.50 | 7.36 | 7.28 | 7.26 | 7.24 | 7.19 | 7.16 |
| J_{24} | 8.20 | 8.09 | 8.05 | 7.99 | 7.94 | 7.88 | 7.84 |
| J_{34} | 2.10 | 2.09 | 2.09 | 2.10 | 2.10 | 2.12 | 2.12 |
| R | 1.91 | 1.63 | 1.56 1.13 | 1.03 | 0.98 | - | - |

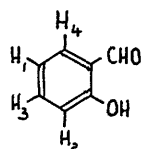
| <u>E(calc)</u> | <u>E(obs)</u> | <u>E(calc)</u> | <u>E(obs)</u> |
|----------------|---------------|----------------|---------------|
| <u>c/s</u> | <u>c/s</u> | <u>c/s</u> | <u>c/s</u> |
| -8.0 | -8.0 | 26.9 | 26.9 |
| -5.8 | -6.0 | 27.8 | |
| -4.0 | -4.0 | 28.5 | 28.4 |
| | | 28.6 | |
| | | 28.9 | |
| -1.8 | -1.5 | 32.6 | |
| -1.5 | | 33.4 | 33.0 |
| -0.6 | -0.5 | 33.9 | 34.0 |
| 0.0 | 0.0 | 34.3 | 34.7 |
| 0.7 | 0.8 | 34.8 | |
| 1.4 | | | |
| | | 36.5 | |
| 2.4 | | 36.8 | 36.5 |
| 3.2 | | | |
| 3.3 | 2.8 | 38.5 | |
| 3.4 | | 38.8 | 38.1 |
| | | | |
| 4.7 | | 40.4 | 40.7 |
| 5.7 | 4.9 | | |
| 6.0 | 6.0 | 42.1 | 41.9 |
| | | | |
| 7.9 | 8.4 | | |
| | | | |
| 10.2 | 10.3 | | |
| | | | |
| 25.2 | 25.4 | | |

TABLE 2

Comparison of observed and calculated transition energies of the sixth order spectrum.

Discussion of observed and calculated spectra

As can be seen from Table 2 and from diagrams I and II, agreement between observed and theoretical spectra is rather good. Differences in relative intensities of the various transitions are small and certainly not appreciably greater than between different observed spectra. Limits to the accuracy of refinement are undoubtedly controlled by instrumental resolution and reproducibility of the detection system. The set of spectral parameters derived by analysis of the spectrum is as follows:-

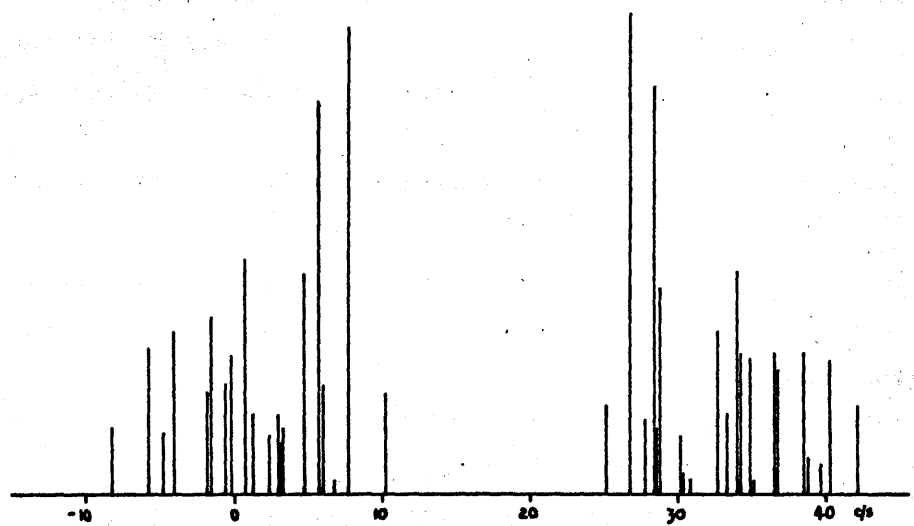


| | c/s. | | c/s. | |
|-------|---------|----------|--------|--|
| H_1 | = 32.68 | J_{12} | = 1.47 | Chemical shifts measured with respect to an arbitrary origin at = 2.65 |
| H_2 | = 33.00 | J_{13} | = 8.48 | |
| H_3 | = 1.82 | J_{14} | = 0.36 | |
| H_4 | = 1.56 | J_{23} | = 7.16 | |
| | | J_{24} | = 7.84 | |
| | | J_{34} | = 2.12 | |

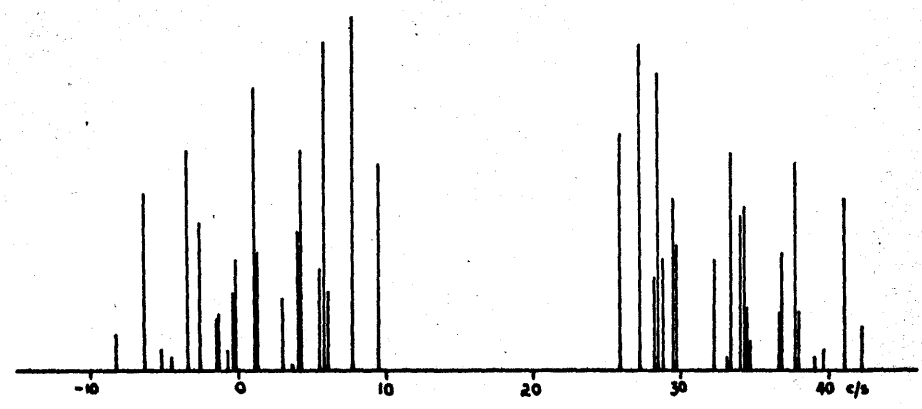
Signs of coupling constants: It is notable that we have assumed all coupling constants to be of the same sign in the analysis. In fact some investigations were carried out to determine the relative signs of the coupling constants. A change of sign of any one ortho coupling constant with respect to the sign of the other two was found to lead to serious deviations between theoretical and observed spectra both in transition energies and intensities. It was therefore concluded that all ortho coupling constants must be of the same sign. These coupling constants could therefore have the same sign as, or different sign from, the meta coupling constants. A spectrum was calculated based upon the refined parameters but with the meta coupling constants given a negative sign. This is compared with the refined spectrum in diagram VI. The transition energies in each spectrum are seen to agree fairly well but relative intensities in the spectrum with negative meta coupling constants are not consistent with those in the observed spectrum. This result was also found in trial calculations with meta coupling constants of different sign. From these calculations it would appear that ortho and meta coupling constants must be of the same sign. No sign was assumed for the

DIAGRAM VI

SPECTRUM WITH J_m POSITIVE



SPECTRUM WITH J_m NEGATIVE

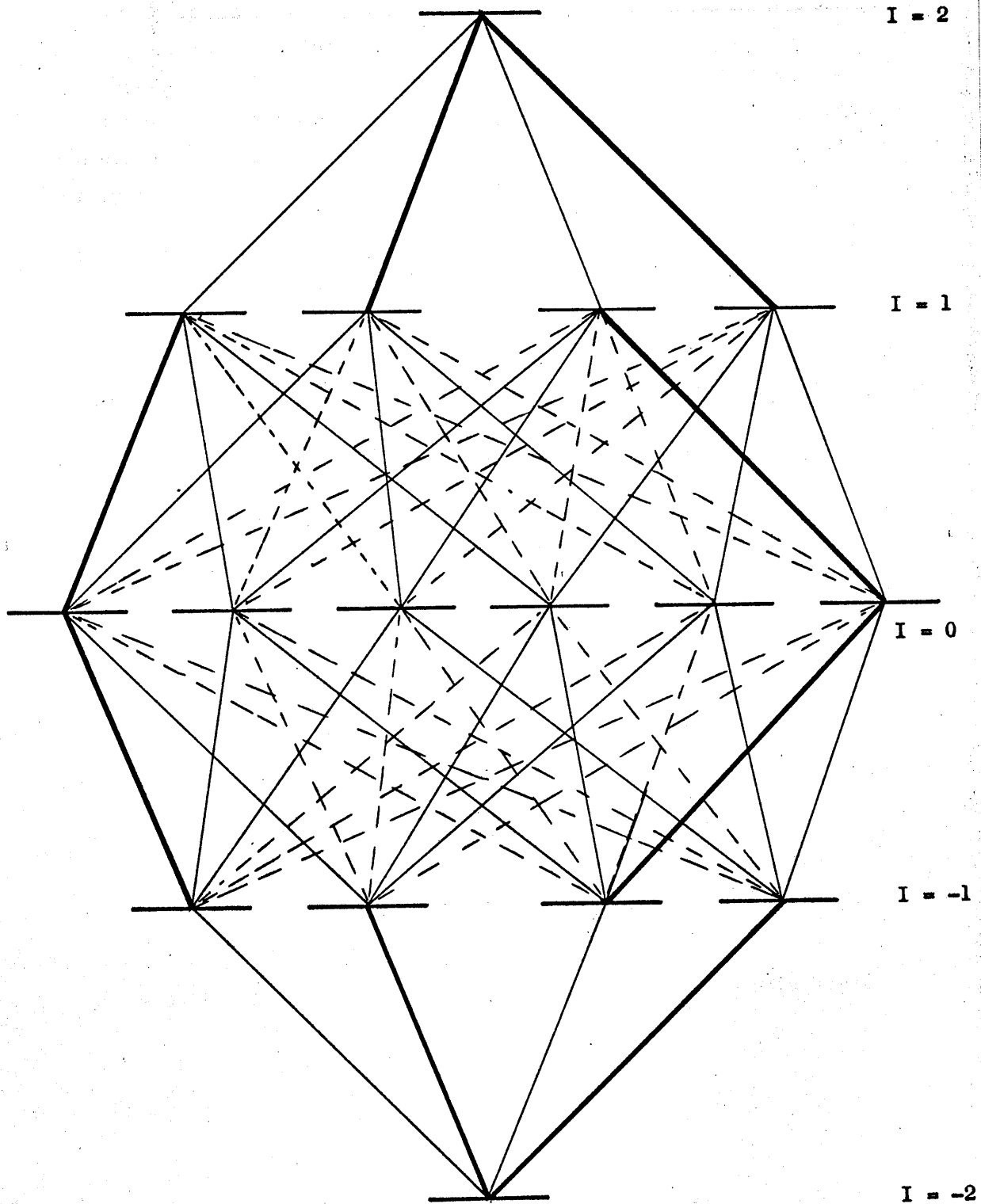


para coupling constant, this being determined by the refinement process itself, the positive sign being most consistent with the signs of the other parameters. All coupling constants were therefore found to be of the same sign, although the absolute value of the sign could not be derived from the spectrum which is invariant to a simultaneous change in sign of all of the coupling constants.

Comparison with the Reilly-Swalen Method of Spectral Analysis.

The most important step in the analysis of the spectrum of salicylaldehyde is undoubtedly not the use of the programmes to refine the calculated spectra, but their use in enabling us to obtain a theoretical spectrum from which assignments can be made. There would seem to be no equivalent step in the Reilly-Swalen method. Diagram VII illustrates the energy level diagram for a four spin system. The transitions represented by solid lines belong to one particular chemical shift term, in the sense that we have previously discussed, the hatched lines belonging to combination transitions. The eight pronounced solid lines in the diagram correspond to the eight transitions upon which we based our initial refinement of the zero order spectrum. It can be seen that these eight transitions alone are insufficient to enable frequency sum rules to be used to initiate refinement.

Diagram VII



Energy level diagram for a four spin system.

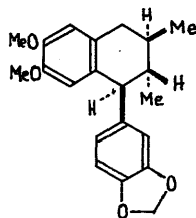
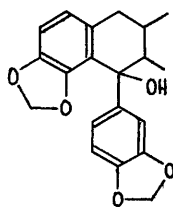
Apart from the examples used to demonstrate the operation of the method, the programmes have been used to solve spectral analysis problems encountered by other workers in the department. So far, the results of two of these investigations have been published:-

- (1) "Lignans of *Myristica otoba*. The Structures of Hydroxy-otobain and Iso-otobain".

by R. Wallace, A.L. Porte, and R. Hodges.

J. Chem. Soc., 1963, 1445.

In this paper, the author's programmes aided the analysis of the P.M.R. spectra of the degradation products of certain naturally occurring molecules, this analysis being in part used to determine the following molecular structures:-

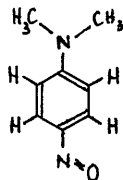


- (2) "Internal Rotation in *p*-nitrosodimethylaniline"

by D. D. MacNicol, R. Wallace, and J. C. D. Brand.

Trans. Faraday Soc., to be published late 1964 or early 1965.

At room temperature, the aromatic protons of *p*-nitrosodimethylaniline



give rise to an A_2X_2 spectrum. At low temperature, the torsion of the NO group is hindered, which removes the magnetic equivalence of

the two protons ortho to the nitroso group. This causes the A_2X_2 spectrum to become an A_2IX spectrum.

The Interpretation of Chemical Shift and
Spin-spin Coupling Constant Parameters
in Terms of Molecular Electronic Structure.

Chapter 5

In the previous chapters the application of the subject of high resolution N.M.R. spectroscopy to the determination of molecular structure has been discussed in some detail. In this application, the subject has been shown to depend upon the use of a vast collection of empirical chemical shift and spin-spin coupling constant data.

To attempt any form of non-empirical interpretation of these magnetic parameters, it is necessary to relate the magnitude of the parameters to the electronic structure of molecules for it is largely this which determines their magnitude. If such an interpretation can be carried out, the results of the non-empirical interpretation of N.M.R. spectra can be compared with similar information derived from other physical and chemical techniques, the sum total of experimental information forming the basis for our chemical concepts. The interpretation of the chemical shift and spin-spin coupling constant parameters will therefore be considered next, so that we might then discuss the interpretation of high resolution N.M.R. spectra from a more fundamental point of view.

Ramsey²⁰ was first to give a complete theory of the chemical shift in molecules. Given a diamagnetic molecule containing N nuclear moments and n electrons, its Hamiltonian in the presence of an applied magnetic field H_0 can be written:-

$$\mathcal{H} - V = \frac{1}{2m} \sum_{k=1}^n \left(p_k + \frac{e}{c} A_k^0 + \frac{e}{c} \sum_{q=1}^N A_k^q \right)^2 \quad (5.2.1)$$

in which e = electronic charge
 c = the velocity of light
 p = the electron linear momentum operator
 m = the electronic mass

In this formula $A_k^0 = \frac{1}{2}(H_0 \wedge r_k)$ is the value, at the position r_k of the k^{th} electron, of the vector potential of the external field H_0 ;

$$A_k^q = (\mu_q \wedge r_{qk}) / r_{qk}^3$$

is the value, at the same point, of the vector potential produced by the nuclear moment μ_q situated at r_q . The origin of the vectors r_k r_q is left unspecified. For an isolated atom it is natural to choose for origin the nucleus of that atom. Clearly all physical results must be independent of the choice of origin, this being a consequence of the general principle of gauge invariance in electromagnetism. In a molecule it may be convenient to select as origin the particular nucleus $\mu_q = \mu$ for which the frequency shift is being calculated. V is the electrostatic energy of the system. For brevity we have omitted the magnetic couplings between the electrons, since they are irrelevant to the problem, and we have also omitted the Zeeman couplings of the nuclei with the applied field H_0 and their dipolar couplings. The expansion of (5.2.1) is shown on the next page. T is the kinetic energy of the electrons and D is their diamagnetic energy. These terms play no part in what follows.

$$\begin{aligned}
\mathcal{H} - v &= \frac{1}{2m} \sum_k p_k^2 && = T \\
&+ \frac{e^2}{2mc^2} \sum_k (A_k^0)^2 && + D \\
&+ \frac{e^2}{2mc^2} \sum_k \sum_{q \neq k} A_k^q \cdot A_q^k && + O_3 \\
&+ \frac{e}{2mc} \sum_k (p_k \cdot A_k^0 + A_k^0 \cdot p_k) && + Z_L \\
&+ \frac{e}{2mc} \sum_k \sum_q (p_k \cdot A_k^q + A_k^q \cdot p_k) && + O_1 \\
&+ \frac{e^2}{2mc^2} \sum_k \sum_q (A_k^0 \cdot A_q^k + A_k^q \cdot A_k^0) && + O_2
\end{aligned}
\tag{5.2.5}$$

$$Z_L = \frac{e}{2mc} \sum_k (p_k \cdot A_k^0 + A_k^0 \cdot p_k) = \beta H_0 \cdot L \quad (5.2.2)$$

is the orbital Zeeman energy of the electrons. O_1 is the magnetic coupling between the n electrons and the N nuclei.

$$O_1 = 2\beta \sum_k \sum_q \frac{\mu_k \cdot l_{qk}}{r_{qk}^3} \quad \text{with } l_{qk} = r_{qk} \wedge p_k \quad (5.2.3)$$

O_2 and O_3 are particularly interesting. The first is bilinear with respect to H_0 and μ_q and the second bilinear in μ_q and μ_q' .

$$O_2 = \frac{e}{2mc} \sum_k \sum_q (H_0 \wedge r_{qk}) \cdot (\mu_q \wedge r_{qk}) / r_{qk}^3 \quad (5.2.4)$$

The term O_2 represents the coupling between the nuclear moments and the magnetic field induced by "Larmor precession" of the electrons in the applied field H_0 . The term O_3 is given by

$$O_3 = \frac{e^2}{2mc} \sum_k \sum_{q,q'} \frac{(\mu_q \wedge r_{qk}) \cdot (\mu_{q'} \wedge r_{q'k})}{r_{qk}^3 r_{q'k}^3} \quad (5.2.6)$$

The chemical shift (and also the indirect interactions) correspond to small modifications of the energy of the system and are calculated by perturbation theory. Furthermore the smallness of the chemical shift is such that it is usually unobservable except in liquid or gaseous samples in which the molecules rotate rapidly. Without specifying how this rotation should be described, we shall represent the ground state of the molecule by the symbol $|0\lambda\rangle$, where λ refers to the orientation of the molecule and $|0\rangle$ to its other degrees of freedom (electronic and possibly vibrational states). In a diamagnetic substance the only terms of the Hamiltonian other than $V, T,$ and D for which the expectation value $\langle 0 | \dots | 0 \rangle$ does not vanish are O_2 and O_3 . The former, bilinear in μ_q and H_0 , clearly provides a contribution to the chemical shift. If we select as origin that particular nucleus for which the shift is being calculated so that r_{ok} becomes just r_k , the first order change in energy is

$$\langle 0_2 \rangle = \frac{e^2}{2mc^2} \langle 0\lambda | \sum_{\mathbf{k}} \frac{(\mathbf{H}^0 \wedge \mathbf{r}_{\mathbf{k}}) \cdot (\boldsymbol{\mu} \wedge \mathbf{r}_{\mathbf{k}})}{r_{\mathbf{k}}^3} | 0\lambda \rangle \quad (5.2.7)$$

This expression can be rewritten as $\langle 0_2 \rangle = \boldsymbol{\mu} \cdot \overline{\frac{\mathbf{H}}{d}} \cdot \mathbf{H}^0$. (The subscript d stands for diamagnetic.) In this expression the tensor $\overline{\frac{\mathbf{H}}{d}}$ can be decomposed into a traceless part $\overline{\frac{\mathbf{H}}{d}}'$ with

$$\overline{\frac{\mathbf{H}}{d}}' = \frac{e^2}{2mc^2} \langle 0\lambda | \sum_{\mathbf{k}} \frac{x_{\mathbf{k}}^p x_{\mathbf{k}}^q}{r_{\mathbf{k}}^3} - \frac{1}{3} \frac{\delta^{pq}}{r_{\mathbf{k}}} | 0\lambda \rangle \quad (5.2.8)$$

and a scalar part $\overline{\frac{\mathbf{H}}{d}}''$ given by $\overline{\frac{\mathbf{H}}{d}}'' = \sigma_d \delta^{pq}$ in which

$$\sigma_d = \frac{e^2}{3mc^2} \langle 0\lambda | \sum_{\mathbf{k}} \frac{1}{r_{\mathbf{k}}} | 0\lambda \rangle \quad (5.2.9)$$

σ_d is independent of the rotational state of the molecule, which need not be specified, and can be written

$$\sigma_d = \frac{e^2}{3mc^2} \langle 0 | \sum_{\mathbf{k}} \frac{1}{r_{\mathbf{k}}} | 0 \rangle \quad (5.2.10)$$

For the traceless part $\overline{\frac{\mathbf{H}}{d}}'$, the average of its values over the various rotational states $|\lambda\rangle$ clearly vanishes, and in a liquid where the molecule passes very rapidly from one state $|\lambda\rangle$ to another, so that only the average over the states is observable, $\overline{\frac{\mathbf{H}}{d}}'$ makes no contribution to the chemical shift, and the change in the Zeeman energy of the nucleus is $\sigma_d \cdot \boldsymbol{\mu} \cdot \mathbf{H}^0$. In contrast to this, in molecular beam experiments where collisions are negligible and molecules are in well defined rotational states $|\lambda\rangle$, the effect of the anisotropic part $\overline{\frac{\mathbf{H}}{d}}'$ is observable. The constant σ_d is always positive, decreasing the applied field \mathbf{H}^0 AT THE NUCLEUS by an amount $\sigma_d \mathbf{H}^0$, whence its name of "diamagnetic shielding constant". A rough estimate of the order of magnitude of σ_d follows from the observation that $e^2/mc^2 = r_0$, the classical radius of the electron = $a_0/(137)^2$ where a_0 is the radius of the first Bohr orbit of the hydrogen atom. If one assumes that $\langle 0 | 1/r_{\mathbf{k}} | 0 \rangle$ is of the order of $1/a_0$, values of σ_d between 10^{-4} and 10^{-5} must be expected.

It is possible to obtain another energy expression Δ , bilinear in μ and H^0 , and thus contributing to the chemical shift, by combining, through second order perturbation theory, a term A of (5.2.5) proportional to μ with a term B proportional to H^0 . There is in fact only one such term

$$\Delta = \sum_n' \frac{(0|C_1|n)(n|Z_L|0)}{E_0 - E_n} \quad (5.2.11)$$

By defining the purely orbital operator

$$C = \frac{|n\rangle\langle n|}{E_0 - E_n} \quad (5.2.12)$$

Δ can then be expressed as follows

$$\Delta = 2\beta^2 \sum_k (0\lambda|(L.H^0)C\left(\frac{\mu \cdot \mathbf{1}_k}{r_k^3}\right)|0\lambda) \quad (5.2.13)$$

This can also be rewritten as a tensor coupling $\mu \cdot \overline{\overline{H}} \cdot H^0$ (the subscript p standing for paramagnetic) with a traceless part

$$\overline{\overline{H}}_{\overline{p}}^{mn} = 2\beta^2 \sum_k (0\lambda|L^m C \frac{\mathbf{1}_k^n}{r_k^3} - \frac{1}{3} \frac{L \cdot \mathbf{1}_k}{r_k^3}|0\lambda) \quad (5.2.14)$$

and a scalar part $\overline{\overline{H}}_{\overline{p}}^{nn} = \sigma_p \delta_{mn}$, where

$$\sigma_p = \frac{2\beta^2}{3} \sum_k (0|\frac{L \cdot C \mathbf{1}_k + \mathbf{1}_k \cdot C L}{r_k^3}|0) \quad (5.2.15)$$

The index λ is omitted in (5.2.15) because the scalar

$$[(L \cdot C \mathbf{1}_k) + (\mathbf{1}_k \cdot C L)] / r_k^3$$

is independent of it. In the same way as for the diamagnetic correction, the contribution of the anisotropic part to the frequency shift vanishes in a liquid.

The calculation of the paramagnetic shielding constant σ_p is far more difficult than that of σ_d for it requires, through the operator C , the knowledge of the excited states of the molecule.

Both σ_d and σ_p depend upon the origin chosen for the vectors r_k in the expression $\frac{1}{2}(\mathbf{H} \wedge \mathbf{r}_k)$ of the vector potential A_k^0 , whilst their sum, $\sigma = \sigma_d + \sigma_p$, which is a measurable quantity, is naturally independent of it. The magnetic shielding constant is related to the chemical shift as described in chapter 1.

Theory of The Spin-Spin Coupling Constant 5.3

The Hamiltonian (5.2.5) contains a term bilinear with respect to the nuclear moments of the molecule, namely the term O_3 , the corresponding nuclear coupling being simply $\langle O_3 \rangle = (\psi_0 | O_3 | \psi_0)$, where ψ_0 is the wavefunction of the ground state of the molecule. Although a first order term, $\langle O_3 \rangle$ is very small. This is essentially because O_3 is a sum of one electron operators:-

$$\frac{(\mu_A \wedge r_{Ak}) \cdot (\mu_B \wedge r_{Bk})}{r_{Ak}^3 r_{Bk}^3}$$

so that when the first factor $(\mu_A \wedge r_{Ak}) / r_{Ak}^3$ is relatively large, the electron k being near the nuclear moment μ_A , the second one is necessarily small. Besides the first order term $\langle O_3 \rangle$, other contributions to the spin-spin coupling may be obtained from second order perturbation theory. There is only one second order term, $(\psi_0 | O_2 C O_2 | \psi_0)$ where C is the operator (5.2.12). Just as was the case with σ_p , this term also depends upon a knowledge of the excited states of the molecule.

A mechanism of spin-spin coupling other than the orbital mechanism which we have just described has been put forward by Ramsey and Purcell.²³ This mechanism depends upon polarization of the electron spins of the diamagnetic molecule by the nuclear spin moments. Because of unequal polarization due to different orientations of the nuclear and electronic spins, a hyperfine magnetic field due to the electrons is thought to exist at the nuclear site. Contributions to nuclear spin-spin coupling arising from this mechanism are expected to be much greater than from the orbital coupling.

Calculation of Chemical Shifts
and Spin-spin Coupling Constants 5.4

Although the theory underlying the calculation of chemical shift and spin-spin coupling constant parameters is well understood, the actual calculation of these parameters pre-supposes a knowledge of both the ground state and excited state electronic wavefunctions of the molecule. In the majority of cases, our knowledge of ground state electronic wavefunctions is somewhat scanty, and that of the excited state wavefunctions is almost non-existent, so that values calculated for chemical shifts and spin-spin coupling constants have, at best, a considerable degree of error.

The appearance in the theory of excited state electronic wavefunctions arises as a result of formulating the theory in terms of Rayleigh-Schrodinger perturbation theory. This complex form of expression has been circumvented by employing variational perturbation theory although sometimes this amounts to little more than selecting one particular excited state wavefunction as the variational perturbation. This can only be justified if the perturbation takes a particularly simple form.

Although the direct calculation of chemical shifts and spin-spin coupling constants is, in all but the simplest cases, extremely difficult, the amount of knowledge which has accumulated as a result of such calculations is extremely great. In particular, a good understanding of the relative importance of the various factors contributing to the chemical shift and coupling constant parameters has been developed. The present state of the methods of calculating chemical shifts and spin-spin coupling constants is clearly illustrated in two recent papers by Pople²⁴ and by Pople and Santry.²⁵ In the next chapter we shall be concerned with the calculation of the chemical shift parameter in the hydrogen and hydrogen deuteride molecules.

**Effects of Isotopic Substitution on the
Magnetic Shielding Constants of Nuclei:**

Contribution of Nuclear Quadrupole Coupling.

Chapter 6

It has been shown²⁶ that, when the group $-\text{CH}_2-$ in certain organic molecules is replaced by $-\text{CHD}-$, then the chemical shift of the proton within the group is moved upfield by a few parts per million. This increase in chemical shift must result from a small increase in the magnetic shielding constant of the proton. It has been suggested²⁷ that the primary cause of this increase is the different vibrational amplitude of the D and H atoms in the molecule.

Gutowsky²⁷ has also pointed out that the effects of the quadrupolar interaction of the deuteron might be partly responsible for the observed change in shielding constant. In this chapter we shall investigate, in a simple way, the contributions of various effects, including quadrupolar coupling, to the observed changes in magnetic shielding constants.

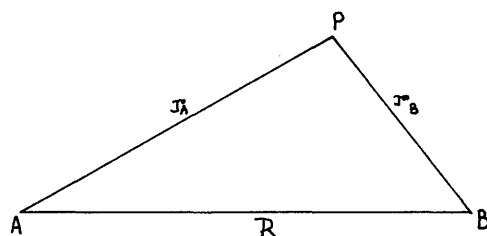
If quadrupolar coupling of the deuteron is important in causing the observed change in shielding constant, then it should have greatest effect in a molecule in which the deuteron is directly bonded to the hydrogen atom as in hydrogen deuteride, rather than in one in which it is one bond removed, as in the $-\text{CHD}-$ group of an organic molecule. For simplicity and convenience, our attention will therefore be restricted to the molecules H_2 and HD.

We shall relate the difference between the proton magnetic shielding constants in these molecules to a change in the orbital exponent of the hydrogen atom electronic wavefunctions. From this change we shall compute, in an approximate way, the resulting change in the electronic energy of the molecule. The quadrupolar interaction of the deuteron will then be shown to contribute insignificantly to this change in electronic energy, contributions due to the different vibrational energies of H_2 and HD being shown to be sufficient to cause the calculated change.

The conclusions drawn from these calculations will be extended to explain changes in the magnetic shielding constants of protons resulting from isotopic substitution in larger molecules.

Differences in Magnetic Shielding
 Constants of the Protons in H_2 and HD 6.2

The nomenclature used to describe the hydrogen and hydrogen deuteride molecules can be understood by making reference to the following diagram:-



A and B are the sites of the nuclei.

R represents the internuclear distance.

r_A and r_B are the position vectors of the electron with position P.

As described in chapter 5.2, the magnetic shielding constant of nucleus A or B is given by

$$\sigma = \sigma_d + \sigma_p$$

Now, from equation (5.2.10), we see that σ_d is proportional to $\langle \frac{1}{r} \rangle$ for the electrons, whereas σ_p is proportional to $\langle \frac{1}{r^3} \rangle$. It follows that σ_d for, say, nucleus A, must be much more susceptible to small changes in electronic environment which occur at some distance from nucleus A than will σ_p .

In the hydrogen deuteride molecule, if nucleus B is regarded as being the deuteron, then the nuclear quadrupole- electron interaction, which is dependent upon $\langle 1/r_B^3 \rangle$, will cause only a small perturbation of the electrons in the vicinity of nucleus B. The effects of this perturbation upon $\langle 1/r_A^3 \rangle$ will be much smaller than upon $\langle 1/r_A \rangle$. To a good degree of approximation the quadrupolar interaction of the deuteron is therefore expected to cause a change primarily in the diamagnetic shielding constant, σ_d , of the proton. In what follows we shall restrict our calculations to those of σ_d .

Re-stating equation (5.2.10), we have:-

$$\sigma_d = \frac{e^2}{3mc^2} \left(0 \left| \sum \frac{1}{r_{Ai}} \right| 0 \right) \quad (6.2.1)$$

Choosing as ground state electronic wavefunction the antisymmetrized Slater function:-

$$|0\rangle = \frac{1}{(2)^{\frac{1}{2}}} \begin{vmatrix} \varphi(1)\alpha(1) & \varphi(2)\alpha(2) \\ \varphi(1)\beta(1) & \varphi(2)\beta(2) \end{vmatrix} \quad (6.2.2)$$

and regarding the two molecular electrons as being equivalent, σ_d can be expressed:-

$$\sigma_d = \frac{2e^2}{3mc^2} \left(\varphi_1 \left| \frac{1}{r_{A1}} \right| \varphi_1 \right) = 3.55 \times 10^{-5} \left(\varphi_1 \left| \frac{1}{r_{A1}} \right| \varphi_1 \right) \quad (6.2.3)$$

Choosing φ_1 to have the simple form:-

$$\varphi_1 = N_1 \left(e^{-kr_{A1}} + e^{-kr_{B1}} \right)$$

the matrix element $\left(\varphi_1 \left| \frac{1}{r_{A1}} \right| \varphi_1 \right)$ can be evaluated by use of spheroidal co-ordinates. Its value is given by:-

$$\left(\varphi_1 \left| \frac{1}{r_{A1}} \right| \varphi_1 \right) = \frac{k(1 + kR) \left[2e^{-kR} - \frac{1}{kR} (1 - e^{-2kR}) \right]}{2 \left[1 + e^{-kR} \left\{ 1 + kR + \frac{(kR)^2}{3} \right\} \right]} \quad (6.2.4)$$

A small increment Δd in d will give rise to a small increment in the matrix element, given by:-

$$\Delta \left(\varphi_1 \left| \frac{1}{r_{A1}} \right| \varphi_1 \right) = \frac{\Delta \sigma_d}{3.55 \times 10^{-5}} \quad (6.2.5)$$

Wimmett²⁸ has measured the differences in shielding constant between the deuterium molecule and the hydrogen molecule, and between the deuterium molecule and hydrogen deuteride. The observed differences are as follows:-

$$\sigma_{D_2} - \sigma_{H_2} = 0.7 \times 10^{-7}$$

$$\sigma_{D_2} - \sigma_{HD} = 0.5 \times 10^{-7}$$

From these measurements we obtain:-

$$\Delta\sigma_{H_2 \rightarrow HD} = \sigma_{HD} - \sigma_{H_2} = 0.2 \times 10^{-7}$$

Using this value for $\Delta\sigma_a$, it follows from equation (6.2.5) that

$$\left(\varphi_1 \left| \frac{1}{r_{Al}} \right| \varphi_1\right) = 0.00056 \text{ (a.u.)}^{-1}$$

We conclude from this calculation that the effect which causes the increase in magnetic shielding constant in going from H_2 to HD must increase the matrix element by the amount calculated. From equation (6.2.4) we see that this increase in the matrix element could arise from a change in R or a change in k. We shall examine each of these possibilities in turn.

Effect of a Small Variation in R upon $(\varphi_1 | \frac{1}{r_{A1}} | \varphi_1)$ 6.3

The equilibrium internuclear distance in H_2 and in HD are given by:-

$$H_2 \quad R_e = 0.7414 \text{ \AA} = 1.4015 \text{ a.u.}$$

$$HD \quad R_e = 0.7415 \text{ \AA} = 1.4017 \text{ a.u.}$$

With the orbital exponent k equal to 1.2350³⁰, we calculate that:-

$$(\varphi_1 | \frac{1}{r_{A1}} | \varphi_1) (R_e = 1.4015 \text{ a.u.}) = 0.9280 \text{ (a.u.)}^{-1}$$

$$(\varphi_1 | \frac{1}{r_{A1}} | \varphi_1) (R_e = 1.4017 \text{ a.u.}) = 0.9280 \text{ (a.u.)}^{-1}$$

It can be seen that the small difference in internuclear distance between H_2 and HD cannot be responsible for the observed difference in proton magnetic shielding constant. Marshall and Pople³¹ come to the same conclusion regarding the variation of σ with internuclear distance.

Effect of a Small Variation in k upon $(\varphi_1 | \frac{1}{r_{A1}} | \varphi_1)$ 6.4

Assuming $R_e = 1.4015$ a.u., a small increase in k results in the following increase in the matrix element:-

| k | $(\varphi_1 \frac{1}{r_{A1}} \varphi_1)$ |
|---------|--|
| 1.23500 | 0.92802 |
| 1.23550 | 0.92830 |

For the required increase in the matrix element of $0.00056(\text{a.u.})^{-1}$, k must increase by 0.001.

An increase in k by this amount will cause a change in the electronic energy of the molecule. Neglecting electron-electron repulsion terms, the increase in the electronic energy of the molecule resulting from an increase in k of 0.001 is calculated to be -4×10^{-4} a.u.

From these very simple calculations we conclude that the effect which leads to the observed difference in magnetic shielding constant between H_2 and HD must perturb the electronic energy by about 10^{-4} a.u.

Perturbation of the Electronic Energy
Caused by Nuclear Quadrupole Coupling. 6.5

The theory of the interaction between the nuclear quadrupole moment and the molecular electric field will be discussed in section 2.

For a nucleus with spin $I = 1$, such as the deuteron, interaction between the quadrupole moment of the deuteron and the molecular electric field leads to two nuclear quadrupolar energy levels given by

$$E_1 = \frac{e^2 q Q}{4} \qquad E_0 = -\frac{e^2 q Q}{2}$$

Ramsey et al. have measured the quadrupolar coupling constant of the deuteron in HD and report the value:-

$$\frac{e^2 q Q}{2h} = -22,454 \pm 6 \text{ c/s}$$

It follows that $E_0 = 3.34 \times 10^{-15} \text{ a.u.}$

$$E_1 = -1.67 \times 10^{-15} \text{ a.u.}$$

The magnitude of the nucleus-electron electrostatic interaction energy must therefore be perturbed by approximately 10^{-15} a.u. by quadrupolar coupling of the deuteron. This is much smaller than the 10^{-4} a.u. perturbation which we calculated necessary to account for the observed difference between the magnetic shielding constant of the proton in H_2 and that in HD.

Although this result seems to constitute the answer to the problem which we set out to solve, it is of interest to examine the validity of our approach by calculating the difference in the vibrational perturbation of the electronic energy of the hydrogen and hydrogen deuteride molecules.

The Vibrational Ground State Energy Levels of H₂ and HD 6.6

According to Herzberg³⁵, the ground state vibrational energy levels of the hydrogen and hydrogen deuteride molecules are given by:-

$$G\left(\frac{1}{2}\right)_{\text{H}_2} = 2170 \text{ cm}^{-1}$$

$$G\left(\frac{1}{2}\right)_{\text{HD}} = 1884 \text{ cm}^{-1}$$

The energy difference between these levels is

$$E = G\left(\frac{1}{2}\right)_{\text{HD}} - G\left(\frac{1}{2}\right)_{\text{H}_2} = -286 \text{ cm}^{-1} = -13 \times 10^{-4} \text{ a.u.}$$

which is of the same order of magnitude as the -4×10^{-4} a.u. difference in electronic energy which we calculated necessary to account for the difference in the magnetic shielding constant of the proton. It follows that the difference in the vibrational perturbation energy of the hydrogen and hydrogen deuteride molecules is sufficient to account for the difference in the magnetic shielding constant.³⁴

In accounting for the difference in the proton chemical shift in the hydrogen and hydrogen deuteride molecules, we have shown that the contribution to this difference arising from nuclear quadrupolar coupling is insignificant with respect to that arising from vibrational perturbation of the electronic energy.

In organic molecules in which the perturbing influence of the deuteron upon the electronic environment of the proton is less than than in hydrogen deuteride, isotopic displacement of the proton chemical shift due to deuteron quadrupolar coupling must certainly be insignificant with respect to that caused by vibrational perturbation of the electrons.

Most of the research which we have so far described was carried out during the author's first fifteen months of research. Towards the end of this initial period, the seriousness of the difficulties encountered in the non-empirical interpretation of chemical shifts and spin-spin coupling constants had been fully realized. As the author's interests were centred mainly around the interpretation of the experimental parameters in terms of electronic structure, there seemed little to be gained by continuing a study N.M.R. spectra. In addition, the related field of N.Q.R. spectroscopy appeared to have greater potential as a tool for studying electronic environment. Of particular interest to us, was the possible application of the technique to problems in transition metal chemistry. The results of Mossbauer, microwave, electron spin resonance, and N.Q.R. measurements supported the idea.

With the help of a grant from the Royal Society and with the aid of departmental funds, it became possible to initiate research in N.Q.R. spectroscopy by building a spectrometer to observe resonances. The material presented in the second section of this thesis describes the progress which we have made in both practical and theoretical aspects of this subject.

Nuclear Quadrupole Resonance Spectroscopy

Section B

Nuclear quadrupole resonance, like nuclear magnetic resonance, is a branch of spectroscopy which provides information concerning electronic distribution in atoms and molecules. Unlike nuclear magnetic resonance spectroscopy, in which primary splitting of the nuclear spin levels is due to interaction of the nucleus with the externally applied magnetic field, the primary splitting of the nuclear levels due to nuclear quadrupolar interaction is due to the electrostatic field gradient set up by the electrons of the molecule. Splitting of the nuclear spin levels due to nuclear quadrupolar interaction is therefore much more sensitive to the electronic environment of the nucleus than is splitting due to nuclear magnetic interaction. By performing suitable experiments, three parameters related to the electronic environment of the nucleus may be derived from nuclear quadrupole resonance spectra. These are:-

- (a) The directions of the principal axes of the electrostatic field gradient tensor at the nuclear site.
- (b) The magnitude of the greatest component of this tensor.
- (c) The degree of asymmetry of the electrostatic field gradient at the nuclear site.

The interest of the chemist in nuclear quadrupole resonance spectroscopy is very much centred around the interpretation of these parameters in terms of molecular and electronic structure.

Before discussing the detection of nuclear quadrupole resonance and the interpretation of spectra we shall outline the theory of the interaction of the nuclear quadrupole moment with the atomic and molecular electric field in order to illustrate the experimental requirements of nuclear quadrupole resonance spectroscopy and the type of information we might expect to derive from such spectra.

Theory of The Nuclear Quadrupole-
Electron Interaction in Atoms. 2.1

If we describe the nucleus and electron cloud distribution in an atom as two charge distributions $\rho_n(\mathbf{r}_n)$ and $\rho_e(\mathbf{r}_e)$, their mutual electrostatic energy is given by

$$W_E = \iint \frac{\rho_n(\mathbf{r}_n) \rho_e(\mathbf{r}_e)}{|\mathbf{r}_n - \mathbf{r}_e|} d\mathbf{r}_n d\mathbf{r}_e \quad (2.1.1)$$

which can be expanded by means of the formula

$$\frac{1}{|\mathbf{r}_n - \mathbf{r}_e|} = 4\pi \sum_{l=0}^{\infty} \sum_{m=-l}^{+l} \frac{1}{2l+1} \cdot \frac{r_c^l}{r_c^{l+1}} Y_l^{m*}(\theta_n \varphi_n) Y_l^m(\theta_e \varphi_e) \quad (2.1.2)$$

to give the following expansion of (2.1.1):-

$$W_E = \iint 4\pi \sum_{l=0}^{\infty} \sum_{m=-l}^{+l} \frac{\rho_n(\mathbf{r}_n) \rho_e(\mathbf{r}_e)}{2l+1} \frac{r_c^l}{r_c^{l+1}} Y_l^{m*}(\theta_n \varphi_n) Y_l^m(\theta_e \varphi_e) d\mathbf{r}_n d\mathbf{r}_e$$

in which the symbols r_c and r_c mean that the larger of the two numbers r_e and r_n is in the denominator, and the smaller in the numerator. If the small penetration of the electron inside the nucleus is neglected, this contribution having negligible effect upon the interaction in any case, we may assume $r_e > r_n$ and write

$$W_E = \sum_{l=0}^{\infty} \sum_{m=-l}^{+l} \frac{4\pi}{2l+1} \left(\int \rho_n(\mathbf{r}_n) r_n^l Y_l^{m*}(\theta_n \varphi_n) d\mathbf{r}_n \right) \left(\int \rho_e(\mathbf{r}_e) r_e^{-(l+1)} Y_l^m(\theta_e \varphi_e) d\mathbf{r}_e \right)$$

Putting:-

$$\left. \begin{aligned} A_l^{m*} &= \frac{4\pi}{2l+1} \int \rho_n(\mathbf{r}_n) r_n^l Y_l^{m*}(\theta_n \varphi_n) d\mathbf{r}_n \\ B_l^m &= \frac{4\pi}{2l+1} \int \rho_e(\mathbf{r}_e) r_e^{-(l+1)} Y_l^m(\theta_e \varphi_e) d\mathbf{r}_e \end{aligned} \right\} \quad (2.1.3)$$

we have:-

$$W_E = \sum_{l=0}^{\infty} \sum_{m=-l}^{+l} A_l^{m*} B_l^m$$

We may transform to quantum mechanics simply by specifying $\rho_n(r_n)$ and $\rho_e(r_e)$ quantum mechanically. If the state of the nucleus is described by a wavefunction $\psi_n(R_1, R_2, \dots, R_A)$ of the coordinates of its A nucleons, the nuclear charge density can be written as the expectation value of the density of charge operator at the point r_n :-

$$\rho_n(r_n) = (\psi_n | \sum_{i=1}^A e_i \delta(r_n - R_i) | \psi_n) \quad (2.1.4)$$

where $e_i = e$ for a proton and zero for a neutron. From (2.1.3) and (2.1.4), A_l^m can be written as the expectation value $A_l^m = \langle \mathcal{A}_l^m \rangle$, in which the nuclear operator \mathcal{A}_l^m is defined by

$$= \frac{\sqrt{4\pi}}{\sqrt{2l+1}} \sum_{i=1}^A e_i R_i Y_l^m(\theta_i, \phi_i) \quad (2.1.5)$$

R_i, θ_i, ϕ_i being the polar coordinates of the A nucleons. Similarly B is the expectation value of the electron operator :-

$$\mathcal{B}_l^m = -e \frac{\sqrt{4\pi}}{\sqrt{2l+1}} \sum_{i=1}^N r_i^{-(l+1)} Y_l^m(\theta_i, \phi_i) \quad (2.1.6)$$

where r_i, θ_i, ϕ_i are the coordinates of the N electrons. The energy of electrostatic interaction between the electrons and the nucleus is then the expectation value of a Hamiltonian

$$\mathcal{H}_E = \sum_{l=0}^{\infty} \sum_{m=-l}^{+l} \mathcal{A}_l^{m*} \mathcal{B}_l^m \quad (2.1.7)$$

From the definitions (2.1.5) and (2.1.6), it is clear that the operators \mathcal{A}_l^m and \mathcal{B}_l^m transform under rotation of the coordinate axes in the same way as spherical harmonics of order l . The tensor operator \mathcal{A} with $2l+1$ components \mathcal{A}_l^m is called the multipole moment of order l of the nucleus. The quadrupole moment of a nucleus depends only upon the expectation value $A_l^m = \langle \mathcal{A}_l^m \rangle$ of the nuclear multipole operator over the wavefunction of the nuclear ground state, that is, l is a constant. Concerning the matrix elements of \mathcal{A}_l^m , odd values of l are forbidden if we assume, as seems well established experimentally, that stationary nuclear states have well defined parities.

Further information and limitation on the values of the matrix elements of the nuclear multipole operators results from their tensor character and is largely based upon the Wigner-Eckart theorem¹, which states that the set of matrix elements for any tensor operator differs from the set for any other tensor operator \mathcal{A}_l' only by a constant factor represented by the reduced matrix element $(\alpha J \| \mathcal{A}_l \| \alpha' J')$. More precisely, it can be shown that a matrix element such as $(\alpha' J' M' | \mathcal{A}_l^m | \alpha J M)$, where $M = J_z$, $M' = J'_z$, is equal to

$$(\alpha' J' M' | \mathcal{A}_l^m | \alpha J M) = (J' M' | \mathcal{A}_l^m | J M) (\alpha' J' \| \mathcal{A}_l \| \alpha J) \quad (2.1.8)$$

where the first factor $(J' M' | \mathcal{A}_l^m | J M)$ is the Clebsh-Gordan coefficient for the coupling of angular momenta. It follows from the well known properties of this coupling that for the matrix element (2.1.8) to be different from zero, it is necessary that

$$|J - J'| \leq l \leq |J + J'|$$

It follows that for a nucleus of spin I ($0 \leq l \leq 2I$), \mathcal{A}_l^m will only be different from zero if $l \leq 2I$. Thus nuclei of spin $I \geq 1$ will have quadrupole moments, nuclei with $I \geq 2$ will have moments of order 4, etc.. The term $l=0$ of the electrostatic interaction between electron and nucleus corresponds to coupling with a point charge Ze . Since the nuclear radius R is much smaller than the electronic radius a , the various terms of W_E , as given by equation (2.1.3), decrease rapidly, roughly as $(R/a)^2$.

Only quadrupolar interactions will be considered from now on. The components \mathcal{A}_2^m of the nuclear quadrupole moment operator can be rewritten as:-

$$\left. \begin{aligned} \mathcal{A}_2^{\pm 2} &= \frac{(6)^{\frac{1}{2}}}{4} \sum_i e_i (x_i \pm iy_i)^2 \\ \mathcal{A}_2^{\pm 1} &= \frac{(6)^{\frac{1}{2}}}{2} \sum_i e_i z_i (x_i \pm iy_i) \\ \mathcal{A}_2^0 &= \frac{1}{2} \sum_i e_i (3z_i^2 - R_i^2) \end{aligned} \right\} \quad (2.1.9)$$

According to the Wigner-Eckart theorem, the \mathcal{A}_2^m have, for a nuclear state of spin I , within the manifold of the $2I + 1$ substates, $I_z = m$, the same matrix elements as the Hermitian tensor operator formed from the components of the vector I :-

$$Q_2^{\pm 2} = \frac{(6)^{\frac{1}{2}}}{4} \sum_i e_i I_{i\pm}^2$$

$$Q_2^{\pm 1} = \frac{(6)^{\frac{1}{2}}}{4} \sum_i e_i [I_{z_i} I_{i\pm} + I_{\pm_i} I_{z_i}]$$

$$Q_2^0 = \frac{1}{2} \sum_i e_i [3I_{z_i}^2 - I_i(I_i + 1)]$$

Since details of nuclear structure are not sufficiently well known to make use of \mathcal{A}_2^m in this form, these relations are normally expressed in the following way:-

$$Q_2^{\pm 2} = \alpha \frac{(6)^{\frac{1}{2}}}{4} (I_{\pm})^2$$

$$Q_2^{\pm 1} = \alpha \frac{(6)^{\frac{1}{2}}}{4} (I_z I_{\pm} + I_{\pm} I_z)$$

$$Q_2^0 = \alpha \frac{1}{2} (3I_z^2 - I(I + 1))$$

The constant α is determined, for instance, from the condition that Q_2^0 and \mathcal{A}_2^0 have the same expectation value in the substate $I_z = I$, denoted as $|I I\rangle$. The usual convention is to represent by the symbol eQ , the quantity

$$eQ = \langle I I | \sum_{i=1}^A e_i (3z_i^2 - R_i^2) | I I \rangle$$

We therefore have:-

$$eQ = 2 \langle I I | \mathcal{A}_2^0 | I I \rangle = 2 \langle I I | Q_2^0 | I I \rangle = \alpha I(2I - 1) \quad (2.1.10)$$

whence

$$\alpha = \frac{eQ}{I(2I - 1)}$$

We can therefore write:-

$$\left. \begin{aligned} Q_{2}^{\pm 2} &= \frac{eQ}{I(2I-1)} \frac{(6)^{\frac{1}{2}}}{4} I_{\pm}^2 \\ Q_{2}^{\pm 1} &= \frac{eQ}{I(2I-1)} \frac{(6)^{\frac{1}{2}}}{4} (I_z I_{\pm} + I_{\pm} I_z) \\ Q_{2}^0 &= \frac{eQ}{I(2I-1)} \frac{1}{2} (3I_z^2 - I(I+1)) \end{aligned} \right\} \quad (2.1.11)$$

The quadrupolar interaction Hamiltonian can now be written

$$\mathcal{H}_E = \sum_{m=-2}^{+2} Q_2^m \mathcal{O}_2^{-m}$$

where Q_2^m involves only nuclear spin operators and \mathcal{O}_2^{-m} involves only electron coordinates. From (2.1.6) \mathcal{O}_2^m can be written

$$\mathcal{O}_2^m = -e \sqrt{\frac{4\pi}{5}} \sum_{i=1}^N r_i^{-3} Y_2^m(\theta_i, \varphi_i) \quad (2.1.12)$$

The five components of this operator constitute the spherical components of the tensor operator

$$T = -e \sum_{i=1}^N \sum_{k,j} \frac{x_{ki} x_{ji}}{r_i^3}$$

which we can write conveniently in matrix form

$$T = -e \sum_{i=1}^N \frac{1}{r_i^3} \begin{bmatrix} x_i^2 & x_i y_i & x_i z_i \\ y_i x_i & y_i^2 & y_i z_i \\ z_i x_i & z_i y_i & z_i^2 \end{bmatrix} \quad (2.1.13)$$

T is known as the electric field gradient tensor. The components of this tensor are closely related to the following combinations of \mathcal{O}_2^m components:-

$$\mathcal{B}_2^0 = -\frac{1}{2} e \sum_{i=1}^N r_i^{-5} (-x_i^2 - y_i^2 + 2z_i^2) \quad (2.1.14)$$

$$\mathcal{B}_2^1 + \mathcal{B}_2^{-1} = \left(\frac{3}{2}\right)^{\frac{1}{2}} e \sum_{i=1}^N r_i^{-5} (2iz_i y_i) \quad (2.1.15)$$

$$\mathcal{B}_2^1 - \mathcal{B}_2^{-1} = \left(\frac{3}{2}\right)^{\frac{1}{2}} e \sum_{i=1}^N r_i^{-5} (2z_i x_i) \quad (2.1.16)$$

$$\mathcal{B}_2^2 + \mathcal{B}_2^{-2} = \left(\frac{3}{8}\right)^{\frac{1}{2}} e \sum_{i=1}^N r_i^{-5} (x_i^2 - y_i^2) \quad (2.1.17)$$

$$\mathcal{B}_2^2 - \mathcal{B}_2^{-2} = \left(\frac{3}{8}\right)^{\frac{1}{2}} e \sum_{i=1}^N r_i^{-5} (4ix_i y_i) \quad (2.1.18)$$

The tensor T is greatly simplified if the axes are transformed in such a way as to diagonalize the matrix of the tensor. The tensor is then said to be described in the "principal axis system". In this case the matrix takes the form

$$T = -e \sum_{i=1}^N \frac{1}{r_i^3} \begin{bmatrix} X_i^2 & 0 & 0 \\ 0 & Y_i^2 & 0 \\ 0 & 0 & Z_i^2 \end{bmatrix} \quad (2.1.19)$$

The only non zero terms of this tensor are derived from expressions (2.1.14) and (2.1.17). From these terms, it is possible to define three new operators which are symmetrical in the principal axes:-

$$\left. \begin{aligned} e \sum_{i=1}^N (3Z_i^2 - r_i^2) r_i^{-5} &= -2 \mathcal{B}_2^0 \\ e \sum_{i=1}^N (3X_i^2 - r_i^2) r_i^{-5} &= -\frac{3}{2} \left(\mathcal{B}_2^2 + \mathcal{B}_2^{-2} \right) + \mathcal{B}_2^0 \\ e \sum_{i=1}^N (3Y_i^2 - r_i^2) r_i^{-5} &= \frac{3}{2} \left(\mathcal{B}_2^2 + \mathcal{B}_2^{-2} \right) + \mathcal{B}_2^0 \end{aligned} \right] \quad (2.1.20)$$

We shall define the expectation value of these operators by:-

$$\left. \begin{aligned} q_{zz} &= \left\langle e \sum_{i=1}^N (3Z_i^2 - r_i^2) r_i^{-5} \right\rangle = -2A \\ q_{xx} &= \left\langle e \sum_{i=1}^N (3X_i^2 - r_i^2) r_i^{-5} \right\rangle = -B + A \\ q_{yy} &= \left\langle e \sum_{i=1}^N (3Y_i^2 - r_i^2) r_i^{-5} \right\rangle = B + A \end{aligned} \right] \quad (2.1.21)$$

where $A = \langle \mathcal{B}_2^0 \rangle$ $B = \left(\frac{3}{2}\right)^{\frac{1}{2}} \langle (\mathcal{B}_2^2 + \mathcal{B}_2^{-2}) \rangle$

The disappearance of expressions (2.1.15) and (2.1.16) in the principal axis system causes two terms in the Hamiltonian to drop out, the resulting expression being

$$E = Q_2^2 \mathcal{B}_2^{-2} + Q_2^{-2} \mathcal{B}_2^2 + Q_2^0 \mathcal{B}_2^0$$

The zero value of expression (2.1.18) implies that

$$\mathcal{B}_2^{-2} = \mathcal{B}_2^2$$

leading to the further simplification

$$\mathcal{H}_E = Q_2^0 \mathcal{B}_2^0 + (Q_2^2 + Q_2^{-2}) \mathcal{B}_2^2$$

Using this expression, the interaction energy becomes:-

$$\begin{aligned} W_E &= \langle Q_2^0 \rangle \langle \mathcal{B}_2^0 \rangle + \langle (Q_2^2 + Q_2^{-2}) \rangle \langle \mathcal{B}_2^2 \rangle \\ &= \langle Q_2^0 \rangle A + \langle (Q_2^2 + Q_2^{-2}) \rangle \frac{B}{(6)^{\frac{1}{2}}} \end{aligned}$$

which, upon substituting for the nuclear operators, becomes:-

$$W_E = \frac{eQ}{4I(2I-1)} \left[\langle (3I_z^2 - I(I+1)) \rangle \cdot 2A + \langle (I_+^2 + I_-^2) \rangle \cdot B \right]$$

The corresponding Hamiltonian is usually written

$$E = - \frac{e^2 q Q}{4I(2I-1)} \left[3I_z^2 - I(I+1) + \eta (I_+^2 + I_-^2) \right] \quad (2.1.22)$$

in which $A = - \frac{eq}{2}$, $B = \eta \cdot 2A = -\eta \cdot eq$

where η is a scalar coefficient.

If, for all the electrons of the atom, $X_i^2 = Y_i^2$, then $\eta = 0$ and the Hamiltonian (2.1.22) becomes:-

$$\mathcal{H}_E = - \frac{e^2 q Q}{4I(2I-1)} \left[3I_z^2 - I(I+1) \right] \quad (2.1.23)$$

In this chapter we have drawn considerable attention to the tensor character of the nuclear quadrupole-electron interaction. This first appeared with the expression of the coupling in terms of spherical harmonics via the expansion (2.1.2). Not only is the tensorial form of expression more elegant than the usual Taylor series expansion³⁵, but, in addition, it has great advantages if we wish to calculate the electric field gradient due to the electrons of the atom or molecule. This will become obvious in subsequent chapters.

Theory of the Nuclear Quadrupole-
Electric Field Interaction in Molecules. 2.2

If the quadrupolar nucleus A forms part of a molecule rather than part of an atom, the electric field gradient operator \mathcal{Q}_2^0 , as given by equation (2.1.12), must be replaced by

$$\mathcal{Q}_2^0 = \left(\frac{4\pi}{5}\right)^{\frac{1}{2}} \sum_{k=1}^M e_k r_{Ak}^{-3} Y_2^0(\theta_{Ak} \varphi_{Ak}) \quad (2.2.1)$$

in which the summation is over all M charged particles of the molecule, excluding the charge of the quadrupolar nucleus itself. This operator is separable into terms involving the nuclear charges of the molecule and those involving the electronic charges:-

$$\mathcal{Q}_2^0 = \left(\frac{4\pi}{5}\right)^{\frac{1}{2}} e \sum_{j=1}^N Z_j r_{jA}^{-3} Y_2^0(\theta_{jA} \varphi_{jA}) - \left(\frac{4\pi}{5}\right)^{\frac{1}{2}} e \sum_{i=1}^n r_i^{-3} Y_2^0(\theta_{Ai} \varphi_{Ai}) \quad (2.2.2)$$

where A refers to the quadrupolar nucleus and the summations are over the N nuclear charges excluding the quadrupolar nucleus, and the n electrons of the molecule. The electric field gradient due to a nuclear charge is simply:-

$$\frac{Ze}{R_j^3} (3\cos^2\theta_j - 1) \quad (2.2.3)$$

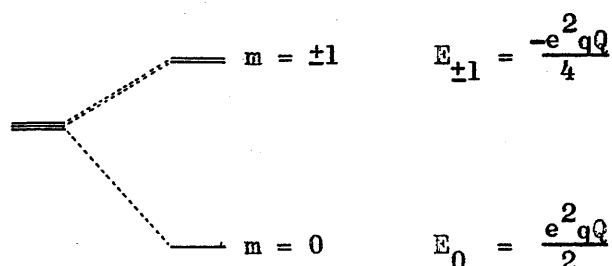
in which nucleus A has been chosen as origin of coordinates, Ze is the nuclear charge of nucleus j, R_j and θ_j are the polar co-ordinates of nucleus j.

The electric field gradient operator for the electrons is identical to that for the atom, although, in the case of a molecule, it operates upon molecular electronic wavefunctions rather than upon atomic wavefunctions.

As a result of the nuclear quadrupole-electric field gradient interaction, the nuclear spin states, which are degenerate in the absence of perturbation by electric or magnetic fields, have energies given by the expectation value of the Hamiltonian (2.1.22) for a non symmetric electric field and (2.1.23) for a cylindrically symmetric electric field. As η is usually fairly small, we shall concentrate our attention upon the nuclear spin energy levels resulting from the interaction of the nuclear quadrupole moment with a cylindrically symmetric electric field. These energy levels are given by:-

$$E_Q = -\frac{e^2 q Q}{4I(2I-1)} \left[3|m|^2 - I(I+1) \right] \quad (2.2.4)$$

For a nucleus such as N^{14} with I equal to one, the nuclear spin levels are split as follows:-



As was the case with nuclear magnetic resonance spectroscopy, this set of energy levels can be detected by radiofrequency spectroscopy, although in this case a sample with its field gradient axes fixed in space must be used rather than one in which the axes rotate rapidly, because rotation of the axes causes the interaction to average to zero. For this reason, crystalline samples are required for nuclear quadrupole resonance spectroscopy.

Experimental Requirements³⁵ of
Nuclear Quadrupole Resonance (N.Q.R.) Spectroscopy ³

The magnitude of the splitting of the nuclear spin energy levels due to interaction of the nuclear quadrupole with the molecular electric field can range from zero to several hundreds or even thousands of megacycles.³⁶ Even for the lighter nuclei which have relatively small quadrupole moments, the resonance frequency may vary over a very considerable range as illustrated in figure 4.1. It is therefore a requirement of a spectrometer that it should operate over a relatively large frequency range. As N.Q.R. absorption signals are very weak, spectrometers must also be extremely sensitive. These requirements tend to be mutually exclusive and in practice a compromise must be reached. Detectors are therefore normally designed to operate over a limited frequency range, there being at present three such ranges:-

- (i) 0 - 20 Mc/s.
- (ii) 15 - 100 Mc/s.
- (iii) > 100 Mc/s.

N.Q.R. absorption of suitable isotopes of first row elements in the periodic table, such as N^{14} , usually occurs in range (i), whereas second row elements may resonate anywhere between zero and one hundred megacycles.

To enable full use to be made of the technique, it is necessary to locate the principal axes of the field gradient tensor and to relate these axes to the crystallographic axes. By doing so, a direction to the quantity q can be given which corresponds to a known direction within the individual molecules of the crystal. Location of the principal axes is best carried out by subjecting the single crystal sample to a small static magnetic field when recording the N.Q.R. spectrum. The perturbing field causes Zeeman splitting of the spectrum which depends upon the orientation of the crystal with respect to the field. Maximum splitting results when the Zeeman field is along the

direction of the principal axis. It is therefore another requirement of a spectrometer that it should provide a magnetic field and facilities for orientating the sample with respect to the field.

Because the N.Q.R. frequency depends upon the average value of the largest component of the field gradient tensor, it is dependent upon molecular motions, hence upon temperature. As a result, it is of interest to study the variation of the N.Q.R. spectrum with sample temperature. Facilities for varying sample temperature should therefore be included in the spectrometer design.

Although, as chemists, our main interest in N.Q.R. is that of interpretation of experimental data, we cannot avoid the experimental problem of detecting N.Q.R. absorption signals for the simple reason that spectrometers are not commercially available and must be constructed by the researcher. In the next chapter we shall describe the design and construction of a spectrometer which fulfills many of the requirements outlined in this chapter and which operates in the frequency range 20 - 70 Mc/s.

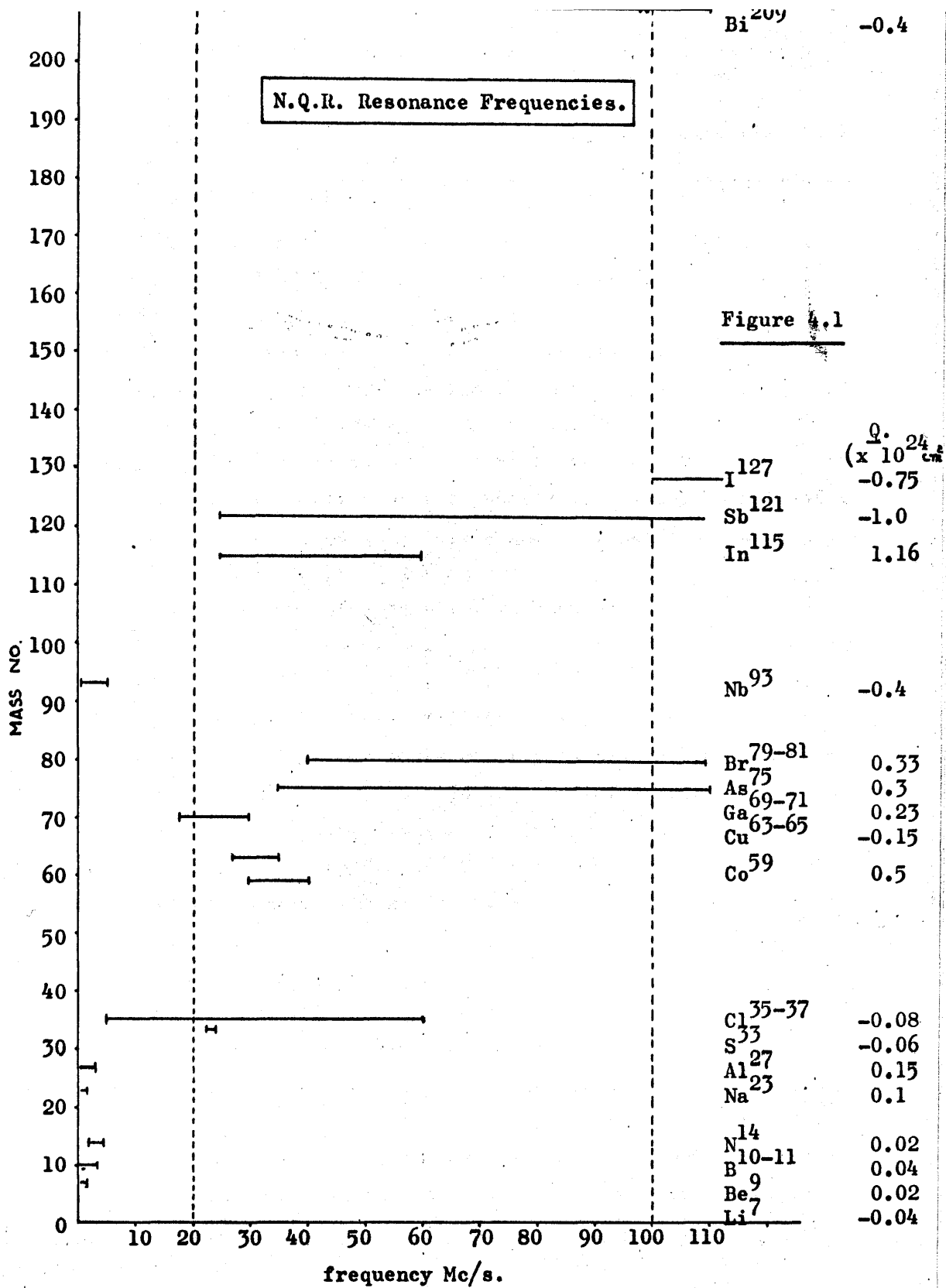
**A Nuclear Quadrupole Resonance Spectrometer
Construction and Operation.**

Chapter 4

The design and construction of the nuclear quadrupole resonance spectrometer which we shall presently describe has constituted the first research in the field of N.Q.R. spectroscopy to be carried out in the Chemistry department of the University of Glasgow.

Our aim in designing a spectrometer has been that it should be suitable for the study of N.Q.R. spectra of nuclei with small electric quadrupole moment and large electric field gradient or with large quadrupole moment and small field gradient. In particular, we have had in mind the possible application of the technique to the study of the electronic environment of transition metal nuclei in complexes. From the survey of N.Q.R. absorption frequencies which is presented in figure 4.1, we concluded that a spectrometer operating in the frequency range 0 - 100 Mc/s. would be suitable for initial investigations. Because of the weakness of N.Q.R. signals and our lack of experience in the field, we desired also that the spectrometer should be highly sensitive.

These requirements, together with the wish to study Zeeman splitting of the resonances, led us to adopt a spectrometer design similar to that proposed by Dean³⁷. As construction progressed and experience was gained in the field of electronics, departures from this design were made. The spectrometer which we shall now describe is therefore of the same type as that proposed by Dean but has its own particular characteristics.



Functional Design of the Spectrometer 4.2

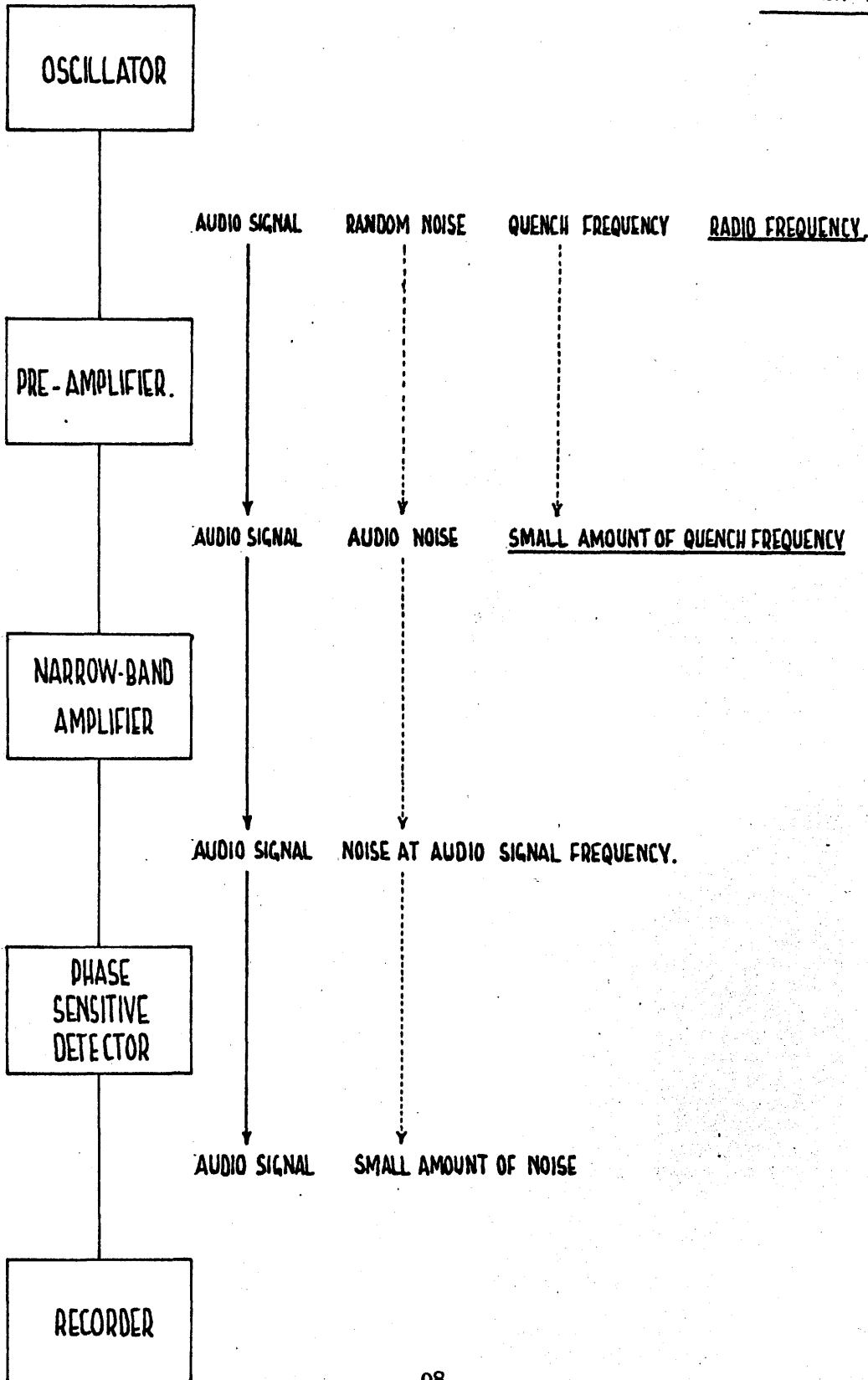
A schematic representation of the mechanism by which N.Q.R. signals are detected by the spectrometer is shown in diagram 4.2 A.

The crystalline sample is placed in the resonant magnetic field contained in the tank coil of the radiofrequency oscillator, the frequency of which is slowly varied so that it passes through the resonance frequency of the sample. The output from the oscillator contains the N.Q.R. signal which is at audio frequency, due to the method of audio-modulation of the oscillator frequency employed in signal detection. As well as this signal, output from the oscillator contains also radiofrequency, quench frequency of about 30 kc/s., and random noise at all frequencies. Before this complex output is passed to the pre-amplifier, the radiofrequency component is removed by passing the oscillator output through a radiofrequency filtering network. The pre-amplifier amplifies audio signal and noise by about fifty times while amplifying the quench frequency component by a smaller amount. The pre-amplifier output is passed to the narrow band amplifier which is tuned to the audio signal frequency, this being the first harmonic of the oscillator modulation frequency. The selectivity of the narrow band amplifier is sharply peaked at 300c/s., so that only audio signal plus random noise in the immediate vicinity of this frequency are amplified, the amplification factor being about 200. Signal voltages at all other frequencies are suppressed by this network. It remains only to remove as much of the resultant noise as possible before displaying the signal on the potentiometric recorder. This is accomplished by passing the output from the narrow-band amplifier through a phase-sensitive detector circuit which converts the 300c/s. signal to a d.c. signal voltage, random fluctuation of the 300c/s. noise level tending to make the d.c. noise level very small indeed.

The function of the other parts of the instrument requires little understanding and will be dealt with in the description of the parts themselves.

DETECTION AND DEVELOPMENT OF THE NQR SIGNAL.
DIAGRAM A.

CHAPTER 4.2.



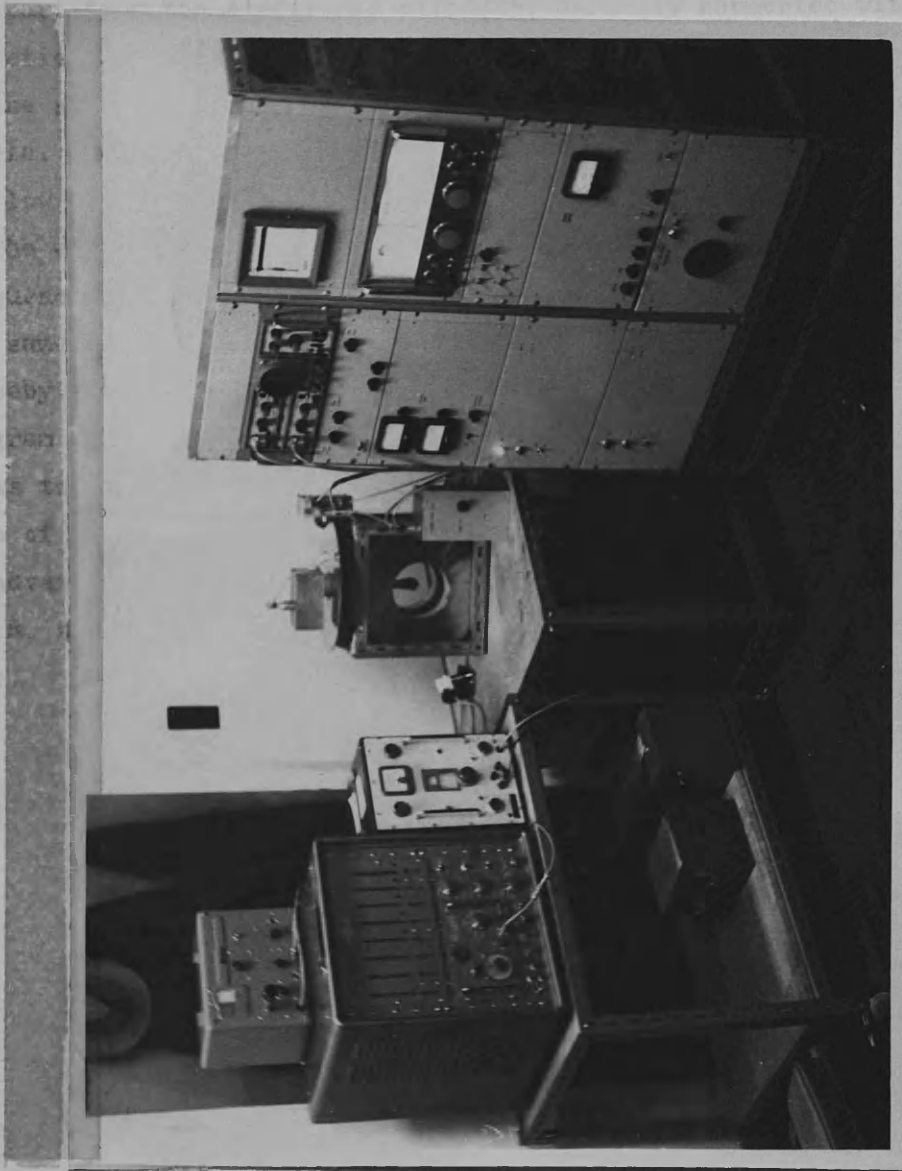
Constructional Design of the Spectrometer 4.3

The complete spectrometer, which is shown in photograph 1, is composed of three separate units, all of which are trolley mounted.

These are:-

- (1) The signal detection unit.
- (2) The console.
- (3) The auxiliary apparatus.

We shall deal with the description of each of these units in turn.



PHOTOGRAPH 1

The Signal Detection Unit 4.3.A

Apart from the electronic circuitry directly connected with detection of the N.Q.R. signal, this unit also contains other parts of the spectrometer which must be situated in close proximity to the sample. The Helmholtz coils for generating the magnetic field and the low temperature apparatus therefore form part of this assembly.

The electronic circuits contained in this section are the radio-frequency oscillator and preamplifier, which have been built into the same housing, and the narrow-band amplifier which is situated closeby. A cut-away drawing of the complete unit is shown in diagram E.

As the radiofrequency oscillator is by far the most important part of the spectrometer, we shall describe the advantages and disadvantages of the various types of oscillator used for observing N.Q.R. signals, and our reasons for choosing to build a particular type.

OSCILLATOR PRE-AMPLIF. HOUSING

JUNCTION BOX

MOTOR TO ROTATE GEARED WHEEL

POLYTHENE SPACERS.

NARROW BAND AMPLIFIER.

HELMHOLTZ COILS

SAMPLE CAVITY

DEWAR TUBE

VIBRATION INSULATION

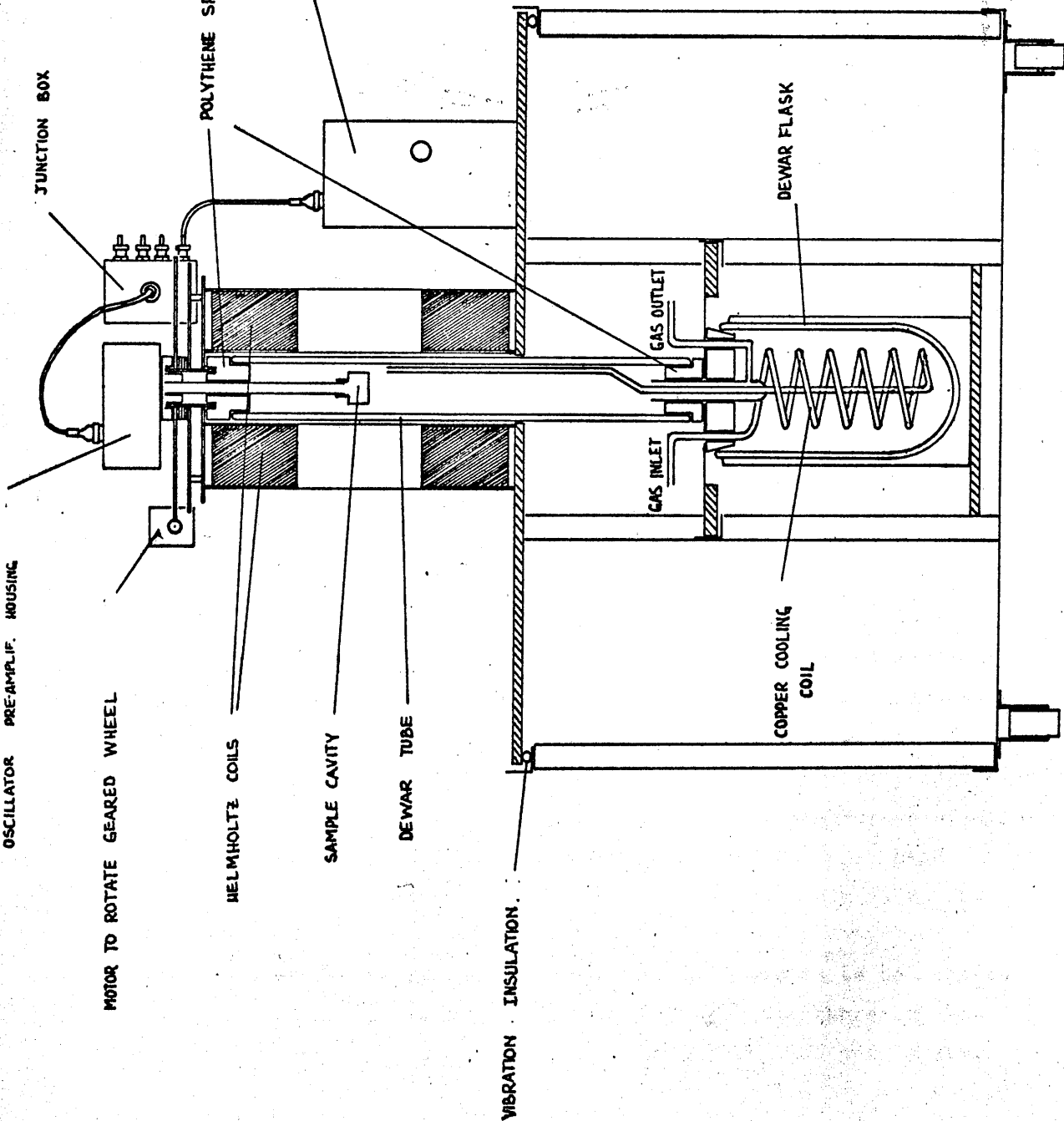
GAS INLET

GAS INLET

COPPER COOLING COIL

DEWAR FLASK

THE SIGNAL DETECTION UNIT
DIAGRAM B
CHAPTER 4.3



(i) Radiofrequency Oscillator Design:
Conditions for Signal Detection.³⁵

The detection of nuclear quadrupole resonance absorption requires application to the sample of a radiofrequency magnetic field at a fixed frequency and at a suitable intensity. The radiofrequency field should not be so large as to saturate the signal, or so small that the signal cannot be detected. In general, quadrupole resonance experiments, because the spin-lattice relaxation times are smaller, require larger r.f. power than magnetic resonance experiments. The r.f. voltage required for a given magnetic field does of course depend on the geometry of the r.f. coil. The oscillator must also have sufficient sensitivity to provide a nuclear signal which measurably exceeds noise level. To search for resonance absorption over a limited frequency range, the applied frequency must be changed continuously, and yet the apparatus must maintain reasonable stability and sensitivity.

Two types of oscillator which measure up to these requirements to different extents have been used to detect N.Q.R. absorption in the frequency range 0 - 100 Mc/s. These are:-

- (a) Regenerative continuous wave detectors.
- (b) Super-regenerative detectors.

Continuous wave detectors provide a simple signal output suitable for the measurement of line shape or the observation of close lying multiplets. Such detectors do, however, suffer from the disadvantage that only a relatively small r.f. power level is required to saturate the spin system. Sensitivity of the detector is necessarily sacrificed by operation at low power levels. An additional disadvantage of this type of detector is that the maintenance of conditions of high sensitivity over a long period and at variable frequency is rather difficult.

Super regenerative detectors cause the spin system to be submitted to bursts of high r.f. power. This type of detector therefore has high sensitivity without much danger of saturating the spin system,

and is particularly suitable , on account of its high power level, for observing resonances with large line-widths. In addition, reasonable sensitivity can be maintained for long periods without serious readjustment. The super-regenerative detector does suffer from the serious disadvantage that the output is complex, hence it is not suitable for measurement of line shape or the observation of close lying multiplets.

It would appear that the high sensitivity of the super-regenerative oscillator, coupled with its ability to detect resonances with large line-widths, renders it more suitable for initial investigations in the field of N.Q.R. than the continuous wave type of oscillator. For these reasons we have employed a super-regenerative detector in our spectrometer.

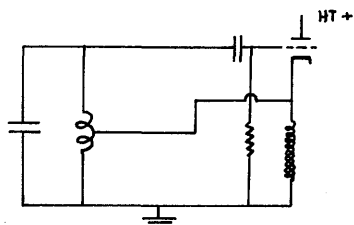
Before describing the oscillator actually employed, we shall first outline the operating fundamentals of the self-quenched super-regenerative oscillator.

Theory of The Self-quenched Super Regenerative Oscillator

(a) Self-quenching Receivers

The self-quenched super regenerative detector is really a squegging oscillator, the waveform generated by its squegging action being known as the quench waveform. The squegging action of this oscillator originates in relaxation oscillations in the circuit itself. The arrangement of the oscillator is such that the time constant in the grid circuit due to the grid leak and associated condenser causes the oscillator to squegg.

In such an oscillator, the oscillations build up from the level of the oscillatory voltage existing in the quiescent circuit. Usually this voltage is provided by thermal and shot noise. The effects upon the circuit of the application of a signal will now be discussed.



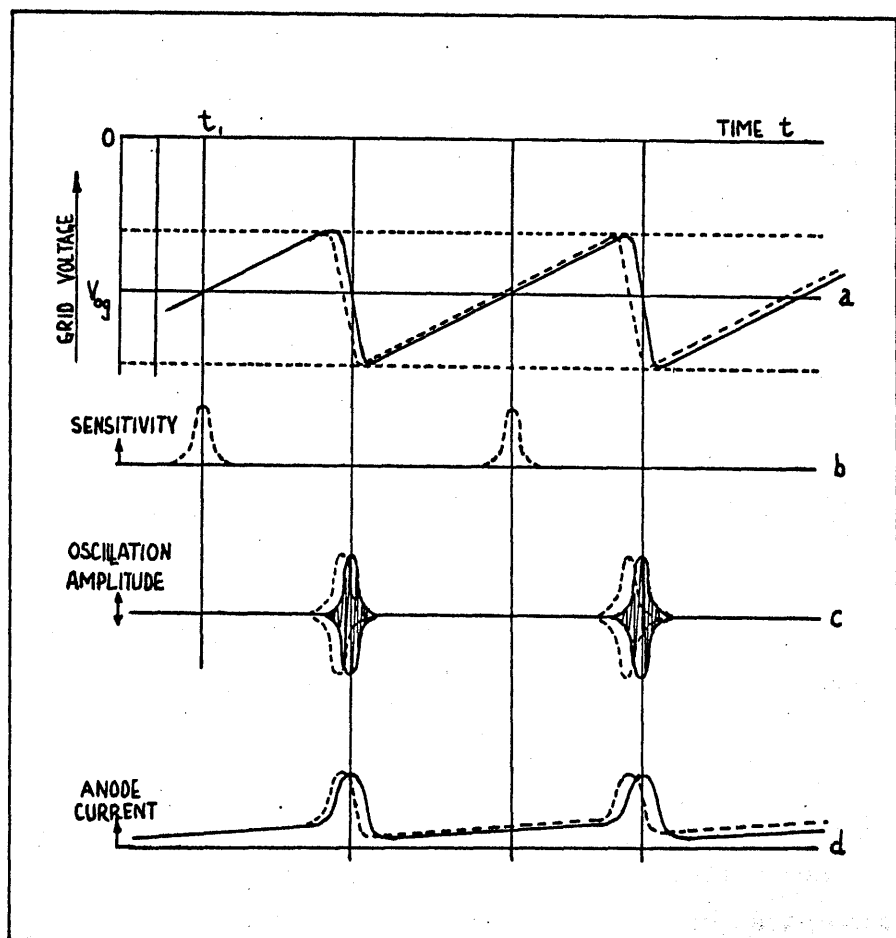
Basic Self-quenched Super Regen.
Oscillator Circuit.

(b) The Self-quenching Cycle

After the oscillator has been switched on for a short time, the relaxation process settles down so that the mean grid voltage is always negative and fluctuates approximately in the manner shown in fig.4.3.1a. It is in this steady state that we are interested. Let us follow the events in a squegging cycle and observe the effects of introducing a signal voltage into the oscillatory circuit. We shall begin our examination of the self-quench cycle when the oscillatory circuit is quiescent and the grid voltage is recovering on the time constant in the grid circuit. Time $t = 0$ is some arbitrary time after which the oscillations from the preceding cycle have died away. As the grid voltage decreases towards zero, a time $t = t_1$ is reached at which the effective circuit conductance is zero corresponding to a grid voltage V_{og} . From this point, oscillations build

CHAPTER 4.3

FIG. 1



SEQUENCE OF OPERATIONS IN THE SELF-QUENCHING CYCLE.

up from the level of circuit noise (solid lines). Initially, the oscillation amplitude is small and has no influence on the continued rise of the grid voltage. The corresponding conductance variation is slow, because it is governed by the slow recovery of the grid potential. As the oscillations grow, grid current begins to flow on the positive peaks. At this stage, it is necessary to imagine an oscillatory voltage superimposed upon the mean grid voltage (this has been omitted from the diagram for clarity). The grid current charges the grid capacitor and causes the mean negative grid voltage to increase in an attempt to follow the oscillation envelope. Eventually the oscillations reach a limiting amplitude at which the valve can only just supply sufficient energy to maintain oscillations. The grid voltage due to persisting grid current continues its negative trend. This reduces the duration of the synchronous bursts of anode current which maintain the oscillations. The effect is cumulative and the oscillations die away. Grid current no longer flows and it only remains for the charge on the grid to leak away in readiness for the next cycle.

When a signal voltage exists in the circuit about time $t = t_1$, the oscillations build up from this new level. Build up starts from exactly the same grid voltage, namely V_{og} . However, the oscillations reach a given amplitude at an earlier time, as shown by the dotted line. The point at which grid current begins to flow is correspondingly advanced, and the grid voltage starts its negative excursion before it has recovered quite so far as it did in the absence of a signal. Fig. 4.3.1c shows the oscillation pulse in relation to the grid voltage waveform. All the succeeding events are advanced by a corresponding amount. The oscillations reach their peak earlier and the sensitive period in the next quench cycle consequently occurs at an earlier time. The effect of applying a steady continuous wave signal, therefore, is to decrease the interval between successive oscillation peaks, thus increasing the quench frequency. This is illustrated by the dotted line in the figure. The variation of mean anode current during the cycle is also shown in the figure. At $t = 0$, it has a value

determined by the grid voltage at that time. It increases gradually as the negative value of the grid voltage is reduced. During the oscillations, however, the mean anode current is greatly increased because it represents the average of bursts at the oscillation frequency. It falls with the oscillation amplitude. By this time, however, the grid potential is more negative, and the anode current drops to a lower value than it had before the oscillations began. On the receipt of a signal, the pulses of anode current become more frequent, and the value of the current, averaged over a number of quench periods, increases with the signal amplitude. If the signal is modulated, this means that the anode current varies at the modulation frequency. The receiver is therefore self detecting.

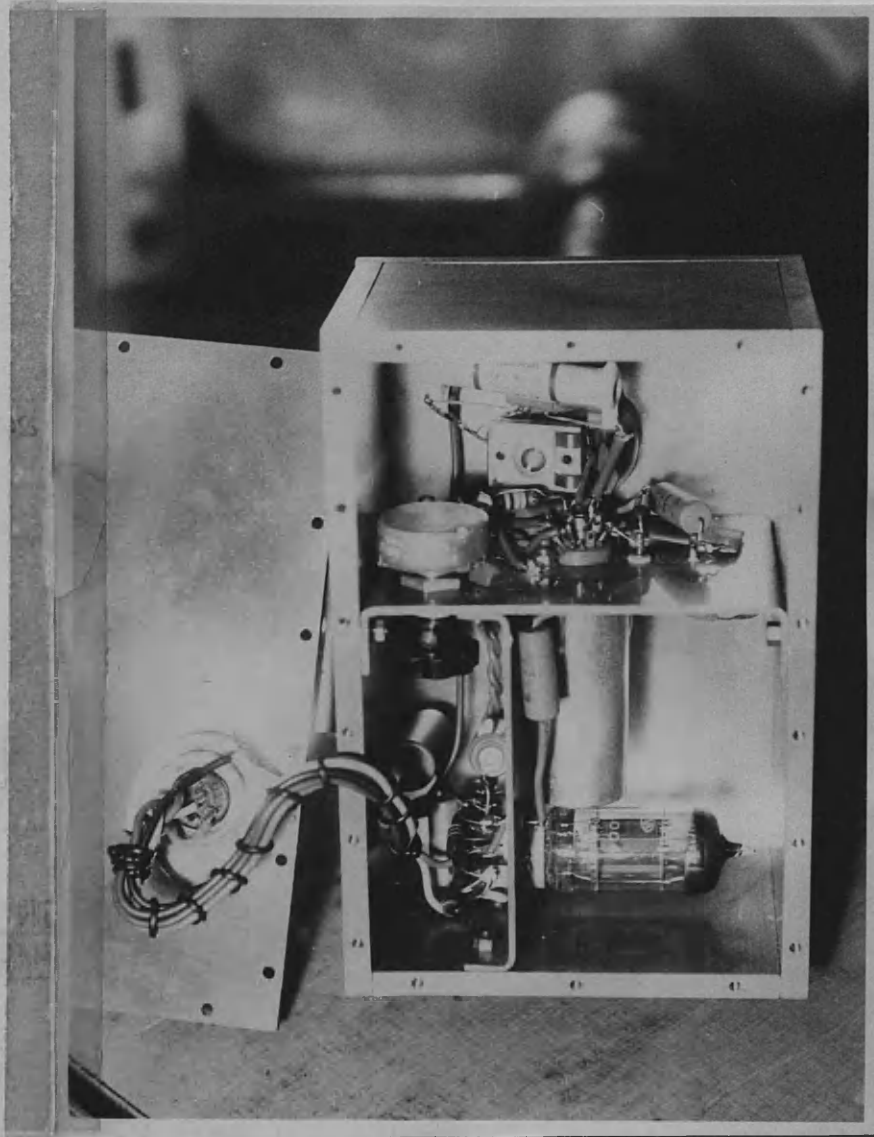
(iii) The Super-regenerative Oscillator:
Practical Design.

The electronic circuitry of the super-regenerative oscillator which we have employed is exactly the same as that proposed by Dean.³⁷ The oscillator and preamplifier have been built into a single housing shown in photograph 2 and diagram C. Electronic circuits are shown in circuit diagram 1.

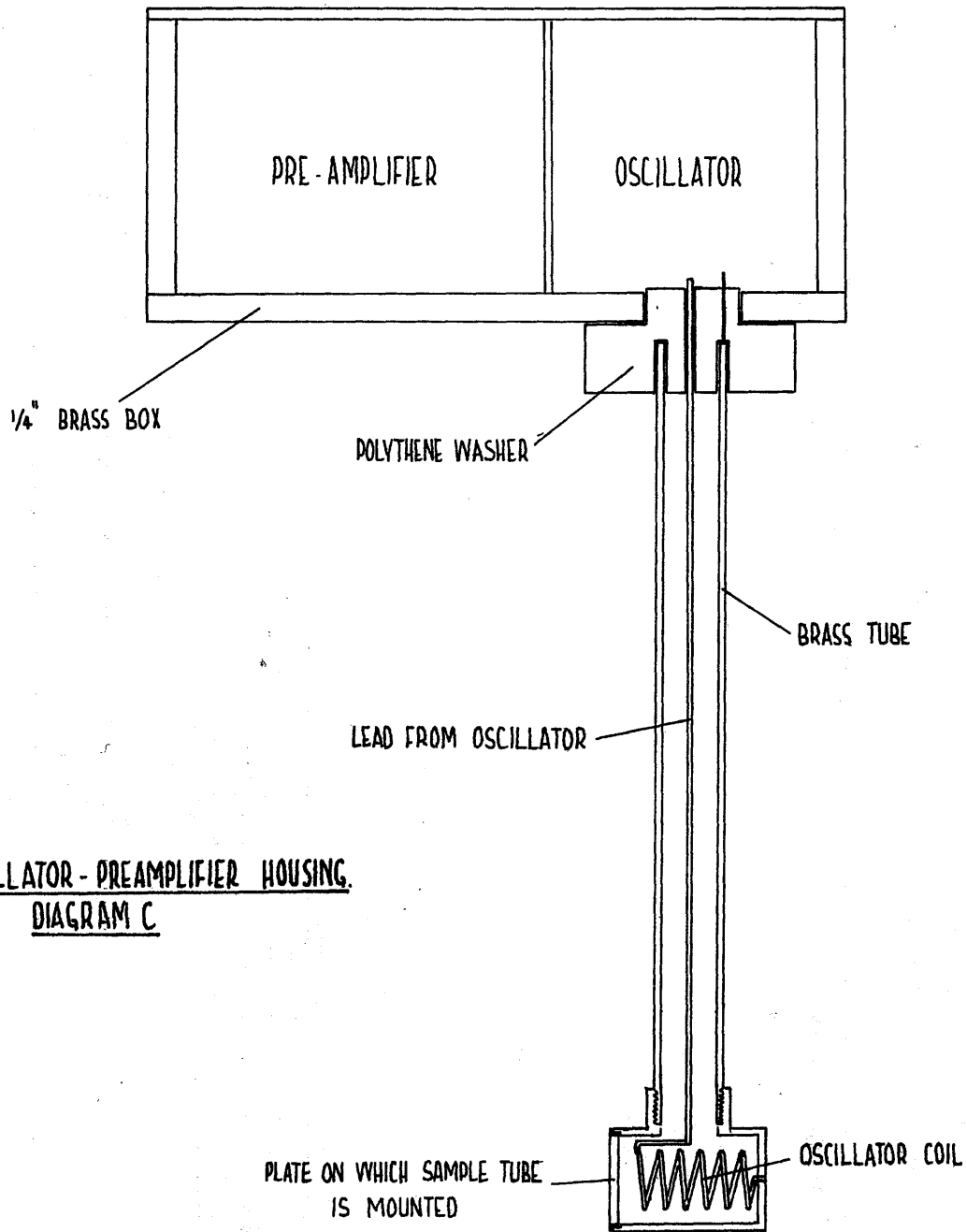
The frequency of the oscillator is set roughly by the 50pf tuning capacitor. Frequency sweep over a small range is carried out electronically by imposing a slowly varying d.c. bias upon the Hughes EC 7001 voltage variable capacitor. Modulation of the oscillator frequency is carried out by superimposing a small a.c. voltage upon this bias. The quench frequency of the oscillator is set by the 1M potentiometer in the grid circuit. Using 18 gauge copper wire coils of dimensions 1" x $\frac{1}{2}$ ", with from six to twelve turns, the frequency range 20 - 70 Mc/s can be covered. On the average, one coil will cover a range in frequency of 7 - 10 Mc/s.

As can be seen from diagram C, the oscillator coil is mounted inside a cylindrical brass housing, at one end of which is a small rotatable brass plate held in place by grub screws. The sample tube is glued to this plate in such a way that, by rotating the plate, the sample can be rotated inside the r.f. coil. When using single crystal samples, this provides one axis about which the sample may be rotated in the magnetic field. The earthy end of the oscillator coil is soldered to the wall of the sample cavity opposite to the brass plate.

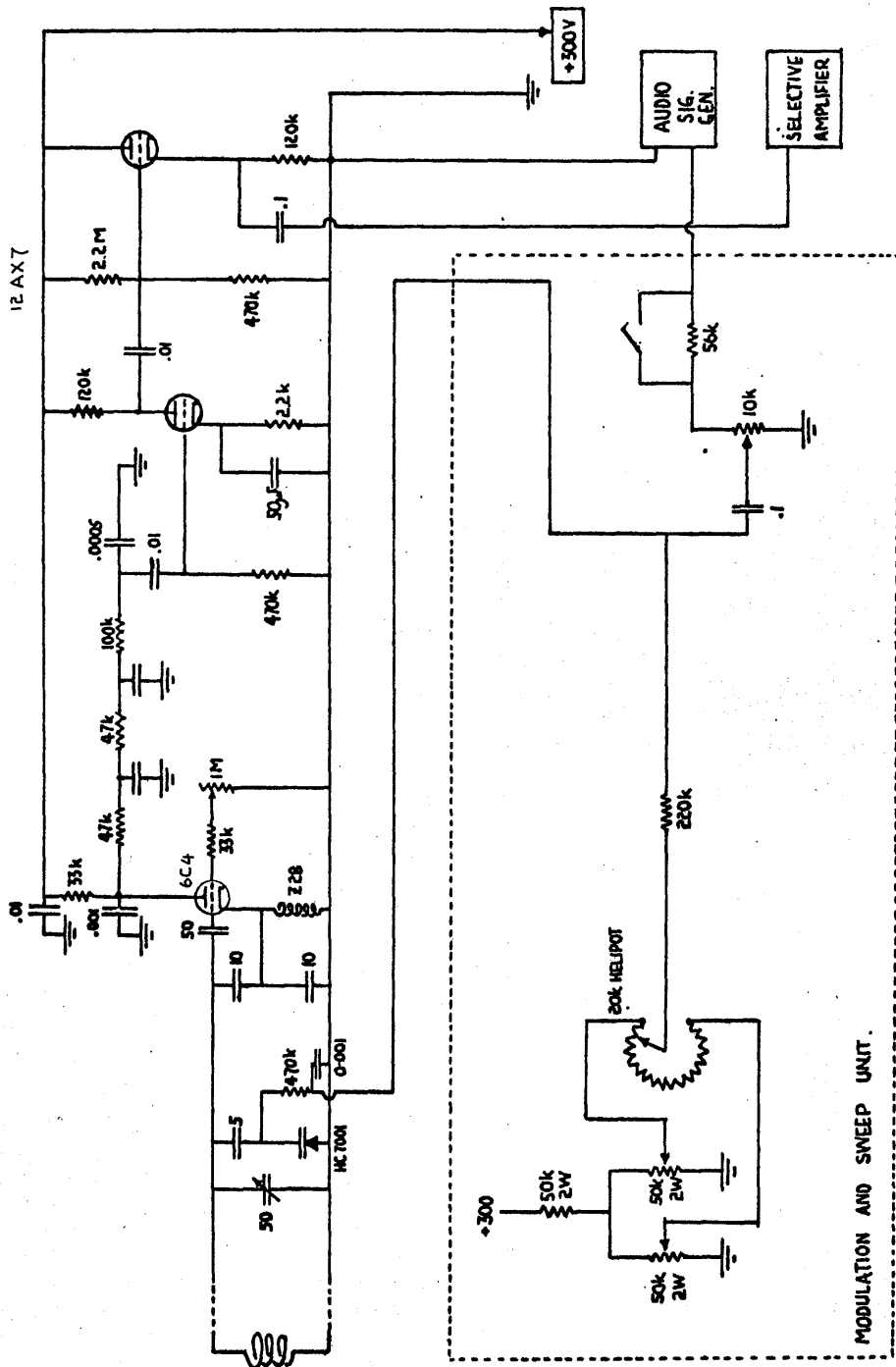
The sample cavity is attached to the oscillator housing by means of a cylindrical brass extension tube. This tube is necessary in order that the sample may be located in the region of homogeneous magnetic field at the centre of the Helmholtz coil assembly. The tube is embedded in a 1" thick polythene spacer which thermally insulates the sample cavity from the remainder of the oscillator. Electronic contact is made by 18 gauge copper pins which have been pushed through the polythene spacer.



PHOTOGRAPH 2



THE OSCILLATOR - PREAMPLIFIER HOUSING.
DIAGRAM C



CIRCUIT DIAGRAM I : OSCILLATOR - PREAMPLIFIER CIRCUIT

The oscillator circuit itself has been built inside a heavy brass box, the edges of which have been milled to improve r.f. shielding, this being a most important consideration as oscillator sensitivity is extremely high. The oscillator valve base is situated close to the leads from the sample coil in order that the components of the circuit can be installed with leads of minimum length, thus minimizing the effects of stray capacitance and inductance originating in the physical configuration of the circuit elements. The oscillator circuit is shielded from the preamplifier in order to minimize pickup and noise.

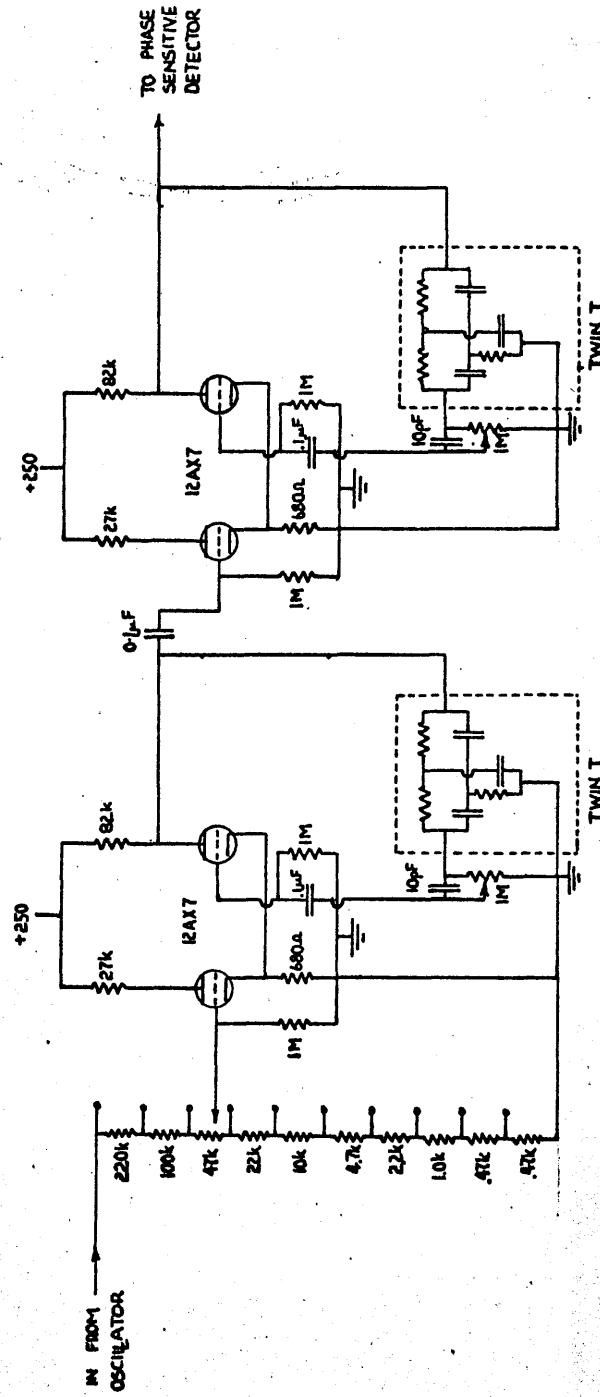
The preamplifier, which is also represented in circuit diagram 1, is simply a one stage audio amplifier followed by a cathode follower. Input and output to the oscillator-preamplifier housing is by a single Plessey plug mounted on the lid of the housing. The complete housing is mounted on top of a large brass gear-wheel which can be made to rotate by a small motor. This provides a second axis of rotation of the sample in the magnetic field.

The leads to the housing are contained in a short shielded cable, the other end of which goes to the junction box (diagram B). High and low tension power supplies are decoupled inside the junction box in order to minimize pickup. The signal output lead to the narrow-band amplifier has also been made as short as possible as pickup in the cable may be large compared to nuclear signal output.

(iv) The Narrow-band Amplifier.

The purpose of the narrow-band amplifier is to select from the random noise input from the oscillator and preamplifier only that component corresponding to the audio signal frequency. As the modulation signal is provided by a stabilized audio frequency generator, the band width of the signal can, at the most, vary over about 3 - 4c/s. Consequently the band width of the narrow-band amplifier should ideally be no more than 5c/s. The single stage twin-T amplifier employed by Dean was found to fall very much short of this requirement. As a replacement for the single stage unit, a pair of stagger-tuned twin-T amplifiers was employed (circuit diagram 2). This circuit was based on a design due to White Instrument Laboratories. The resulting narrow-band amplifier was found to have sharp frequency response characteristics, and a gain of about two hundred at the frequency to which it was tuned, compared to a gain of about fifty for the single stage amplifier. The twin-T networks were built as plug-in units so that the detection frequency could be changed with ease.

CIRCUIT DIAGRAM 2: NARROWBAND AMPLIFIER.



(v) The Helmholtz Coil Assembly.

The assembly is seen most clearly in photograph 3 and figuratively in diagram B. Each coil former is made from 3/16" brass sheet, inside surfaces being lined with thin sheet Tufnol which acts as an electrical insulator. The dimensions of each coil former are:-

external diameter = 14"
internal diameter = 6"
internal width = $2\frac{3}{4}$ "

Each coil former has been wound with double cotton covered 18 gauge copper wire, two coatings of I.C.I. Tensol polystyrene cement being applied after each second layer of wire. The final layer of wire has been protected by a sheet of plastic material.

The coils have been mounted inside an aluminium Handy Angle frame which also serves as a support for the large gear-wheel on which the oscillator housing is mounted. Power supply input to the coils, which are in series, is by means of a Belling-Lee socket mounted on the aluminium frame which is grounded as a safeguard against shock.



PHOTOGRAPH 3

(vi) The Low Temperature Apparatus

The sample cavity is cooled by being placed in a long Dewar tube, the top and bottom of which fit snugly on to polythene spacers as shown in diagram B. The top spacer fits tightly round the extension tube from the oscillator, the small gap between this spacer and the polythene spacer immediately below the oscillator being packed with cotton wool. The bottom spacer fits snugly round a glass gas inlet and annular outlet tube which passes directly into a Dewar flask containing liquid nitrogen. The inlet to the Dewar tube is connected to a copper cooling coil.

A flow of nitrogen is made to enter the system via the gas inlet, is cooled by the liquid nitrogen bath, then circulates round the Dewar tube, passing eventually to the atmosphere via the gas outlet tube. At present, no mechanism of controlling the temperature has been included in the system.

The Console 4.3.(B)

The function of the console is to house the majority of the electronic circuitry of the spectrometer. The power supplies for the electronic circuits, magnet power supply circuits, and apparatus for detection and display of N.Q.R. absorption signals are located in this unit. As well as these items, there is also an oscilloscope and general purpose radio receiver. The layout of the console is shown in diagram D. In the following pages the circuits contained in each chassis of the console will be described.

(1) High tension and low tension power supplies.

(a) 300 v.d.c./ 6.3 v.a.c. power supply

(b) 250 v.d.c./ 6.3 v.a.c. power supply

These are provided by stock International Electronics Ltd. power supplies.

(c) 6 v.d.c.

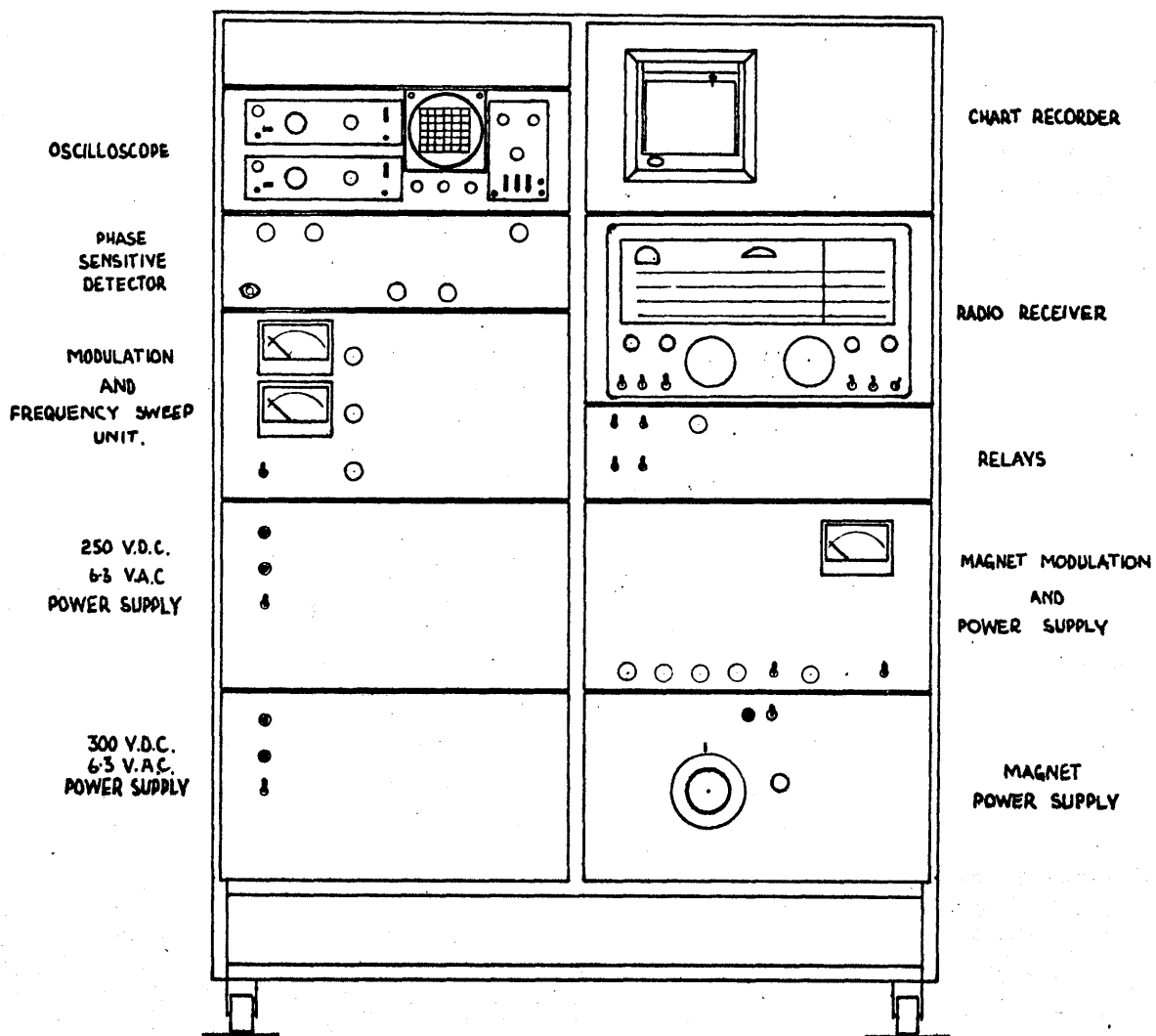
A large six volt car battery is installed in a shielded box behind the 300 v.d.c. power supply. This battery provides power for the valve heaters of the oscillator preamplifier valves in preference to a.c. heaters in order to minimize noise and pickup.

(2) Circuits concerned with signal detection

(a) Modulation and frequency sweep unit:

The purpose of this unit is to provide a continuously varying d.c. bias and an a.c. waveform to be applied to the Hughes diode in the oscillator circuit in order to effect frequency sweep and modulation. The electronic circuit of this unit is extremely simple and is shown along with the oscillator preamplifier circuit in circuit diagram 1. The slowly varying d.c. bias is provided by driving the 20k helipot by means of an electric motor which has been geared down so that fifteen rotations of the shaft of the

THE CONSOLE : DIAGRAM D.

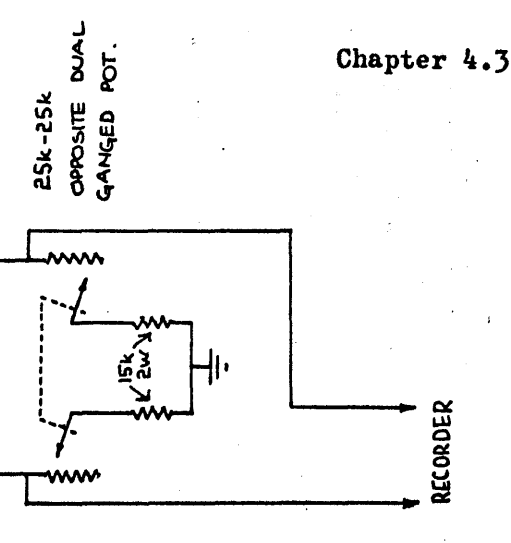
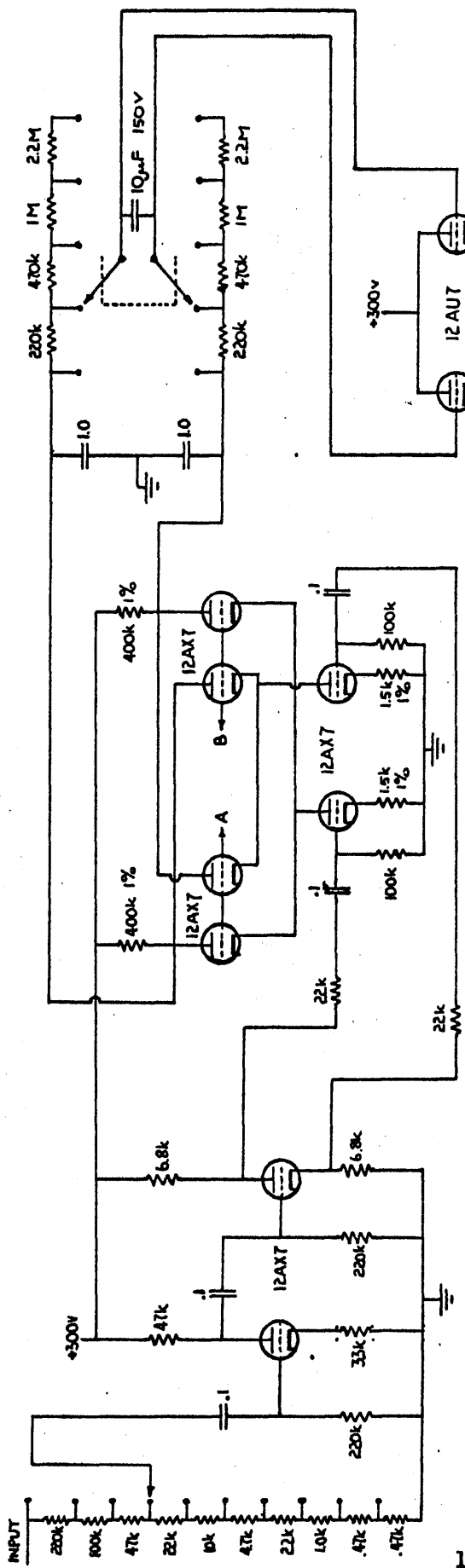


helipot are completed in a seven hour period. In order to provide a continuous sweep and to prevent the helipot shaft from being overrun, a mechanism has been installed which causes the motor driving the helipot to reverse its direction of travel automatically at the end of each sweep. Care has been taken to minimize pickup as slight modulation of the oscillator frequency could arise from a.c. pickup at this stage. The d.c. bias range is from about 0 - 60 volts, giving a frequency sweep range of some 300 kc/s.

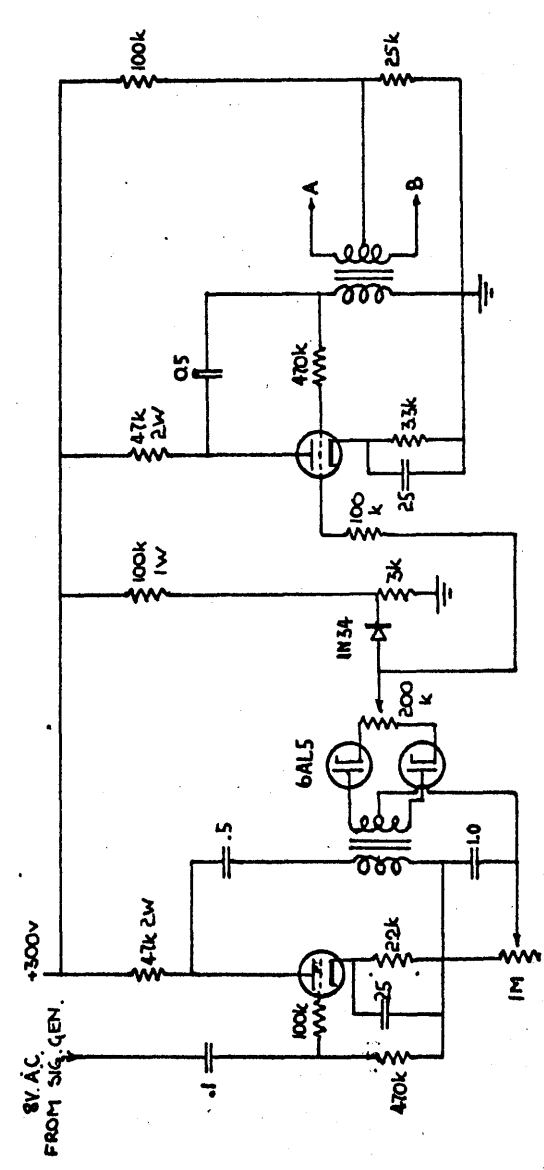
(b) Phase sensitive detector.

Circuit diagram 3A shows the layout of the phase-sensitive detector, this being exactly the same as that employed by Dean. The circuit shown at the top of the page is the phase sensitive detector itself, that at the bottom being the reference generator for switching grids A and B. The integrating time of the detector is from about two to ten seconds.

This circuit has been found to function fairly well, although the rather crude square wave reference signal has caused us to redesign the reference generator. Circuit diagram 3B illustrates the new reference circuit which generates square waves with a very short rise and fall time. Small variations in the d.c. level of grids A and B have little effect upon the on-off times of these grids when the redesigned reference circuit is used hence baseline drift is minimized.

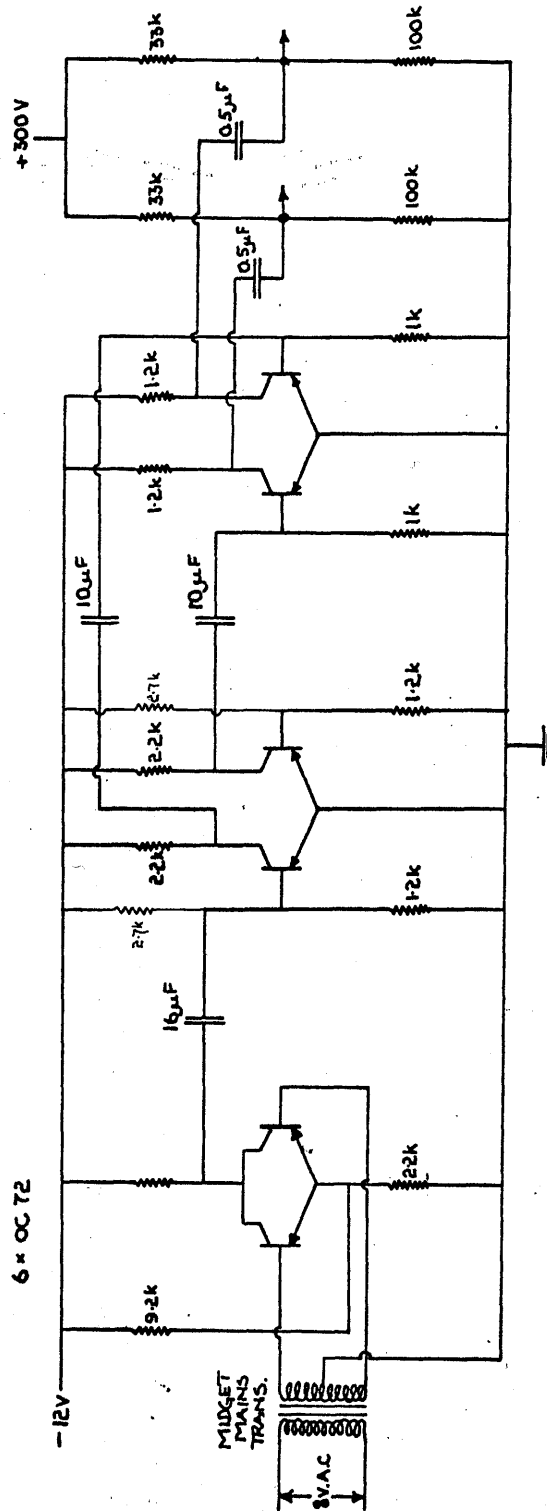


Chapter 4.3



CIRCUIT DIAGRAM 3A: THE PHASE SENSITIVE DETECTOR.

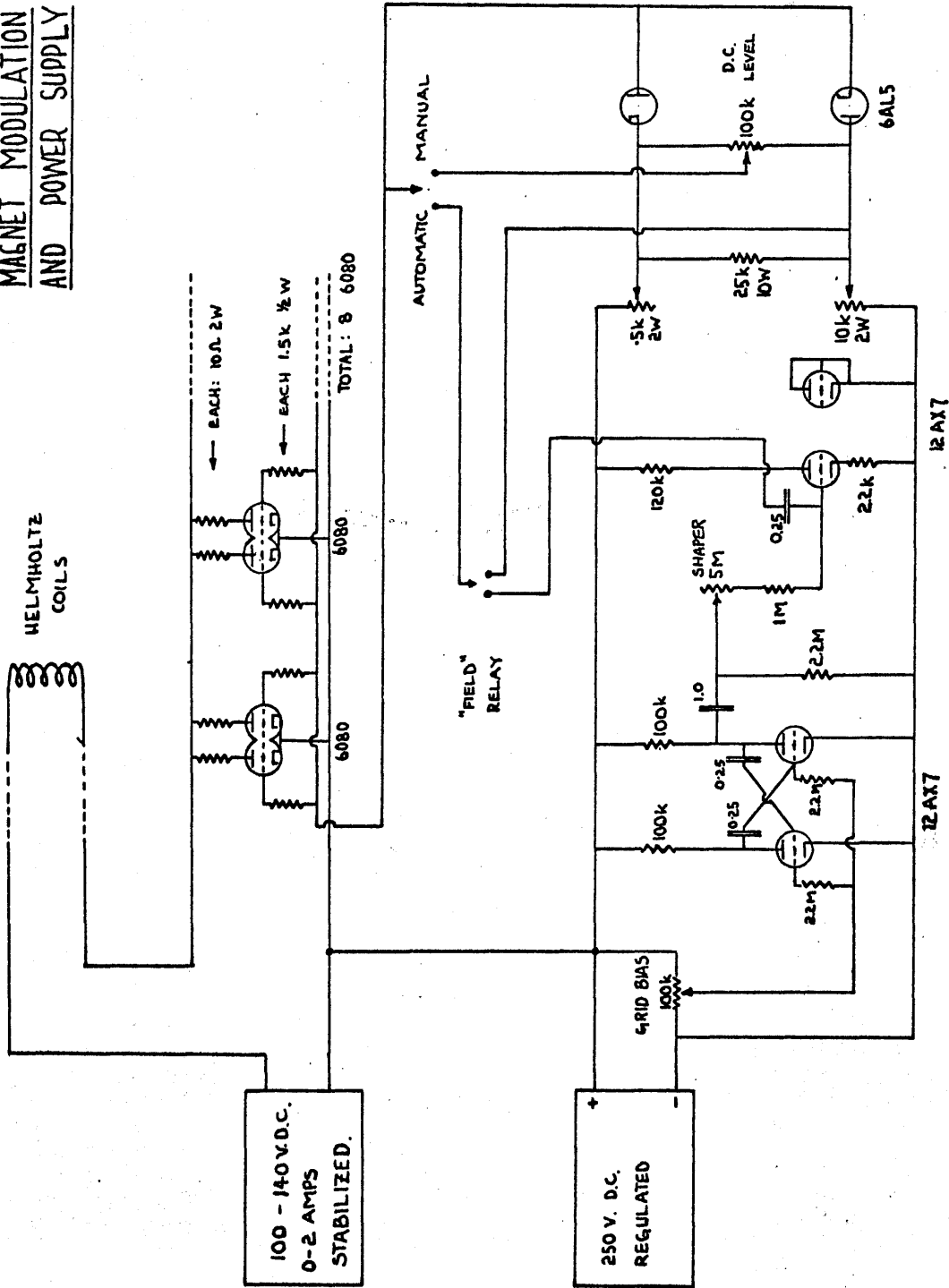
CIRCUIT DIAGRAM 38: SQUARE WAVE REFERENCE GENERATOR.



(c) The magnet power supply and modulation unit.

In chapter 3 the technique for locating the principal axes of the electrostatic field gradient tensor was discussed. This is usually carried out by subjecting the crystalline sample to a small static magnetic field³⁵ while recording the N.Q.R. spectrum, the orientation of the sample for maximum Zeeman splitting being determined. An alternative and sometimes more convenient method³⁷ is to locate what is known as the "zero splitting locus". This is done by arranging the experimental conditions so that only the unsplit components of the Zeeman spectrum are recorded, and is most simply carried out by slowly modulating the Zeeman field, Zeeman split components not being recorded under these conditions. The magnet power supply and field modulation circuits are shown in circuit diagram 4. The 100-140 V. D.C. power supply is of standard design. Leads to a relay circuit controlling the automatic operation of the spectrometer have been included although the relay circuit itself has not yet been completed. Output to the magnet consists of a D.C. current upon which can be superimposed a sawtooth current waveform with a period of one tenth to ten seconds. Magnetic field modulation caused by this sawtooth waveform renders the Zeeman split components unobservable.

CIRCUIT DIAGRAM 4
MAGNET MODULATION
AND POWER SUPPLY



Auxiliary Apparatus 4.3.(C).

The following three pieces of equipment constitute the auxiliary apparatus:-

(A) An Advance Components L.F. Signal Generator Type 81A which is used to provide the modulation signal waveform and reference signal for the phase-sensitive detector.

(B) A Marconi Counter Frequency Meter Type TF 1345/2 which is used to measure the oscillator radiofrequency, quench frequency, and is employed in general as an accurate frequency meter.

(C) An Advance Components Type E Model 2 radiofrequency signal generator which is used as a piece of test equipment for the radiofrequency sections of the apparatus, and, along with the frequency meter, is used to measure the frequency of the r.f. oscillator.

(1) Method of Detection

Although we have explained at length the theory and construction of the super regenerative detector, we have not yet described how the signal which is detected originates from audio modulation of the oscillator frequency. This process is represented in Diagram 4.4.F. Frequency sweep of the oscillator is illustrated in part (a) of this diagram, which contains also a schematic representation of modulation of the oscillator frequency. As the frequency approaches the region of resonance absorption, the crests of the r.f. waves begin to sweep into the resonance. This stage is illustrated more clearly in part (b) of the diagram. The signal which is generated corresponds in frequency to the frequency of modulation hence it is not detected. As the oscillator frequency increases, the r.f. waves begin to sweep back and forth through through the resonance as illustrated in part (c) of the diagram. For each cycle of modulation, the resonance condition is satisfied twice over so that the signal generated has twice the frequency of the modulation signal. It is this frequency, the first harmonic of the modulation frequency, that the spectrometer is tuned to receive.

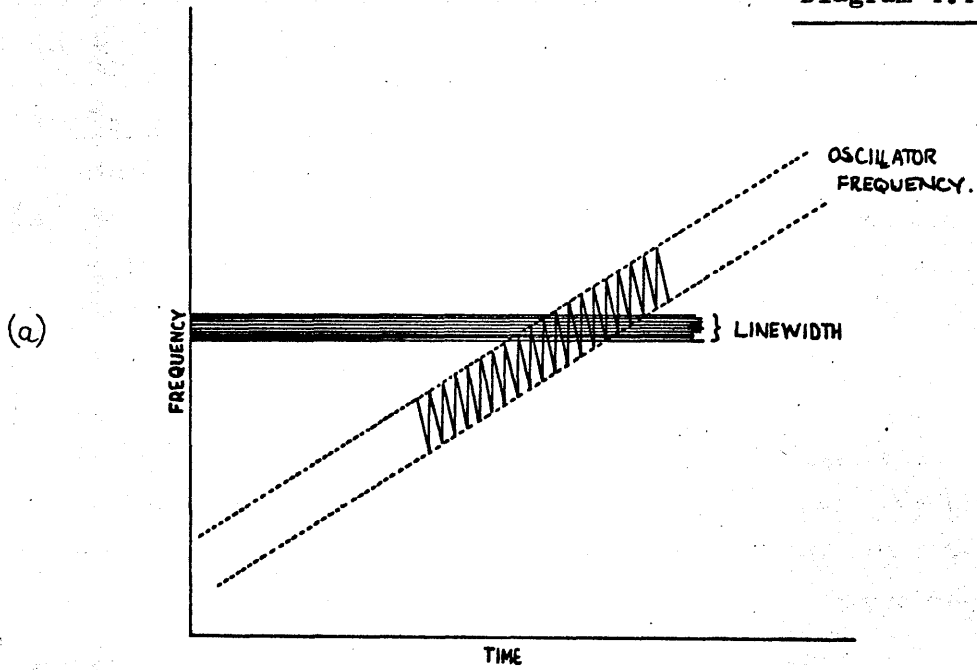
The frequency of audio modulation is somewhat arbitrary, though it must be small compared to the quench frequency. To minimize the effects of mains pickup, a modulation frequency of 150 c/s and corresponding detection frequency of 300 c/s have been employed in the spectrometer. The twin-T networks in the narrow band amplifier are therefore tuned to 300 c/s.

Operation of the Spectrometer.

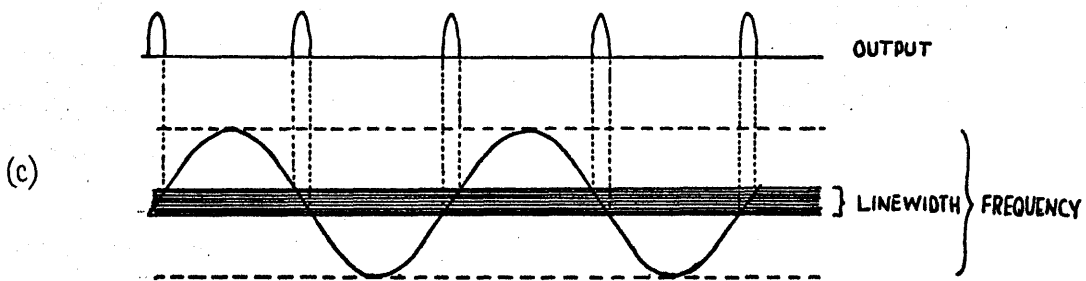
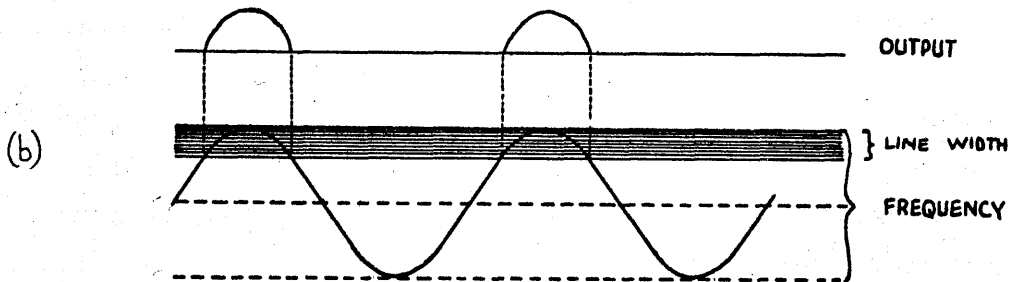
Neglecting the operation of the magnetic field circuits for the moment, operation of the spectrometer is best considered in two stages, the first being concerned with the oscillator-preamplifier and the second with all detection stages subsequent to this.

Before attempting to detect a resonance there are four instrumental

Diagram 4.4.F.



Detection of N.Q.R. Absorption.



parameters to be set which govern the operation of the oscillator.

These are:-

- (1) The oscillator frequency which is set roughly by the tuning capacitor in the grid circuit of the oscillator.
- (2) The quench frequency of the oscillator which is determined by the grid-leak potentiometer in the oscillator circuit.
- (3) The frequency scanning width which is governed by the setting of the potentiometers in the modulation and frequency sweep unit.
- (4) The modulation amplitude which is also controlled by a potentiometer in the modulation and frequency sweep unit.

In the operation of all the other detector stages put together, there are really only three controls which require to be set. These are:-

- (1) The input attenuation to the narrow band amplifier :

In practice it has been found that the gain of the narrow band amplifier is sufficiently great that the input must be fully attenuated to avoid overloading the circuit.

- (2) Input attenuation to the phase sensitive detector.

This is simply determined by the intensity of the detected signal.

- (3) Time constant of the phase sensitive detector: This control is largely responsible for determining the signal to noise ratio of the recorded signal. For maximum sensitivity it is best to use a slow frequency sweep rate and a large time constant.

Of the seven parameters which we have just described, the frequency scanning width, the input attenuation to the narrow band amplifier and to the phase sensitive detector, can be regarded as characteristics of the instrument alone. The time constant of the phase sensitive detector depends both upon the characteristics of the instrument and those of the resonance. The setting of the three remaining parameters depends entirely upon the characteristics of the resonance. Difficulties in locating resonances are therefore centred around the selection of the correct value for the following parameters:-

- (a) The oscillator frequency
- (b) The quench frequency
- (c) the modulation amplitude.

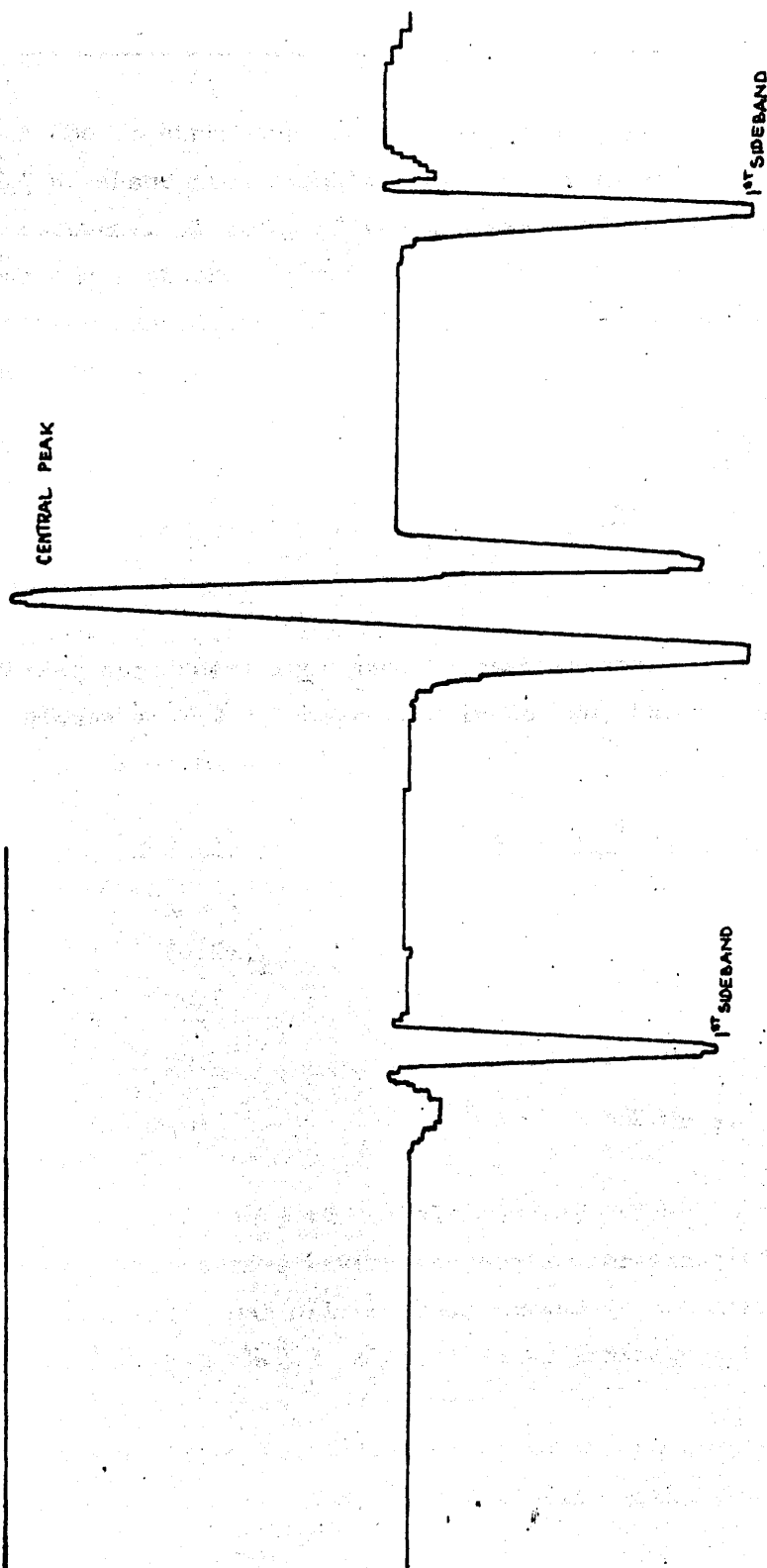
(3) Testing spectrometer sensitivity

The sensitivity of the spectrometer may easily be tested by recording a resonance of known frequency and linewidth. The nuclear quadrupole resonance absorption of the Cl^{35} isotope in polycrystalline sodium chlorate is well suited to this purpose. A reproduction of this spectrum, obtained on the spectrometer operating at a frequency sweep rate of 0.75 kc/minute, is shown in Diagram E.. Noise level in this spectrum is very small indeed.

As a test of comparative sensitivity, the Cl^{35} resonance of K_2PtCl_6 was recorded using three grams of polycrystalline material. The observed signal to noise ratio was approximately fifteen to one. Under similar experimental conditions, and using nine grams of material, Nakamura et al⁴⁰, in a recent paper, have been unable to report a signal to noise ratio higher than three to one for this compound. The sensitivity of the spectrometer which we have built would therefore seem to compare favourably with those of other groups engaged in this field of research.

DIAGRAM E

^{35}Cl NUCLEAR QUADRUPOLE RESONANCE IN NaClO_3
AT 29.8 Mc/s QUENCH FREQ. = 34 kc/s



Searches for N.Q.R. Spectra of Transition Metal Nuclei. 5.1
 Problem of Signal Detection Renewed.

As soon as the spectrometer became operational, we decided to try to obtain N.Q.R. absorption signals from some transition metal containing compounds. A study of the nuclear quadrupole moments and isotopic abundances of the elements of the first, second, and third transition series showed the following nuclei to be potentially suitable for study:-

$\cdot \quad V\left(\frac{7}{2}\right) \quad \cdot \quad Mn\left(\frac{5}{2}\right) \quad \cdot \quad Co\left(\frac{7}{2}\right) \quad \cdot \quad Cu\left(\frac{3}{2}\right) \quad \cdot$
 $\cdot \quad Nb\left(\frac{9}{2}\right) \quad \cdot \quad \cdot \quad \cdot \quad \cdot \quad Pd\left(\frac{5}{2}\right) \quad \cdot \quad \cdot$
 $\cdot \quad Ta\left(\frac{7}{2}\right) \quad \cdot \quad Re\left(\frac{5}{2}\right) \quad \cdot \quad Ir\left(\frac{3}{2}\right) \quad \cdot \quad Au\left(\frac{3}{2}\right) \quad Hg\left(\frac{1}{2}\right)$

isotopic nuclear spin being indicated in parentheses.

Of these elements, N.Q.R. absorption in Co, Cu, Nb, and Hg compounds has already been detected:-

| <u>Nucleus</u> | <u>Compound</u> | <u>Range of frequencies</u> |
|----------------|-------------------------|-----------------------------|
| Co | $Co(C_5H_5)_2 ClO_4$ | 24-36 Mc/s. |
| Cu | $K Cu(CN)_2$ Cu_2O | 26-33 Mc/s. |
| Nb | $K NbO_3$ | 2-3 Mc/s. |
| Hg | $HgCl_2$ | 362 Mc/s. |

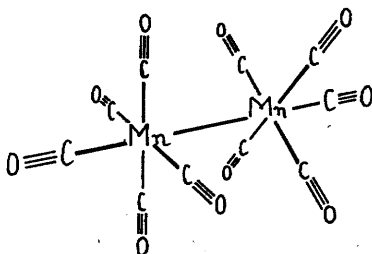
Of these five compounds, only the cobalt complex exists in the form of molecular ions, the others having macromolecular structures. A second point to note is that all of these compounds are diamagnetic, difficulties in detecting N.Q.R. absorption in paramagnetic materials having been pointed out by various workers.³⁹⁻⁴⁰

For an initial study of transition metal nuclei in complexes, the compound which we select for study should ideally satisfy the following requirements:-

- (1) The nucleus should have a relatively small quadrupole moment, hence nuclei of the first transition series are, in general, most suitable.
- (2) The electric field gradient at the nucleus should be small, and, in addition, cylindrically symmetric.
- (3) The compound should be diamagnetic.
- (4) The crystal structure should be simple.

In addition to these requirements, it is an added advantage if a nucleus with a high spin quantum number is chosen, there being for such nuclei two or three widely spaced transitions which facilitate detection of the resonance.

The compound, di-manganese decacarbonyl, would appear to satisfy the above requirements rather well, and is, in addition, rather interesting on account of abnormally long Mn-Mn bond which occurs in the molecule:-

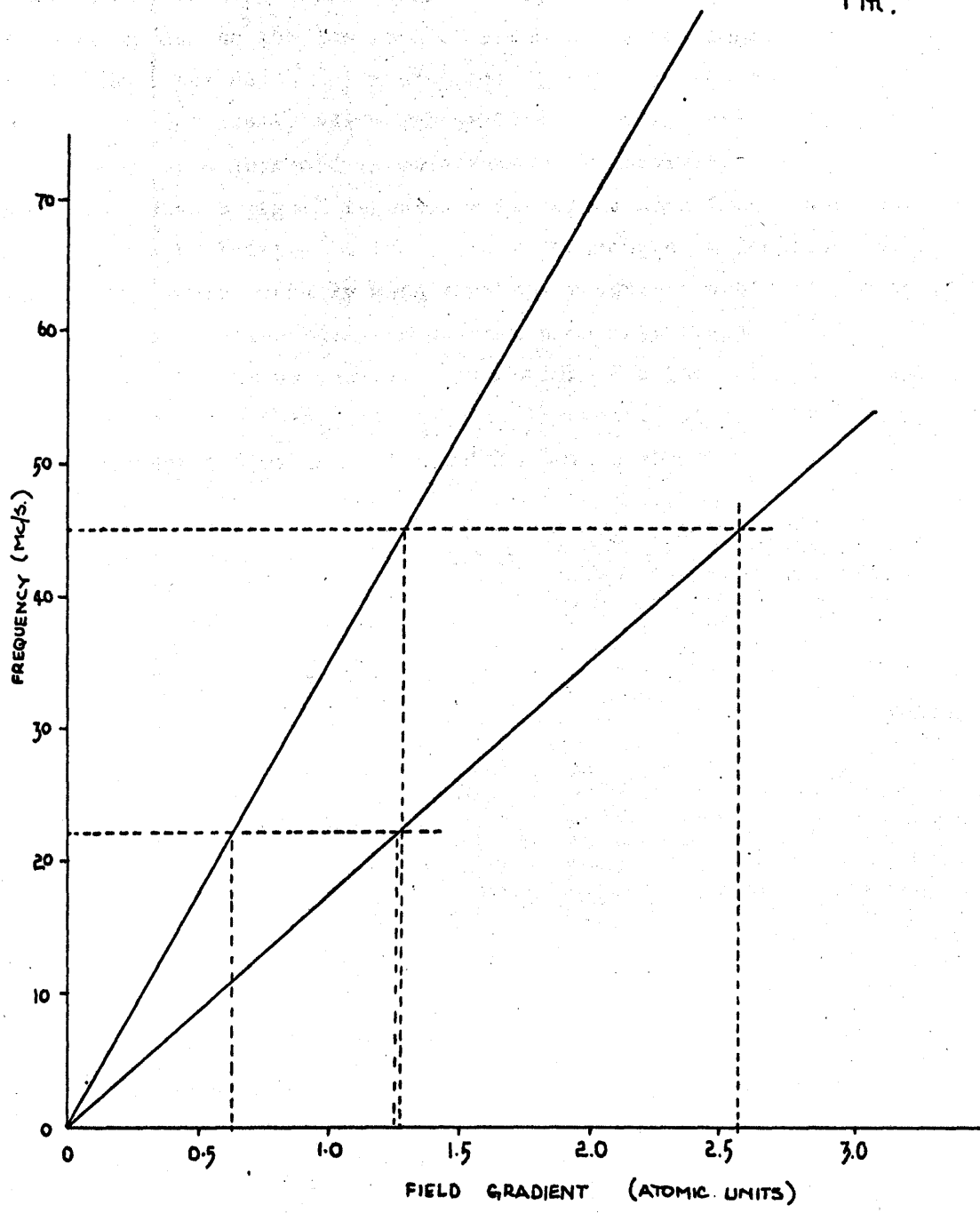


Each Mn atom is surrounded by five carbonyl groups and one other Mn atom, hence the electric field gradient at the nucleus would be expected to be fairly small and should also be cylindrically symmetric. The crystals which these molecules form are extremely simple, the axis of each molecule in the crystal pointing in the same direction.

Diagram G shows the N.Q.R. frequencies of the Mn^{55} nucleus plotted against the electric field gradient at the nucleus. From the diagram we see that, by scanning the oscillator frequency from 22 Mc/s to 45 Mc/s, it should be possible to cover a range in field gradient from 0.6 (a.u.)^{-3} to 2.6 (a.u.)^{-3} . A search for this resonance over the frequency range 22 - 45 Mc/s was carried out but with no success. The conclusion drawn from this rather arduous four week search employing continuous operation of the spectrometer was that the

DIAGRAM G.

M_{π}^{55}



spectrometer, though quite suitable for the study of resonances at known frequencies, is quite inefficient in searching for resonances. The same conclusion has subsequently been drawn from a number of searches for resonances over limited frequency ranges.

The inefficiency of the oscillator system in searching for resonances is entirely due to the low rate of frequency sweep employed, this being about 1 Mc/s per day. Any reasonable increase in the rate of frequency sweep would not really solve the problem, as this would inevitably be accompanied by a decrease in spectrometer sensitivity. As many resonances have a signal to noise ratio of no more than ten to one even after optimization of the circuit parameters, a decrease in sensitivity would probably mean that the resonance would not be detected at all. This problem seems to be common to most types of N.Q.E. spectrometer and is undoubtedly responsible for the delay in applying the technique to problems of chemical interest. In chapter 5.2 we shall consider a "working solution" to this problem.

Design of a "Search Detector". 5.2

From the practical experience we have gained of the self-quenched super-regenerative oscillator, the following characteristics have become obvious:-

- (1) It is reliable,
- (2) It is inexpensive,
- (3) It is simple to construct.
- (4) It can be operated for a month or more without serious attention.

On account of these characteristics, it has occurred to the author that it might be possible to operate a battery of such oscillators simultaneously but at different frequencies. Furthermore, this battery could be accommodated in the present spectrometer system merely by replacing the single oscillator-preamplifier by twenty similar oscillators operating in parallel. Each of these oscillators would be designed to operate over a three megacycle frequency range, frequencies from twenty to sixty megacycles being covered. The successful operation of an assembly of this type would of course depend upon how well each oscillator could be r.f. decoupled from all of the others. The oscillator-preamplifier housings would be built as plug-in units in a large chassis, leads to each housing being r.f. decoupled. Output from the twenty detectors would be fed into the narrow band amplifier. This output could be expressed as follows:-

$$O = \sum_{n=1}^{20} \begin{bmatrix} \text{random} \\ \text{noise} \end{bmatrix}_n + \begin{bmatrix} \text{audio mod.} \\ \text{signal} \end{bmatrix}_n + \begin{bmatrix} \text{N.Q.R.} \\ \text{signal} \end{bmatrix}_i$$

The sum of random noise voltages from from twenty detectors should be less than that from one detector so that a decrease in noise level might be expected. As all the audio modulation signals are derived from the same source, the sum of such signals will be at the same frequency and at a greater intensity than for one oscillator. The selectivity of the narrow band amplifier should, however, be able to cope with this larger modulation signal. This leaves the N.Q.R.

signal which is present only in the i^{th} detector, the other detectors operating at different frequencies. At the present frequency sweep rate of 1 Mc/s per oscillator per day, 20 Mc/s per day could be covered. This would be a vast improvement upon the present system.

The search detector which has just been proposed has not yet been constructed. The nearest approach to it has been the simultaneous operation of two detectors. The N.Q.R. spectrum of Cl^{35} in sodium chlorate was successfully recorded at 29.8 Mc/s while operating the second oscillator at between 32 and 33 Mc/s.

Our proposed solution to the detection problem, though by no means elegant, may be the only solution until such times as highly sensitive and versatile detectors are developed.

**The Contribution of the Electron Distribution in Molecules
to the Electric Field Gradient at the Nuclear Site.**

Chapter 7

When discussing the theory of nuclear quadrupolar interactions, we derived operators whose expectation values were seen to describe the electric field gradient at the nuclear site. By development of that theory, it turns out that zero field gradient would be expected at the nuclei of S- state atoms and ions. In other atoms, ions, or in molecules, those electrons having s-character with respect to the quadrupolar nucleus are expected to make no contribution to the field gradient at the nuclear site. It would therefore be expected that the core electrons of the atom containing the quadrupolar nucleus would make zero contribution to the field gradient.

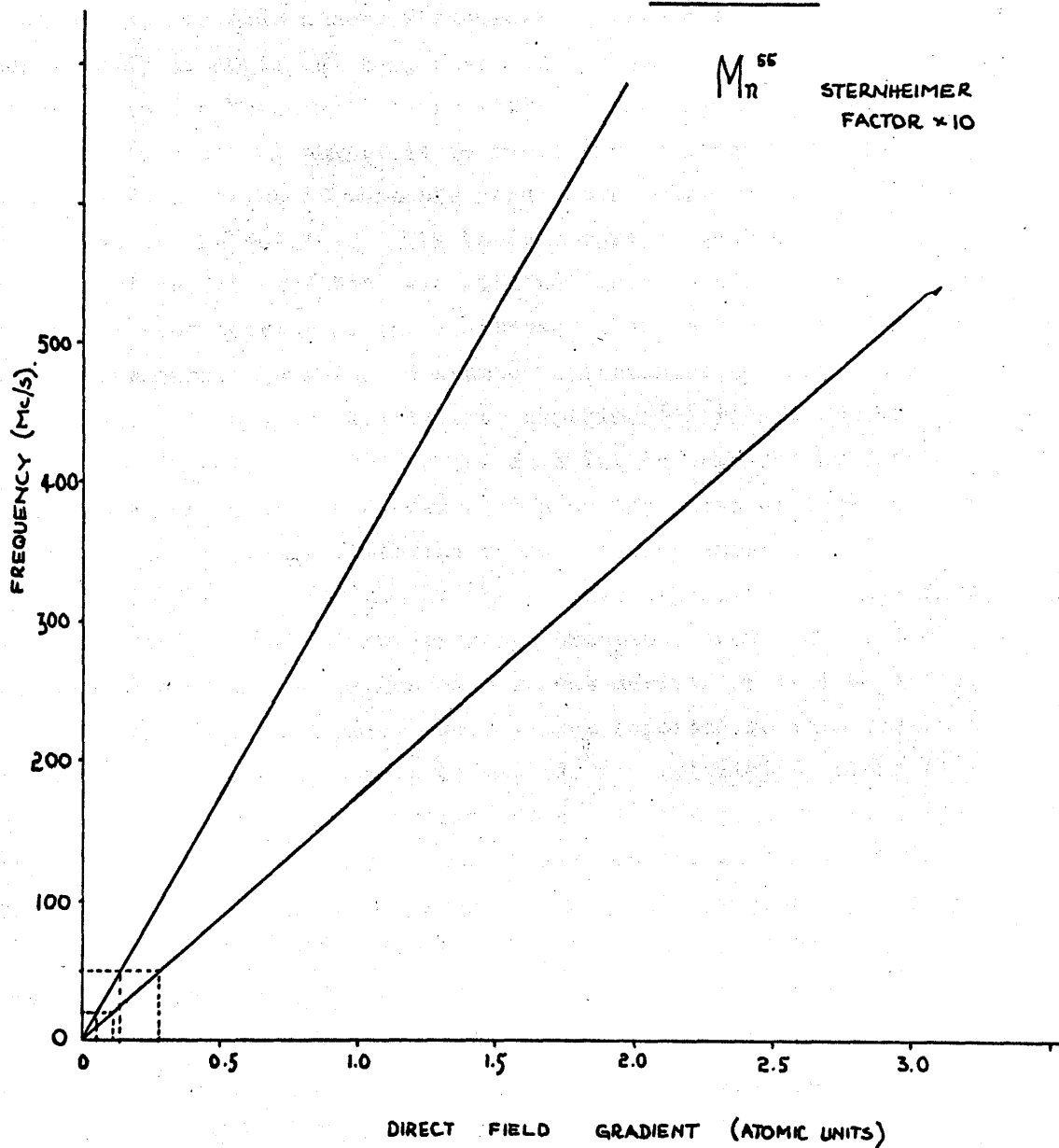
In ionic molecules, such as gaseous KCl, the field gradient at the Cl nucleus would be expected, from the preceding theory, to be very small. In fact, the field gradient observed in such molecules is nearly always ten to one hundred times greater than calculated. Even if the approximate nature of the wavefunctions used in such calculations is taken into account, it is obvious that some mechanism of enhancement of the electric field gradient is operating. This mechanism has become known as the Sternheimer anti-shielding effect and has been investigated by a number of workers.⁴⁵⁻⁴⁶ This enhancement is in fact due to a quadrupole moment being induced in the core electrons in the vicinity of the nucleus by the nuclear quadrupole moment itself. The quadrupole moment experienced by charges external to the core is not simply the nuclear quadrupole moment, but, in addition, the induced electronic quadrupole moment.

Calculation of the induced moment involves second order perturbation theory and is, at best, rather approximate. It turns out that, for first row atoms and molecules, core polarization by the nuclear quadrupole moment can account for about 20 - 30% of the field gradient due to charges external to the core, this field gradient now being called the direct field gradient. For nuclei with large quadrupole moments, such as Cl, Cu, the induced field gradient may be one or two powers of ten greater than the direct field gradient. For the Cl⁻ ion, it has been

estimated⁴⁷ that there is almost a fifty fold enhancement of the direct field gradient due to an external charge. An additional reason can now be seen for the difficulty in detecting N.Q.R. absorption in transition metal complexes. If we reconsider di-manganese decacarbonyl and assume that the induced field gradient can amplify the direct field gradient by, say, a factor of ten, then if we plot, not as in Diagram G, frequency versus field gradient, but as in Diagram H, frequency versus direct field gradient, it can be seen that an oscillator coverage of 22 - 45 Mc/s will only cover a direct field gradient range of from 0.1 to 0.3 (a.u.)⁻³, which is very small indeed. N.Q.R. spectra of transition metal nuclei are therefore likely to occur over a very wide frequency range.

Although the magnitude of the induced field gradient is in many cases enormous with respect to the direct field gradient, it is necessary, in order to interpret the observed spectra in terms of electronic and molecular structure, to have some method of calculating the direct field gradient. We have previously shown how the field gradient operator can be partitioned into a nuclear and an electronic operator, and the method of calculating the nuclear contribution to the field gradient has been described. In the following chapters we shall concern ourselves with the development of methods for evaluating the direct field gradient due to the electrons in molecules.

DIAGRAM H



Importance of Molecular Calculations 7.2

As chemists, our main interest in physical techniques such as N.M.R. and N.Q.R., is not centred around the technique itself, but is concerned with those results of experiments which relate molecular properties. The measurement of chemical shifts, for example, provides us with no more than a set of numbers to which certain dimensions may be attached. To make a more fundamental interpretation of these numbers than results by empirical comparison of one number with another, this latter procedure being well illustrated by the organic chemist's usage of the chemical shift, it is necessary to interpret the measurements in terms of what are regarded as more fundamental properties of the molecule. The basic theory of such an interpretation has been given for the chemical shift and spin-spin coupling constant in chapter 5 of section A, and in chapter 2 of this section for the nuclear quadrupole coupling constant. Unfortunately, electronic wavefunctions cannot be derived from experimental results by present day quantum theory, the best we can do being to compare the theoretical magnitude of the observable, calculated on the basis of some approximate electronic wavefunction, with the value measured experimentally. The importance of this comparison of theory with experiment can hardly be overemphasized as much of our present conceptual knowledge of the electronic structure of molecules has been derived by this approach.

In the period during which the research reported in this thesis was carried out, no computational methods for calculating chemical shifts, nuclear quadrupole coupling constants, etc., were available within the group or within the department. A few matrix elements of an operator similar to the nuclear quadrupole interaction Hamiltonian had been reported in the literature⁴⁸, but certain of these had been shown to be erroneous.⁵⁵

To provide a basis for the calculation by computer of properties such as chemical shifts and nuclear quadrupole coupling constants, the author decided to study existing methods of calculating such properties analytically. In this chapter we shall consider only the

calculation of the electronic contribution to the electric field gradient at the nuclear site, though the methods used could equally well be applied to the calculation of any electronic property dependent upon the first order density matrix^{49,50} for the electrons.

The methods used for the evaluation of most of the matrix elements are essentially those of Barnett and Coulson^{51,52}, and of Pitzer, Kern, and Lipscomb,⁵³ although both these methods have been modified by the author by the inclusion of quantities known as "3-j symbols". The 3-j symbols and the advantages accompanying their use will be subsequently demonstrated.

In this chapter we have attempted to present sufficient mathematical detail to make the use of the methods of calculation clear. At the same time we have been forced to omit many algebraic manipulations. The important results concerning the electronic contribution to nuclear quadrupole coupling will be summarized at the end of the chapter.

Formulation of the Theory 7.3

Excellent background reading to the formulation of the quadrupolar interaction Hamiltonian and the evaluation of its expectation value in terms of electronic density matrices, determinantal wavefunctions, and so on, has recently been presented by Scrocco.⁴⁹

The operator representing the electronic contribution to the electric field gradient at a given nucleus A in a molecule has already been introduced in equation 2.2.2. which we shall rewrite in the form:-

$$\mathcal{E} = \sum_i \mathcal{B}_2^0(e)_{Ai} = -e \left(\frac{4\pi}{5} \right)^{\frac{1}{2}} \sum_i r_{Ai}^{-3} Y_2^0(\theta_{Ai}, \varphi_{Ai}) \quad (7.2.1)$$

in which $\mathcal{B}_2^0(e)_{Ai}$ is the contribution of electron i to the electric field gradient at nucleus A, the other terms being exactly the same as for equation (2.2.2).

To evaluate the matrix elements of the operator (7.2.1), some form of electronic wavefunction for the molecule must be formulated. By choosing Slater determinantal wavefunctions⁵⁴ composed of anti-symmetrized products of one electron wavefunctions, the calculation of the electronic contribution to the field gradient amounts to the evaluation of a sum of one electron matrix elements of the form:-

$$\langle \chi_i | \mathcal{B}_2^0(e)_{Ai} | \chi_i \rangle \quad (7.2.2)$$

in which the χ_i are one electron wavefunctions.

These one electron functions are usually written as a linear combination of atomic orbitals:-

$$\chi_i = \sum_F c_{iF} \psi_{iF}^S \quad (7.2.3)$$

centred upon the F atoms of the molecule. As we shall now be concerned only with the evaluation of one ~~electron~~ ^{electron} matrix elements, the subscript i will be dropped for simplicity. By virtue of expansion (7.2.3), each matrix element is split into a sum of one electron multicentre matrix elements of the type:-

$$(\psi_F | \mathcal{B}_2^0(e)_A | \psi_R)$$

involving centres F, A, and R in the molecule. The one and two centre matrix elements are the only ones which contribute significantly to the electron field gradient and so the evaluation of these alone will be described. In molecular calculations, the one centre orbitals most extensively employed are the Slater orbitals which are defined in the following way:-

$$\psi(nl\mathfrak{m}) = N_n \cdot R_n(r) \cdot Y_l^{\mathfrak{m}}(\theta \varphi)$$

where N_n is a normalization constant,
 $R_n(r)$ describes the radial distribution of the wavefunction,
 $Y_l^{\mathfrak{m}}(\theta \varphi)$ describes the angular distribution of the wavefunction. A list of Slater orbitals with principal quantum number $n \leq 3$ is given in Table 7.2.1. The matrix elements which require to be evaluated are of three types:-

$$(A) \text{ One centre } (\psi_A | \mathcal{B}_2^0(e)_A | \psi_A)$$

$$(B) \text{ Two centre (i) } (\psi_B | \mathcal{B}_2^0(e)_A | \psi_B)$$

$$(ii) (\psi_A | \mathcal{B}_2^0(e)_A | \psi_B)$$

Each type of matrix element must be evaluated in a different way and we shall consider each in turn. Before doing so, however, we shall introduce the 3-j symbols.

Expressions for Slater Orbitals $\psi(nlm) = N \frac{R}{r} Y_l^m(\theta, \phi)$

$$\psi(100) = N_1 e^{-cr} Y_0^0(\theta, \phi) \quad N_1^2 = 4c^3$$

$$\psi(200) = N_2 r e^{-cr/2} Y_0^0(\theta, \phi)$$

$$\psi(210) = N_2 r e^{-cr/2} Y_1^0(\theta, \phi)$$

$$\psi(211) = N_2 r e^{-cr/2} Y_1^1(\theta, \phi)$$

$$\psi(21-1) = N_2 r e^{-cr/2} Y_1^{-1}(\theta, \phi)$$

$$N_2^2 = c^5/24$$

$$\psi(300) = N_3 r^2 e^{-cr/3} Y_0^0(\theta, \phi)$$

$$\psi(310) = N_3 r^2 e^{-cr/3} Y_1^0(\theta, \phi)$$

$$\psi(311) = N_3 r^2 e^{-cr/3} Y_1^1(\theta, \phi)$$

$$\psi(31-1) = N_3 r^2 e^{-cr/3} Y_1^{-1}(\theta, \phi)$$

$$\psi(320) = N_3 r^2 e^{-cr/3} Y_2^0(\theta, \phi)$$

$$\psi(321) = N_3 r^2 e^{-cr/3} Y_2^1(\theta, \phi)$$

$$\psi(32-1) = N_3 r^2 e^{-cr/3} Y_2^{-1}(\theta, \phi)$$

$$\psi(322) = N_3 r^2 e^{-cr/3} Y_2^2(\theta, \phi)$$

$$\psi(32-2) = N_3 r^2 e^{-cr/3} Y_2^{-2}(\theta, \phi)$$

$$N_3^2 = 8c^7/5 \times 3^9$$

All of the integrals which require to be evaluated are separable into integrals over the radial coordinate r_A and integrals over angular coordinates θ_A, φ_A which have the form:-

$$\int_0^{2\pi} \int_0^\pi Y_{l_1}^{m_1}(\theta_A \varphi_A) Y_{l_2}^{m_2}(\theta_A \varphi_A) Y_{l_3}^{m_3}(\theta_A \varphi_A) \sin \theta_A d\theta_A \cdot d\varphi_A \quad (7.4.6)$$

If one of the orbitals has centre B as origin, then its expansion about centre A involves a doubly infinite sum of integrals such as that above (see page 163). The number of non zero integrals and their evaluation can be derived most rapidly by use of quantities known as 3-j symbols. As these are not particularly well known, we shall define the 3-j symbols and briefly discuss their properties. Our discussion closely follows that of Edmonds.⁵⁵

The concept of contragredient quantities.

Consider the coupling of two angular momentum eigenvectors with the same j to form a state with zero angular momentum. This gives

$$u_1(j,m) u_2(j,-m)(-1)^{j-m} = (2j+1)^{\frac{1}{2}} v(j,j,0,0)$$

Since the right hand side is invariant under rotations, we may say that the quantities $(-1)^{j-m} u(j,-m)$ transform under rotations contragrediently to the $u(j,m)$. We may also introduce a quantity which behaves like a metric tensor, namely

$$\begin{pmatrix} j & \\ m & m' \end{pmatrix} = (-1)^{j+m} \delta_{m,-m'}$$

that is, we have

$$u(j,m) u(j,m') \begin{pmatrix} j & \\ m & m' \end{pmatrix} = \text{invariant}$$

The concept of contragredient quantities leads to the conclusion that the vector coupling coefficients are components of mixed tensors, this giving some explanation of their unsymmetric properties. The concept of contragredience is clearly illustrated by Fano and Racah. A more symmetric quantity may be found by carrying out an operation corresponding to raising or lowering of indices in tensor algebra. Such a result is obtained by considering not the coefficient associated with coupling of j_1 and j_2 to give j_3 , but with the coupling of three angular momenta j_1, j_2 , and j_3 to give a resultant zero.

The 3-j symbol of Wigner is defined by

$$\begin{pmatrix} j_1 & j_2 & j_3 \\ m_1 & m_2 & m_3 \end{pmatrix} = (-1)^{j_1 - j_2 - m_3} (2j_3 + 1)^{-\frac{1}{2}} (j_1 m_1 j_2 m_2 | j_1 j_2 j_3 - m_3)$$

Its symmetry properties are easily derived from those of the vector coupling coefficient. An even permutation of the columns leaves the numerical value unchanged:-

$$\begin{pmatrix} j_1 & j_2 & j_3 \\ m_1 & m_2 & m_3 \end{pmatrix} = \begin{pmatrix} j_2 & j_3 & j_1 \\ m_2 & m_3 & m_1 \end{pmatrix} = \begin{pmatrix} j_3 & j_1 & j_2 \\ m_3 & m_1 & m_2 \end{pmatrix}$$

While an odd permutation is equivalent to multiplication by $(-1)^{j_1 + j_2 + j_3}$

$$(-1)^{j_1 + j_2 + j_3} \begin{pmatrix} j_1 & j_2 & j_3 \\ m_1 & m_2 & m_3 \end{pmatrix} = \begin{pmatrix} j_2 & j_1 & j_3 \\ m_2 & m_1 & m_3 \end{pmatrix}$$

We also have

$$\begin{pmatrix} j_1 & j_2 & j_3 \\ m_1 & m_2 & m_3 \end{pmatrix} = (-1)^{j_1 + j_2 + j_3} \begin{pmatrix} j_1 & j_2 & j_3 \\ -m_1 & -m_2 & -m_3 \end{pmatrix}$$

It may be seen from symmetry properties that certain 3-j symbols must be identically zero. In this class, for example, is any symbol with $m_1 = m_2 = m_3 = 0$ and $j_1 + j_2 + j_3$ odd. Symbols of the type:-

$$\begin{pmatrix} j_1 & j_2 & j_3 \\ m_1 & 0 & m_3 \end{pmatrix}$$

are identically zero unless $m_1 = -m_3$. The numerical value of a 3-j symbol is seldom found from the general definition, but from some specialized formula. Numerical values for 3-j symbols have been tabulated by Rotenberg, Bivins, Metropolis, and Wooten.⁵⁷

Formulae which we shall find useful in the evaluation of matrix elements are the following:-

$$\int_0^{2\pi} \int_0^{\pi} Y_{l_1}^{m_1}(\theta, \varphi) Y_{l_2}^{m_2}(\theta, \varphi) Y_{l_3}^{m_3}(\theta, \varphi) \sin \theta \cdot d\theta \cdot d\varphi$$

$$= \left[\frac{(2l_1+1)(2l_2+1)(2l_3+1)}{4\pi} \right]^{\frac{1}{2}} \begin{pmatrix} l_1 & l_2 & l_3 \\ 0 & 0 & 0 \end{pmatrix} \begin{pmatrix} l_1 & l_2 & l_3 \\ m_1 & m_2 & m_3 \end{pmatrix}$$

(7.4.7)

$$Y_{l_1}^{m_1}(\theta, \varphi) Y_{l_2}^{m_2}(\theta, \varphi) = \sum_{l=0}^{\infty} \sum_{m=-l}^{+l} \left[\frac{(2l_1+1)(2l_2+1)(2l+1)}{4\pi} \right]^{\frac{1}{2}} Y_l^m(\theta, \varphi)$$

$$\times \begin{pmatrix} l_1 & l_2 & l \\ m_1 & m_2 & m \end{pmatrix} \begin{pmatrix} l_1 & l_2 & l \\ 0 & 0 & 0 \end{pmatrix} \quad (7.4.8)$$

$Y_{l_1}^{m_1}(\theta, \varphi)$ and $Y_{l_2}^{m_2}(\theta, \varphi)$ in the latter formula being spherical harmonics with the same angles for argument.

$Y_l^{m*}(\theta, \varphi)$ is defined in the following manner:-

$$Y_l^{m*}(\theta, \varphi) = (-1)^m Y_l^{-m}(\theta, \varphi)$$

Evaluation of One-centre Matrix Elements 7.5

$$(\psi_L | \mathcal{B}_2^0(e)_A | \psi'_L)$$

Substituting expression (7.3.5) for ψ in the expression for the matrix element, we get:-

$$(\psi_A | \mathcal{B}_2^0(e)_A | \psi'_A) = \langle N(n_5)R_{n_5}(r_A) Y_{l_5}^{m_5}(\theta_A \varphi_A) | -e\sqrt{\frac{4\pi}{5}} r_A^{-3} Y_2^0(\theta_A \varphi_A) | N(n_1)R_{n_1}(r_A) Y_{l_1}^{m_1}(\theta_A \varphi_A) \rangle \quad (7.5.9)$$

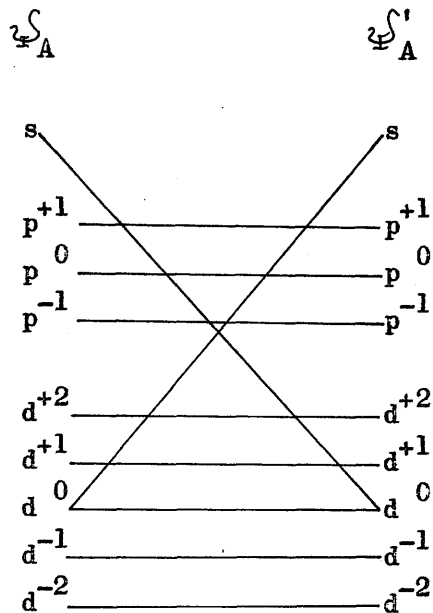
which is separable into a product of matrix elements involving radial and angular coordinates:-

$$(\psi_A | \mathcal{B}_2^0(e)_A | \psi'_A) = -e\sqrt{\frac{4\pi}{5}} [N(n_5)N(n_1)] \langle R_{n_5}(r_A) | r_A^{-3} | R_{n_1}(r_A) \rangle \langle Y_{l_5}^{m_5}(\theta_A \varphi_A) | Y_2^0(\theta_A \varphi_A) | Y_{l_1}^{m_1}(\theta_A \varphi_A) \rangle$$

The matrix element involving angular coordinates can be solved with the aid of expression (7.4.7), giving:-

$$(\psi_A | \mathcal{B}_2^0(e)_A | \psi'_A) = -e\sqrt{\frac{4\pi}{5}} [N(n_5)N(n_1)] \langle R_{n_5}(r_A) | r_A^{-3} | R_{n_1}(r_A) \rangle \times \sqrt{\frac{5(2l_5+1)(2l_1+1)}{4\pi}} \begin{pmatrix} l_5 & 2 & l_1 \\ 0 & 0 & 0 \end{pmatrix} \begin{pmatrix} l_5 & 2 & l_1 \\ -m_5 & 0 & m_1 \end{pmatrix} (-1)^{m_5}$$

It follows from the properties of the 3-j symbols that the matrix element is zero unless $m_1 = m_5$. The non zero matrix elements for $l_5 \geq l_1$ are listed in table 7.5.1, the remaining matrix elements for $l_1 < l_5$ having values identical with the corresponding matrix elements for $l_5 > l_1$. The wavefunctions connected by the operator $\mathcal{B}_2^0(e)_A$ are the following:-



The evaluation of the radial integrals is simply carried out by using the integrals tabulated in appendix III. The integrals are defined by

$$\langle R_{n_5}(r_A) | r_A^{-3} | R_{n_1}(r_A) \rangle = \int_0^{\infty} R_{n_5}(r_A) \cdot R_{n_1}(r_A) \cdot r_A^{-1} \cdot dr_A$$

$$\left\langle \psi_A(n_5 l_5 m_5) \left| -e \sqrt{\frac{4\pi}{5}} r_A^{-3} Y_2^0(\theta_A, \phi_A) \right| \psi_A(n_1 l_1 m_1) \right\rangle \quad \text{Table 7.5.1}$$

$$\left\langle \psi_A(n_5 2 0) \left| \beta_2^0(e) \right| \psi_A(n_1 0 0) \right\rangle = -\left[\frac{1}{5}\right]^{\frac{1}{2}} e \left[N(n_5) N(n_1) \right] \left\langle R_{n_5}(r_A) \left| r_A^{-3} \right| R_{n_1}(r_A) \right\rangle$$

$$\begin{aligned} \left\langle \psi_A(n_5 1 1) \left| \beta_2^0(e) \right| \psi_A(n_1 1 1) \right\rangle &= \left[\frac{1}{5}\right] e \left[N(n_5) N(n_1) \right] \left\langle R_{n_5}(r_A) \left| r_A^{-3} \right| R_{n_1}(r_A) \right\rangle \\ \left\langle \psi_A(n_5 1 -1) \left| \beta_2^0(e) \right| \psi_A(n_1 1 -1) \right\rangle &= \left[\frac{1}{5}\right] e \left[N(n_5) N(n_1) \right] \left\langle R_{n_5}(r_A) \left| r_A^{-3} \right| R_{n_1}(r_A) \right\rangle \end{aligned}$$

$$\left\langle \psi_A(n_5 1 0) \left| \beta_2^0(e) \right| \psi_A(n_1 1 0) \right\rangle = -\left[\frac{2}{5}\right] e \left[N(n_5) N(n_1) \right] \left\langle R_{n_5}(r_A) \left| r_A^{-3} \right| R_{n_1}(r_A) \right\rangle$$

$$\begin{aligned} \left\langle \psi_A(n_5 2 2) \left| \beta_2^0(e) \right| \psi_A(n_1 2 2) \right\rangle &= \left[\frac{2}{7}\right] e \left[N(n_5) N(n_1) \right] \left\langle R_{n_5}(r_A) \left| r_A^{-3} \right| R_{n_1}(r_A) \right\rangle \\ \left\langle \psi_A(n_5 2 -2) \left| \beta_2^0(e) \right| \psi_A(n_1 2 -2) \right\rangle &= \left[\frac{2}{7}\right] e \left[N(n_5) N(n_1) \right] \left\langle R_{n_5}(r_A) \left| r_A^{-3} \right| R_{n_1}(r_A) \right\rangle \end{aligned}$$

$$\begin{aligned} \left\langle \psi_A(n_5 2 1) \left| \beta_2^0(e) \right| \psi_A(n_1 2 1) \right\rangle &= -\left[\frac{1}{7}\right] e \left[N(n_5) N(n_1) \right] \left\langle R_{n_5}(r_A) \left| r_A^{-3} \right| R_{n_1}(r_A) \right\rangle \\ \left\langle \psi_A(n_5 2 -1) \left| \beta_2^0(e) \right| \psi_A(n_1 2 -1) \right\rangle &= -\left[\frac{1}{7}\right] e \left[N(n_5) N(n_1) \right] \left\langle R_{n_5}(r_A) \left| r_A^{-3} \right| R_{n_1}(r_A) \right\rangle \end{aligned}$$

$$\left\langle \psi_A(n_5 2 0) \left| \beta_2^0(e) \right| \psi_A(n_1 2 0) \right\rangle = -\left[\frac{2}{7}\right] e \left[N(n_5) N(n_1) \right] \left\langle R_{n_5}(r_A) \left| r_A^{-3} \right| R_{n_1}(r_A) \right\rangle$$

Evaluation of $\langle \psi_A^*(n_2 l_2 m_2) | \mathcal{G}_2^0(e) | \psi_A(n_1 l_1 m_1) \rangle$ for $n_2, n_1 = 1, 2$. 7.6

In molecules made up of first row atoms, e.g. CO, N₂, etc., the electrons occupy 1s, 2s, and 2p atomic orbitals (neglecting configuration interaction, etc.). It is therefore of great interest to have explicit expressions for the matrix elements corresponding to the electronic contribution to the field gradient at nuclei in such molecules. In fact there are only two non zero one centre matrix elements, these having the value

$$(2p_A^0 | \mathcal{G}_2^0(e)_A | 2p_A^0) = -\frac{64}{15} c^3 e$$

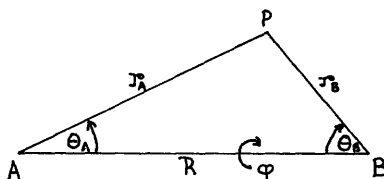
$$(2p_A^{\pm 1} | \mathcal{G}_2^0(e)_A | 2p_A^{\pm 1}) = +\frac{32}{15} c^3 e$$

The Evaluation of Two Centre Matrix Elements of the Type

$$\langle \psi_B^*(n_2, l_2, m_2) | \mathcal{O}_2^0(e) | \psi_B(n_1, l_1, m_1) \rangle \quad 7.7$$

Matrix elements of this type are conveniently evaluated by expanding the operator centred upon nucleus A about a new origin centred at nucleus B. The necessary expansion formulae have recently been derived by Pitzer, Kern, and Lipscomb and it is essentially their method which we shall use.

The coordinate system employed will be as follows:-



In this figure, $(r_A, \theta_A, \varphi_A)$ and $(r_B, \theta_B, \varphi_B)$ are the polar coordinates of a point, referred to the two nuclei A and B as origins, and the lines AB and BA respectively are polar axes. From the figure we note that $\varphi_A = \varphi_B = \varphi$.

The expansion of a solid spherical harmonic on one centre in terms of solid spherical harmonics on another centre is given by Hobson. For solid spherical harmonics of degree $-n-1$, it is

$$\frac{P_n^m(\cos \theta_A)}{r_A^{n+1}} = \frac{1}{R^n} \sum_{l=n}^{\infty} \binom{l+n}{n-m} \frac{r_B^l}{R^{l+1}} P_l^m(\cos \theta_B) \quad \text{if } r_B < R \quad (7.7.1a)$$

$$\frac{P_n^m(\cos \theta_A)}{r_A^{n+1}} = \frac{(-1)^{n-m}}{R^n} \sum_{l=n}^{\infty} \binom{l-m}{n-m} \frac{R^l}{r_B^{l+1}} P_l^m(\cos \theta_B) \quad \text{if } r_B > R \quad (7.7.1b)$$

where the $\binom{i}{j}$ are the binomial coefficients, defined by the equation:-

$$\binom{i}{j} = i! (j!)^{-1} (i-j)!^{-1}$$

The integration involved in the evaluation of the matrix element is done in spherical coordinates about centre B by dividing the range of integration of r_B into three parts, 0 to $R - \epsilon$, $R - \epsilon$ to $R + \epsilon$,

and $R + \epsilon$ to ∞ ($\epsilon > 0$). Using the appropriate series for inner and outer parts, the integration is performed and then ϵ is allowed to go to zero. Since the radial functions in (7.7.1) are well behaved at $r_B = R$, ϵ can be set equal to zero initially in these two parts.

Using equation (7.7.1), the operator $\beta_{2(e)_A}^0$ can be expanded:-

$$\frac{-e \sqrt{\frac{4\pi}{5}} Y_2^0(\theta_A \varphi_A)}{r_A^3} = -\frac{e}{R^2} \sum_{l=0}^{\infty} \binom{l+2}{2} \frac{r_B^l}{R^{l+1}} \sqrt{\frac{4\pi}{2l+1}} Y_l^0(\theta_B \varphi_B) \quad \text{if } r_B < R \quad (7.7.2a)$$

$$\frac{-e \sqrt{\frac{4\pi}{5}} Y_2^0(\theta_A \varphi_A)}{r_A^3} = -\frac{e}{R^2} \sum_{l=2}^{\infty} \binom{l}{2} \frac{R^l}{r_B^{l+1}} \sqrt{\frac{4\pi}{2l+1}} Y_l^0(\theta_B \varphi_B) \quad \text{if } r_B > R \quad (7.7.2b)$$

In the following sections, the integrals occurring in each range of integration will be evaluated.

(i) Evaluation of Matrix Elements in the Range $r_B < R$

By expressing the operator $\beta_2^0(e)_A$ in terms of expansion (7.7.2a) and by using 3-j symbols, we obtain the following expression:-

$$\begin{aligned} \langle \psi_B(n_5 l_5 m_5) | \beta_2^0(e)_A | \psi_B(n_1 l_1 m_1) \rangle &= -e [N(n_5)N(n_1)] \\ &\times \left\langle \left(\frac{R_{n_5}(r_B) R_{n_1}(r_B)}{R^2} \right) (-1)^{m_5} \sum_{l=0}^{\infty} \binom{l+2}{2} \sqrt{\frac{4\pi}{2l+1}} \cdot \frac{r_B^l}{R^{l+1}} \left[\frac{(2l_5+1)(2l+1)(2l_1+1)}{4\pi} \right]^{\frac{1}{2}} \right. \\ &\quad \left. \times \begin{pmatrix} l_5 & l & l_1 \\ 0 & 0 & 0 \end{pmatrix} \begin{pmatrix} l_1 & l & l_5 \\ m_1 & 0 & -m_5 \end{pmatrix} \right\rangle \quad (7.7.3) \end{aligned}$$

The first simplification of this expression results from the properties of the 3-j symbols, for the matrix element is non zero only for $m_1 = m_5$. Further simplification results only by specification of l_1 or l_5 . All necessary matrix elements can be evaluated by calculating merely those for which $l_5 \geq l_1$. The expression derived for each case of interest is shown in Table 7.7.2 on the next page. In this table the following shorthand notation is used:-

$$\langle \psi_B(n_5 l_5 m_5) | \beta_2^0(e)_A | \psi_B(n_1 l_1 m_1) \rangle = \langle \psi_B | \beta_2^0(e)_A | \psi_B \rangle$$

The radial integrals which occur are evaluated by means of the integrals tabulated in Appendix IV.

TABLE 7.1

$$\langle \psi_{B_2}^{m_5} | \beta_2^0(e) | \psi_{B_0}^0 \rangle_{L_5 \rightarrow 0}^{R \leftarrow \epsilon} = -e [N(m_2)N(m_1)] \binom{L_5+2}{2} \binom{L_5+2}{L_5+1} \int_0^{R \leftarrow \epsilon} \frac{R_{m_5}(r_B) R_{m_1}(r_B) r_B^{L_5+2}}{R^{L_5+3}} dr_B$$

$$\langle \psi_{B_1}^{m_5} | \beta_2^0(e) | \psi_{B_1}^{m_1} \rangle_{L_5 \rightarrow 0}^{R \leftarrow \epsilon} = -e [N(m_2)N(m_1)] (-1)^{m_5} \left\langle \left(\frac{R_{m_5}(r_B) R_{m_1}(r_B)}{R^2} \right) \left[\sqrt{3} \begin{pmatrix} 1 & 0 & 1 \\ -m_5 & 0 & m_1 \end{pmatrix} + 18 \sqrt{\frac{2}{15}} \frac{r_B^2}{R^3} \begin{pmatrix} 1 & 2 & 1 \\ -m_5 & 0 & m_1 \end{pmatrix} \right] \right\rangle_{0}^{R \leftarrow \epsilon}$$

$$\langle \psi_{B_2}^{m_5} | \beta_2^0(e) | \psi_{B_1}^{m_1} \rangle_{L_5 \rightarrow 0}^{R \leftarrow \epsilon} = -e [N(m_2)N(m_1)] (-1)^{m_5} \left\langle \left(\frac{R_{m_5}(r_B) R_{m_1}(r_B)}{R^2} \right) \left[\frac{3\sqrt{2} r_B^3}{R^2} \begin{pmatrix} 2 & 1 & 1 \\ -m_5 & 0 & m_1 \end{pmatrix} - \sqrt{7} \frac{r_B^4}{R^3} \begin{pmatrix} 2 & 3 & 1 \\ -m_5 & 0 & m_1 \end{pmatrix} \right] \right\rangle_{0}^{R \leftarrow \epsilon}$$

$$\langle \psi_{B_2}^{m_5} | \beta_2^0(e) | \psi_{B_2}^{m_1} \rangle_{L_5 \rightarrow 0}^{R \leftarrow \epsilon} = -e [N(m_2)N(m_1)] (-1)^{m_5} \left\langle \left(\frac{R_{m_5}(r_B) R_{m_1}(r_B)}{R^2} \right) \left[\sqrt{5} \begin{pmatrix} 2 & 0 & 2 \\ -m_5 & 0 & m_1 \end{pmatrix} - 6 \sqrt{\frac{10}{7}} \frac{r_B^2}{R^3} \begin{pmatrix} 2 & 2 & 2 \\ -m_5 & 0 & m_1 \end{pmatrix} + 15 \sqrt{\frac{10}{7}} \frac{r_B^4}{R^5} \begin{pmatrix} 2 & 4 & 2 \\ -m_5 & 0 & m_1 \end{pmatrix} \right] \right\rangle_{0}^{R \leftarrow \epsilon}$$

(ii) Evaluation of Matrix Elements in the Range $r_B > R$

Using equation (7.7.2b), we derive the following expression:-

$$\langle \mathcal{Y}_B(n_5, l_5, m_5) | \mathcal{B}_2^0(e)_A | \mathcal{Y}_B(n_1, l_1, m_1) \rangle = -e [N(n_5)N(n_1)]$$

$$\left(\frac{R_{n_5}(r_B) R_{n_1}(r_B)}{R^2} \right) (-1)^{m_5} \sum_{l=2}^{\infty} \binom{l}{2} \frac{R^l}{r_B^{l+1}} \sqrt{\frac{4\pi}{2l+1}} \left[\frac{(2l_5+1)(2l+1)(2l_1+1)}{4\pi} \right]^{1/2} \begin{pmatrix} l_5 & l & l_1 \\ 0 & 0 & 0 \end{pmatrix} \begin{pmatrix} l_5 & l & l_1 \\ -m_5 & 0 & m_1 \end{pmatrix}$$

(7.7.4)

Again there is the simplification that the matrix element is non zero only if $m_1 = m_5$.

As in the previous section, we need only evaluate matrix elements for $l_5 > l_1$. The expression derived for each case of interest is shown in table 2. The radial integrals can be evaluated by use of the integrals shown in Appendix V.

(iii) Evaluation of Matrix Elements in the Range $R-\epsilon < r_B < R+\epsilon$.

Evaluation of matrix elements in this range is fully discussed in the appendix of the article by Pitzer, Kern, and Lipscomb.⁵³ Here we shall state only the value of the integral for the operator $\mathcal{B}_2^0(e)_A$. This value is given by:-

$$\langle \mathcal{Y}_B(n_5, l_5, m_5) | \mathcal{B}_2^0(e)_A | \mathcal{Y}_B(n_5, l_5, m_5) \rangle = \frac{e}{3} [N(n_5)N(n_1)]$$

$$\sqrt{\frac{(2l_5+1)(2l_1+1)(l_5+m_5)!(l_1-m_1)!}{(l_5-m_5)!(l_1+m_1)!}} (-1)^{m_5} R_{n_5}(r_B) R_{n_1}(r_B) \delta(r_B - R)$$

(7.7.5)

The delta function implies that the product of the radial functions is zero unless $r_B = R$.

TABLE 7.72

$$\langle \psi_{B_2}^0 | \beta_2^0(e) | \psi_{B_0}^0 \rangle_{R^+ \epsilon} = -e [N(\eta_2) N(\eta_1)] \frac{1}{5} \int_{R^+ \epsilon}^{\infty} \frac{R_{\eta_2}(r_B) R_{\eta_1}(r_B)}{r_B} dr_B$$

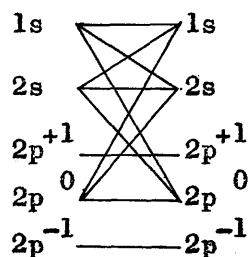
$$\langle \psi_{B_1}^{m_1} | \beta_2^0(e) | \psi_{B_1}^{m_1} \rangle_{R^+ \epsilon} = -e [N(\eta_2) N(\eta_1)] \sqrt{\frac{6}{5}} \begin{pmatrix} 1 & 2 & 1 \\ -m_1 & 0 & m_1 \end{pmatrix} (-1)^{m_1} \int_{R^+ \epsilon}^{\infty} \frac{R_{\eta_2}(r_B) R_{\eta_1}(r_B)}{r_B} dr_B$$

$$\langle \psi_{B_2}^{m_2} | \beta_2^0(e) | \psi_{B_2}^{m_2} \rangle_{R^+ \epsilon} = -e [N(\eta_2) N(\eta_1)] \frac{9}{7} \begin{pmatrix} 2 & 3 & 1 \\ -m_2 & 0 & m_2 \end{pmatrix} (-1)^{m_2} \int_{R^+ \epsilon}^{\infty} \frac{R_{\eta_2}(r_B) R_{\eta_1}(r_B)}{r_B^2} dr_B$$

$$\langle \psi_{B_2}^{m_2} | \beta_2^0(e) | \psi_{B_2}^{m_1} \rangle_{R^+ \epsilon} = -e [N(\eta_2) N(\eta_1)] (-1)^{m_2} \left\langle \frac{R_{\eta_2}(r_B) R_{\eta_1}(r_B)}{R^2} \right\rangle \left[-\sqrt{\frac{10}{7}} \frac{R^2}{r_B^3} \begin{pmatrix} 2 & 2 & 2 \\ -m_2 & 0 & m_1 \end{pmatrix} + 6\sqrt{\frac{10}{7}} \frac{R^4}{r_B^5} \begin{pmatrix} 2 & 4 & 2 \\ -m_2 & 0 & m_1 \end{pmatrix} \right]$$

Evaluation of Matrix Elements in the Range $r_B = 0 \rightarrow \infty$

In the previous three sub-sections we have evaluated matrix elements in the ranges $r_B = 0$ to $R - \epsilon$, $R - \epsilon$, to $R + \epsilon$, and $R + \epsilon$ to ∞ . By adding appropriate expressions we can therefore derive formulae for the integrals evaluated over the range $r_B = 0$ to ∞ . Such expressions are rather complicated and in practice it is simpler to evaluate the integrals in each range separately then add the resulting expressions. Matrix elements have been evaluated in this way for 1s, 2s, and 2p atomic orbitals. The resulting expressions are shown on the next page. The following orbitals situated on nucleus B are connected by the operator:-



Evaluation of $\langle \langle \psi_B^0(100) | 0_A | \psi_B^0(100) \rangle \rangle$
 $\langle \langle \psi_B^0(21_{5m_5}) | 0_A | \psi_B^0(21_{1m_1}) \rangle \rangle$ in the range $r_B = 0 \rightarrow \infty$

By addition of the partial integrals for each range of evaluation, we derive the following expressions:-

$$(1s_B | 0_A | 1s_B) = -\frac{e}{R^3} \left[1 - \exp(-a) \left(\frac{a^3}{6} + \frac{a^2}{2} + a + 1 \right) \right] \quad a = 2cR$$

$$(2s_B | 0_A | 2s_B) = -\frac{e}{R^3} \left[1 - \exp(-2b) \left(\frac{4b^5}{9} + \frac{2b^4}{3} + \frac{4b^3}{3} + 2b^2 + 1 \right) \right] \quad b = \frac{cR}{2}$$

$$(2p_B^0 | 0_A | 2p_B^0) = -\frac{e}{R^3} \left[1 + \frac{18}{b^2} - \exp(-2b) \left(\frac{4b^5}{3} + 2b^4 + 6b^3 + 14b^2 + \frac{26b}{b^2} + 37 + \frac{36}{b} + \frac{18}{b^2} \right) \right]$$

$$(2p_B^0 | 0_A | 2s_B) = -\frac{e}{\sqrt{3}R^3} \left[\frac{15}{2b} - \exp(-2b) \left(\frac{4b^5}{3} + 2b^4 + 5b^3 + 10b^2 + 15b + 15 + \frac{15}{2b} \right) \right]$$

$$(2p_B^{\pm 1} | 0_A | 2p_B^{\pm 1}) = -\frac{e}{R^3} \left[1 - \frac{9}{b^2} + \exp(-2b) \left(\frac{4b^5}{3} + b^3 + 4b^2 + 10b + 17 + \frac{18}{b} + \frac{9}{b^2} \right) \right]$$

$$(2s_B | 0_A | 1s_B) = -\frac{e}{R^3} \left(\frac{k^3 c^5}{6} \right)^{\frac{1}{2}} \left[\frac{3}{8h^4} - \exp(-2hR) \left(\frac{R^4}{3} + \frac{R^3}{2h} + \frac{3R^2}{4h^2} + \frac{3R}{4h^3} + \frac{3}{8h^4} \right) \right]$$

$$(2p_B^0 | 0_A | 1s_B) = -\frac{e}{R^4} \left(\frac{k^3 c^5}{2} \right)^{\frac{1}{2}} \left[\frac{3}{4h^5} - \exp(-2hR) \left(\frac{R^5}{3} + \frac{R^4}{2h} + \frac{R^3}{h^2} + \frac{3R^2}{2h^3} + \frac{3R}{2h^4} + \frac{3}{4h^5} \right) \right]$$

$$h = (k + c/2).$$

$k = 1s$ ORBITAL EXPONENT.

ON THIS PAGE $0_A = \beta_2^0(e)_A$.

Evaluation of Two Centre Matrix Elements of the Type

$$\langle \psi_A | G_2^0(e)_A | \psi_B \rangle$$

7.8

These matrix elements are more difficult to evaluate than the others which we have previously described. The most obvious method of evaluation is to expand the wavefunction ψ_B about a new origin of coordinates situated at centre A. The resulting series of one centre matrix elements can be expressed analytically in terms of certain Z functions of a standard mathematical type. This method of evaluating the matrix elements is essentially that of Barnett and Coulson. By modifying this method by the introduction of 3-j symbols, the doubly infinite sum of one centre matrix elements which results from the expansion of ψ_B about centre A is seen to be reduced to a few terms in a clear and simple manner.

We shall first derive the expansion of ψ_B about a new origin of coordinates situated at centre A. Following this, a general expression will be derived for the complete matrix element. Finally, the value for particular matrix elements will be calculated.

Expansion of a Slater wavefunction about a new centre.

Using the same coordinate system as in chapter 7.7, we obtain from equations (5) and (6) of reference the following expansion formulae:-

$$r_B^l Y_l^m(\theta_B, \varphi_B) = (-1)^{2m} \sqrt{\frac{(2l+1)(l-m)!}{(l+m)!}} \sum_{j=|m|}^l (-1)^{j+m} \binom{m+l}{m+j} r_A^j R^{l-j} \sqrt{\frac{(j+m)!}{(2j+1)(j-m)!}} Y_j^m(\theta_A, \varphi_A) \quad (7.8.1)$$

$$r_B^{s-1} e^{-\beta r_B} = \beta^{-s+1} \sum_{k=0}^{\infty} \frac{2k+1}{\sqrt{t\tau}} \sqrt{\frac{4\pi}{2k+1}} Y_k^0(\theta_A, \varphi_A) \zeta_{s,k}(l, t; \tau) \quad (7.8.2)$$

in which $t = \beta r_A$, $\tau = \beta R$, and the $\zeta_{s,k}(l, t; \tau)$ are functions of the variables

t and which are related to other functions of standard mathematical form which we shall call Z functions. Equations (7.8.1) and (7.8.2) have been expressed in terms of spherical harmonics $Y_{\ell}^m(\theta, \phi)$ which are related to the Associated Legendre Functions, $P_{\ell}^m(\cos \theta)$, used by Barnett and Coulson by the formula:-

$$P_{\ell}^m(\cos \theta) \exp(i m \phi) = (-1)^m \left[\frac{4\pi(\ell+m)!}{(2\ell+1)(\ell-m)!} \right]^{\frac{1}{2}} Y_{\ell}^m(\theta, \phi) \quad (7.8.3)$$

A Slater type orbital situated on centre B can be expressed as follows:-

$$\begin{aligned} \chi_B^{\ell}(n_1 \ell m_1) &= N(n_1) r_B^{n_1-1} \exp(-\beta r_B) Y_{\ell}^{m_1}(\theta_B, \phi_B) & \beta &= c/n \\ &= N(n_1) \left[r_B^{n_1-\ell-1} \cdot \exp(-\beta r_B) \right] \left[r_B^{\ell} Y_{\ell}^{m_1}(\theta_B, \phi_B) \right] \end{aligned} \quad (7.8.4)$$

Substituting equations (7.8.1) and (7.8.2) for the quantities in square brackets in this expression, and using equation (7.4.8), we obtain the expansion of $\chi_B^{\ell}(n_1 \ell m_1)$ shown in equation (7.8.5) on the next page. On substituting this expression in the formula for the complete matrix element, and using equation (7.4.7) for the integral over three spherical harmonics, we obtain a general expression for the matrix element which is given by equation (7.8.6). Simplification of this rather cumbersome expression results from the properties of the 3-j symbols. We note first that the 3-j symbols have a non zero value only if $m_1 = -m_4 = m_5$. This condition removes the sum over m_4 from the general expression. Putting $m_1 = m_5 = m$, we obtain expression (7.8.7) for the non zero matrix elements.

$$\phi_B(n_1, l_1, m_1) = N(n_1, l_1, m_1) \beta^{2m_1} (-1)^{m_1} \left[\frac{i^{(m_1+1)} (2l_1+1)}{(2l_1+1)^2} \right]^{1/2} \sum_{s_1=0}^{m_1} \sum_{t_1=0}^{m_1-s_1} \sum_{u_1=0}^{m_1-s_1-t_1} \left[\frac{2\sqrt{2}}{(1+\epsilon_1^2)^{1/2}} \right]^{1/2} \left[\frac{i^{(l_1-u_1)} (1-\epsilon_1^2)^{m_1}}{(1+\epsilon_1^2)^{m_1+1}} \right]^{1/2} \rho_{l_1, m_1, s_1, t_1, u_1}^{v_1}$$

$$(5.8.2) \quad \begin{pmatrix} m_1 & 0 & 0 & 0 \\ l_1 & s_1 & t_1 & u_1 \end{pmatrix} (v_1 \delta v_1 \theta)_{l_1, m_1} \rho_{l_1, m_1, s_1, t_1, u_1}^{v_1} \times$$

$$\langle \psi_A(n_5, l_5, m_5) | \beta_2^0(e_A) | \psi_B(n_1, l_1, m_1) \rangle$$

$$= -e [N(n_5)N(n_1)] (-1)^{2m_1+m_5} \left[\frac{(2l_1+1)(l_1-m_1)!}{(l_1+m_1)!} \right]^{1/2} \int_{-t_5^{5/2}}^{t_5^{5/2}} \frac{\beta}{\sqrt{\tau}} \exp(-k\tau) \sum_{l_3=0}^{\infty} \sum_{l_4=0}^{l_3} \sum_{m_3=-l_3}^{l_3} \sum_{m_4=-l_4}^{l_4} (-1)^{l_2-l_2} \binom{m_1+l_1}{m_1+l_2} \left[\frac{(2l_5+1)(l_2+m)!}{(l_2-m)!} \right]^{1/2} dt \quad (7.8.6)$$

$$\times t_2 \beta^{l_1-l_2} \sum_{m_1=-l_1}^{l_1} \sum_{m_2=-l_2}^{l_2} \sum_{m_3=0}^{l_3} \sum_{m_4=0}^{l_4} \binom{l_1}{m_1} \binom{l_2}{m_2} \binom{l_3}{0} \binom{l_4}{0} \binom{l_5}{-m_5} \binom{l_2}{0} \binom{l_4}{0} \binom{l_5}{0} \binom{l_2}{-m} \binom{l_4}{0} \binom{l_5}{-m}$$

$$K = \alpha/\beta$$

(α IS EXPONENT OF $\beta(n_5, l_5, m_5)$)

$$\langle \psi_A(n_5, l_5, m) | \beta_2^0(e_A) | \psi_B(n_1, l_1, m) \rangle$$

$$= -e [N(n_5)N(n_1)] (-1)^m \left[\frac{(2l_1+1)(l_1-m)!}{(l_1+m)!} \right]^{1/2} \int_{-t_5^{5/2}}^{t_5^{5/2}} \frac{\beta}{\sqrt{\tau}} \exp(-k\tau) \sum_{l_3=0}^{\infty} \sum_{l_4=0}^{l_3} \sum_{m_3=-l_3}^{l_3} \sum_{m_4=-l_4}^{l_4} (-1)^{l_2-l_2} \binom{m+l_1}{m+l_2} \left[\frac{(2l_5+1)(l_2+m)!}{(l_2-m)!} \right]^{1/2} \times t_2 \beta^{l_1-l_2} \sum_{m_1=-l_1}^{l_1} \sum_{m_2=-l_2}^{l_2} \sum_{m_3=0}^{l_3} \sum_{m_4=0}^{l_4} \binom{l_1}{m_1} \binom{l_2}{m_2} \binom{l_3}{0} \binom{l_4}{0} \binom{l_5}{-m} \binom{l_2}{m} \binom{l_4}{0} \binom{l_5}{-m} \binom{l_2}{0} \binom{l_4}{0} \binom{l_5}{0} dt \quad (7.8.7)$$

Simplification of the general integral

Equation (7.8.7) can be simplified further only by specification of l_1, l_5 , or m . If m is specified first, we can derive expressions for the three matrix elements of interest, namely:-

$$(a) \langle \Psi_A(n_5 l_5 0) | \mathcal{B}_2^0(e)_A | \Psi_B(n_1 l_1 0) \rangle$$

$$(b) \langle \Psi_A(n_5 l_5 \pm 1) | \mathcal{B}_2^0(e)_A | \Psi_B(n_1 l_1 \pm 1) \rangle$$

$$(c) \langle \Psi_A(n_5 l_5 \pm 2) | \mathcal{B}_2^0(e)_A | \Psi_B(n_1 l_1 \pm 2) \rangle$$

It is next convenient to specify l_5 so that each of the different types of matrix element is split into three sub-types, those for type (a) becoming:-

$$(ai) \langle \Psi_A(n_5 0 0) | \mathcal{B}_2^0(e)_A | \Psi_B(n_1 l_1 0) \rangle$$

$$(aii) \langle \Psi_A(n_5 1 0) | \mathcal{B}_2^0(e)_A | \Psi_B(n_1 l_1 0) \rangle$$

$$(aiii) \langle \Psi_A(n_5 2 0) | \mathcal{B}_2^0(e)_A | \Psi_B(n_1 l_1 0) \rangle$$

Finally l_1 is specified. Because of the equality:-

$$\langle \Psi_A(n_5 l_5 m) | \mathcal{B}_2^0(e)_A | \Psi_B(n_1 l_1 m) \rangle = \langle \Psi_B(n_1 l_1 m) | \mathcal{B}_2^0(e)_A | \Psi_A(n_5 l_5 m) \rangle$$

only those matrix elements for $l_5 \leq l_1$ need be evaluated. All of the integrals occurring can be reduced in a manner which we shall shortly demonstrate to a sum of Z functions which are defined by:-

$$Z_{m,n}(\kappa, \nu) + \frac{1}{2} = \int_0^{\infty} \exp(-\kappa t) \cdot \zeta_{m,n}(1, t; \nu) t^{\nu + \frac{1}{2}} dt$$

The evaluation of the matrix elements in terms of the Z functions is straightforward. The method of evaluation will be illustrated for the matrix element $\langle \Psi_A(n_5 0 0) | \mathcal{B}_2^0(e)_A | \Psi_B(n_1 0 0) \rangle$, the result alone being stated for the other matrix elements.

Evaluation of $\langle \mathcal{Z}_A^{\mathcal{S}}(n_5 0 0) | \mathcal{B}_2^0(e)_A | \mathcal{Z}_B^{\mathcal{S}}(n_1 0 0) \rangle$

Stage 1; In equation (7.8.7) put $m = 0$

$$\langle \mathcal{Z}_A^{\mathcal{S}}(n_5 l_5 0) | \mathcal{B}_2^0(e)_A | \mathcal{Z}_B^{\mathcal{S}}(n_1 l_1 0) \rangle = -e [N(n_5)N(n_1)] \sqrt{\frac{2l_1+1}{\gamma}} \beta^{-n_1-n_5+l_1+3} \times$$

$$\int_0^{\infty} t^{n_5-5/2} \exp(-\kappa t) \sum_{l_3=0}^{\infty} \sum_{l_4=0}^{\infty} \sum_{l_2=0}^{l_1} (-1)^{l_2} \beta^{-l_2} (2l_5+1)^{1/2} \begin{pmatrix} l_1 \\ l_2 \end{pmatrix} t^{l_2} R^{l_1-l_2} \begin{bmatrix} (l_1, t; \kappa) \\ n_1-l_1, l_3 \end{bmatrix} (2l_3+1)(2l_4+1) \begin{pmatrix} l_3 & l_2 & l_4 \\ 0 & 0 & 0 \end{pmatrix}^2 \begin{pmatrix} l_5 & 2 & l_4 \\ 0 & 0 & 0 \end{pmatrix}^2 dt.$$

Stage 2; Put $l_5 = 0$

$$\langle \mathcal{Z}_A^{\mathcal{S}}(n_5 0 0) | \mathcal{B}_2^0(e)_A | \mathcal{Z}_B^{\mathcal{S}}(n_1 l_1 0) \rangle = -e [N(n_5)N(n_1)] \sqrt{\frac{2l_1+1}{\gamma}} \beta^{-n_1-n_5+l_1+3} \times$$

$$\int_0^{\infty} t^{n_5-5/2} \exp(-\kappa t) \sum_{l_3=0}^{\infty} \sum_{l_4=0}^{\infty} \sum_{l_2=0}^{l_1} (-1)^{l_2} \beta^{-l_2} \begin{pmatrix} l_1 \\ l_2 \end{pmatrix} t^{l_2} R^{l_1-l_2} \begin{bmatrix} (l_1, t; \kappa) \\ n_1-l_1, l_3 \end{bmatrix} (2l_3+1)(2l_4+1) \begin{pmatrix} l_3 & l_2 & l_4 \\ 0 & 0 & 0 \end{pmatrix}^2 \begin{pmatrix} 0 & 2 & l_4 \\ 0 & 0 & 0 \end{pmatrix}^2 dt$$

Now the 3-j symbol :-

$$\begin{pmatrix} 0 & 2 & l_4 \\ 0 & 0 & 0 \end{pmatrix}$$

is zero unless $l_4 = 2$. When $l_4 = 2$, it has the value $(1/5)^{1/2}$. The expression therefore simplifies to:-

$$\langle \mathcal{Z}_A^{\mathcal{S}}(n_5 0 0) | \mathcal{B}_2^0(e)_A | \mathcal{Z}_B^{\mathcal{S}}(n_1 l_1 0) \rangle = -e [N(n_5)N(n_1)] \sqrt{\frac{2l_1+1}{\gamma}} \beta^{-n_1-n_5+l_1+3} \times$$

$$\int_0^{\infty} t^{n_5-5/2} \exp(-\kappa t) \sum_{l_3=0}^{\infty} \sum_{l_2=0}^{l_1} (-1)^{l_2} \beta^{-l_2} \begin{pmatrix} l_1 \\ l_2 \end{pmatrix} t^{l_2} R^{l_1-l_2} \begin{bmatrix} (l_1, t; \kappa) \\ n_1-l_1, l_3 \end{bmatrix} (2l_3+1) \begin{pmatrix} l_3 & l_2 & 2 \\ 0 & 0 & 0 \end{pmatrix}^2 dt$$

Stage (iii) Putting $l_1 = 0$, l_2 can have only one value for which the matrix element is non zero, this value being $l_2 = 0$.
The matrix element reduces to:-

$$\langle \psi_A(n_5 \ 0 \ 0) | \beta_2^0(e) | \psi_E(n_1 \ 0 \ 0) \rangle = -e [N(n_5)N(n_1)] \frac{\beta^{-n_1-n_5+3}}{\sqrt{\gamma}} \times$$

$$\int_0^{\infty} t^{n_5-5/2} \exp(-\kappa t) \sum_{l_3=0}^{\infty} \begin{Bmatrix} (1, t; \gamma) \\ n_1, l_3 \end{Bmatrix} (2l_3+1) \begin{pmatrix} l_3 & 0 & 2 \\ 0 & 0 & 0 \end{pmatrix}^2 dt$$

In this expression, the 3-j symbol is zero unless $l_3 = 2$, so that the sum over l_3 reduces to a single term, the expression becoming:-

$$\langle \psi_A(n_5 \ 0 \ 0) | \beta_2^0(e) | \psi_B(n_1 \ 0 \ 0) \rangle = -e [N(n_5)N(n_1)] \frac{\beta^{-n_1-n_5+3}}{\sqrt{\gamma}} \int_0^{\infty} t^{n_5-5/2} \exp(-\kappa t) \begin{Bmatrix} (1, t; \gamma) \\ n_1, 2 \end{Bmatrix} dt$$

$$= -e [N(n_5)N(n_1)] \frac{\beta^{-n_1-n_5+3}}{\sqrt{\gamma}} Z_{n_1, 2, n_5-5/2}(1, t; \gamma)$$

In a similar manner, all the matrix elements can be evaluated in terms of the Z functions. The resulting expressions are listed on the following two pages.

$$\langle \psi_A(n_3 00) | \hat{Q}_A | \psi_B(n_1 00) \rangle$$

$$= -E [N(n_2) N(n_1)] \beta^{\eta_1 \eta_2 \eta_3} / \sqrt{2} Z_{\eta_1 \eta_2 \eta_3}(\kappa, \tau)$$

$$\langle \psi_A(n_3 00) | \hat{Q}_A | \psi_8(n_1 10) \rangle$$

$$= -E [N(n_2) N(n_1)] \beta^{\eta_1 \eta_2 \eta_3} / \sqrt{2} \cdot \sqrt{3} [BR Z_{\eta_1 \eta_2 \eta_3}(\kappa, \tau) - \frac{2}{5} Z_{\eta_1 \eta_2 \eta_3}(\kappa, \tau) - \frac{3}{5} Z_{\eta_1 \eta_2 \eta_3}(\kappa, \tau)]$$

$$\langle \psi_A(n_3 00) | \hat{Q}_A | \psi_6(n_1 20) \rangle$$

$$= -E [N(n_2) N(n_1)] \beta^{\eta_1 \eta_2 \eta_3} / \sqrt{2} \cdot \sqrt{5} [BR \{ \frac{4}{5} Z_{\eta_1 \eta_2 \eta_3}(\kappa, \tau) - BR \{ \frac{4}{5} Z_{\eta_1 \eta_2 \eta_3}(\kappa, \tau) + \frac{6}{5} Z_{\eta_1 \eta_2 \eta_3}(\kappa, \tau) \} + \{ \frac{1}{5} Z_{\eta_1 \eta_2 \eta_3}(\kappa, \tau) + \frac{2}{7} Z_{\eta_1 \eta_2 \eta_3}(\kappa, \tau) + \frac{18}{35} Z_{\eta_1 \eta_2 \eta_3}(\kappa, \tau) \}]$$

$$\langle \psi_A(n_3 10) | \hat{Q}_A | \psi_8(n_1 10) \rangle$$

$$= -E [N(n_2) N(n_1)] \beta^{\eta_1 \eta_2 \eta_3} / \sqrt{2} \cdot 3 [BR \{ \frac{2}{5} Z_{\eta_1 \eta_2 \eta_3}(\kappa, \tau) + \frac{3}{5} Z_{\eta_1 \eta_2 \eta_3}(\kappa, \tau) \} - \{ \frac{2}{15} Z_{\eta_1 \eta_2 \eta_3}(\kappa, \tau) + \frac{11}{21} Z_{\eta_1 \eta_2 \eta_3}(\kappa, \tau) + \frac{12}{35} Z_{\eta_1 \eta_2 \eta_3}(\kappa, \tau) \}]$$

$$\langle \psi_A(n_3 10) | \hat{Q}_A | \psi_6(n_1 20) \rangle$$

$$= -E [N(n_2) N(n_1)] \beta^{\eta_1 \eta_2 \eta_3} / \sqrt{2} \cdot \sqrt{5} [BR \{ \frac{2}{5} Z_{\eta_1 \eta_2 \eta_3}(\kappa, \tau) + \frac{3}{5} Z_{\eta_1 \eta_2 \eta_3}(\kappa, \tau) \} - (BR) \{ \frac{2}{5} Z_{\eta_1 \eta_2 \eta_3}(\kappa, \tau) + \frac{4}{15} Z_{\eta_1 \eta_2 \eta_3}(\kappa, \tau) + \frac{12}{35} Z_{\eta_1 \eta_2 \eta_3}(\kappa, \tau) \} + \{ \frac{11}{35} Z_{\eta_1 \eta_2 \eta_3}(\kappa, \tau) + \frac{2}{5} Z_{\eta_1 \eta_2 \eta_3}(\kappa, \tau) + \frac{2}{7} Z_{\eta_1 \eta_2 \eta_3}(\kappa, \tau) \}]$$

$$\langle \psi_A(n_3 20) | \hat{Q}_A | \psi_8(n_1 20) \rangle$$

$$= -E [N(n_2) N(n_1)] \beta^{\eta_1 \eta_2 \eta_3} / \sqrt{2} \cdot 5 [BR \{ \frac{2}{5} Z_{\eta_1 \eta_2 \eta_3}(\kappa, \tau) + \frac{2}{7} Z_{\eta_1 \eta_2 \eta_3}(\kappa, \tau) + \frac{18}{35} Z_{\eta_1 \eta_2 \eta_3}(\kappa, \tau) \} - \{ \frac{2}{5} Z_{\eta_1 \eta_2 \eta_3}(\kappa, \tau) + \frac{2}{7} Z_{\eta_1 \eta_2 \eta_3}(\kappa, \tau) + \frac{12 \times 9}{11 \times 35} Z_{\eta_1 \eta_2 \eta_3}(\kappa, \tau) + \frac{18}{77} Z_{\eta_1 \eta_2 \eta_3}(\kappa, \tau) \}]$$

ON THIS PAGE $\hat{Q}_A = \hat{Q}_2^0(e)_A$, AND -E REPLACES -e

$$\langle \psi_A(\eta_2=1) | Q_A | \psi_B(\eta_1=1) \rangle$$

$$= -E [N(\eta_2) N(\eta_1)] \beta^{-\eta_1-\eta_2+3} / \sqrt{2} \left[-\frac{1}{5} Z(\kappa, \nu) + \frac{2}{7} Z(\kappa, \nu) - \frac{10}{35} Z(\kappa, \nu) \right]$$

$$\langle \psi_A(\eta_2=1) | Q_A | \psi_B(\eta_2=1) \rangle$$

$$= -E [N(\eta_2) N(\eta_1)] \beta^{-\eta_1-\eta_2+3} / \sqrt{2} \cdot 3\sqrt{5} (BR) \left\{ -\frac{1}{15} Z(\kappa, \nu) + \frac{2}{21} Z(\kappa, \nu) - \frac{6}{35} Z(\kappa, \nu) \right\} - \left\{ \frac{1}{35} Z(\kappa, \nu) + \frac{1}{15} Z(\kappa, \nu) - \frac{2}{21} Z(\kappa, \nu) \right\}$$

$$\langle \psi_A(\eta_2=1) | Q_A | \psi_B(\eta_2=1) \rangle$$

$$= -E [N(\eta_2) N(\eta_1)] \beta^{-\eta_1-\eta_2+3} / \sqrt{2} \cdot 5 \left[3(BR) \left\{ \frac{1}{7} Z(\kappa, \nu) + \frac{5}{21} Z(\kappa, \nu) - \frac{2}{21} Z(\kappa, \nu) \right\} - \frac{1}{7} \left\{ -Z(\kappa, \nu) + \frac{1}{7} Z(\kappa, \nu) + \frac{150}{77} Z(\kappa, \nu) + \frac{12}{11} Z(\kappa, \nu) \right\} \right]$$

$$\langle \psi_A(\eta_2=2) | Q_A | \psi_B(\eta_2=2) \rangle$$

$$= -E [N(\eta_2) N(\eta_1)] \beta^{-\eta_1-\eta_2+3} / \sqrt{2} \cdot \frac{1}{7} \left[-2 Z(\kappa, \nu) + 5 Z(\kappa, \nu) + \left(\frac{12\sqrt{60-66}}{77} \right) Z(\kappa, \nu) + \frac{6\sqrt{70}}{11} Z(\kappa, \nu) \right]$$

ON THIS PAGE $Q_A = \Theta_2^0(e_A)$, AND $-E$ REPLACES $-e$.

Summary of Calculation Methods
Evaluation of the Z Functions. 7.9

The analytical and numerical evaluation of the Z functions has been fully described by Barnett and Coulson. It would be a relatively simple matter to programme an electronic computer to calculate the Z functions numerically.

By the methods which we have described, it is possible to evaluate all the important matrix elements of the nuclear quadrupole interaction Hamiltonian for molecules. In fact it would not be difficult to programme the computer to calculate the quantities q and σ from some trial wavefunction. If this was done, simple and rapid correlations could be made between experimental observations and theoretical predictions.

Conclusions Regarding the Development of N.Q.R. Research. 8.

After a mere eighteen months of research in the field of N.Q.R. spectroscopy, almost all of which has been taken up by the construction of apparatus, it is too soon to say whether or not our hopes will be realized. It is certainly true that a satisfactory solution to the detection problem will have to be found before the technique can really be exploited. This problem is undoubtedly the greatest single factor hampering research at the moment.

The interpretation of N.Q.R. in terms of electronic structure is complicated to a large extent at the moment by lack of detailed knowledge concerning the magnitude of the Sternheimer effect. Although the importance of this effect is difficult to estimate, it is liable to become much less formidable as more extensive measurements of nuclear quadrupole coupling constants are made.

General Conclusions and Reflections

In the three year period during which this research has been carried out, a great deal of extremely useful experience in chemistry, physics, computing, and electronics has been gained, as well as confidence in how to go about constructing new and complex apparatus. This sort of experience is, in the author's view, much more desirable than that which would have resulted from the study of some specialized chemical topic. Largely as a result of the wide variety of fields covered, the author's interests have moved away from the simple correlation of observations with electronic structure, and have become more directed towards developing new methods for studying "chemically interesting observables at a molecular level".

APPENDIX 1: Operating Instructions for programme R.W. 1

R.W. 1A Input: 1) Programme except last two cards.
 2) Binary normalized vectors, i.e. output from
 normalization prog. in order, and with
 parameter cards.
 3) Last two cards.

Output: 1) T matrix.

R.W. 1B Input: 1) Programme
 2) T matrix, i.e. output from R.W. 1A.
 3) Binary H matrix.
 4) Binary E(obs) matrix.
 5) Binary C matrix.

Output: 1) E(calc) matrix.
 2) Refined H matrix.
 3) The parameter R

Output is decimalized using LK06

Additional Facilities:

R.W. 1A : Inputs (2) and (3) may be read in continuously.

R.W. 1B : Data can be read in continuously.

APPENDIX 2: Operating Instructions for programme R.W.2

(Four Spin Programmes)

R.W. 2A : As for R.W. 1A

R.W. 2B : Inputs (1) to (4) identical to those of R.W. 1B.
Input (5), C matrix, now put in as two 28x28 "mesh
matrices".

Appendix III. The Integrals $\int_0^{\infty} r^n e^{-cr} dr$

$$\int_0^{\infty} r^0 e^{-cr} dr = \frac{1}{c}$$

$$\int_0^{\infty} r^6 e^{-cr} dr = \frac{5 \times 3^2 \times 2^4}{c^7}$$

$$\int_0^{\infty} r^1 e^{-cr} dr = \frac{1}{c^2}$$

$$\int_0^{\infty} r^7 e^{-cr} dr = \frac{35 \times 3^2 \times 2^4}{c^8}$$

$$\int_0^{\infty} r^2 e^{-cr} dr = \frac{2}{c^3}$$

$$\int_0^{\infty} r^8 e^{-cr} dr = \frac{35 \times 3^4 \times 2^7}{c^9}$$

$$\int_0^{\infty} r^3 e^{-cr} dr = \frac{6}{c^4}$$

$$\int_0^{\infty} r^9 e^{-cr} dr = \frac{35 \times 3^4 \times 2^7}{c^{10}}$$

$$\int_0^{\infty} r^4 e^{-cr} dr = \frac{24}{c^5}$$

$$\int_0^{\infty} r^{10} e^{-cr} dr = \frac{5^2 \times 7 \times 3^4 \times 2^8}{c^{11}}$$

$$\int_0^{\infty} r^5 e^{-cr} dr = \frac{15 \times 2^3}{c^6}$$

$$\int_0^{\infty} r^n e^{-cr} dr = \frac{n}{c} \int_0^{\infty} r^{n-1} e^{-cr} dr$$

Appendix IV.

The Integrals $\int_0^{R-\epsilon} r^n e^{-2cr} dr$
 $\lim_{\epsilon \rightarrow 0}$

$$\int_0^{R-\epsilon} r^0 e^{-2cr} dr = \frac{1}{2c} - e^{-2cR} \frac{1}{2c}$$

$$\int_0^{R-\epsilon} r^1 e^{-2cr} dr = \frac{1}{4c^2} - e^{-2cR} \left[\frac{1}{4c^2} + \frac{R}{2c} \right]$$

$$\int_0^{R-\epsilon} r^2 e^{-2cr} dr = \frac{1}{4c^3} - e^{-2cR} \left[\frac{1}{4c^3} + \frac{R}{2c^2} + \frac{R^2}{2c} \right]$$

$$\int_0^{R-\epsilon} r^3 e^{-2cr} dr = \frac{3}{8c^4} - e^{-2cR} \left[\frac{3}{8c^4} + \frac{3R}{4c^3} + \frac{3R^2}{4c^2} + \frac{R^3}{2c} \right]$$

$$\int_0^{R-\epsilon} r^4 e^{-2cr} dr = \frac{3}{4c^5} - e^{-2cR} \left[\frac{3}{4c^5} + \frac{3R}{2c^4} + \frac{3R^2}{2c^3} + \frac{R^3}{c^2} + \frac{R^4}{2c} \right]$$

$$\int_0^{R-\epsilon} r^5 e^{-2cr} dr = \frac{15}{8c^6} - e^{-2cR} \left[\frac{15}{8c^6} + \frac{15R}{4c^5} + \frac{15R^2}{4c^4} + \frac{5R^3}{2c^3} + \frac{5R^4}{4c^2} + \frac{R^5}{2c} \right]$$

$$\int_0^{R-\epsilon} r^6 e^{-2cr} dr = \frac{45}{8c^7} - e^{-2cR} \left[\frac{45}{8c^7} + \frac{45R}{4c^6} + \frac{45R^2}{4c^5} + \frac{15R^3}{2c^4} + \frac{15R^4}{4c^3} + \frac{3R^5}{2c^2} + \frac{R^6}{2c} \right]$$

Appendix V. The Integrals $\int_{R+\epsilon}^{\infty} r^n e^{-2cr} dr$
 $\lim_{\epsilon \rightarrow 0}$

$$\int_{R+\epsilon}^{\infty} r^0 e^{-2cr} dr = \frac{1}{2c} e^{-2cR}$$

$$\int_{R+\epsilon}^{\infty} r^1 e^{-2cr} dr = \frac{1}{2c} e^{-2cR} \left(R + \frac{1}{2c} \right)$$

References

1. "Irreducible Tensorial Sets", Fano and Racah, Academic Press, 1959.
2. "Characteristic NMR Shielding Values for Hydrogen in Organic Structures", by G. Van Dyke Tiers. Minnesota Mining and Manuf. Co.
3. "Nuclear Magnetic Resonance Spectroscopy", by L.M. Jackman, Pergamon, 1959.
4. J.A. Pople, W.G. Schneider, H.J. Bernstein, "High Resolution Nuclear Magnetic Resonance Spectroscopy", M^cGraw-Hill, 1959.
5. J.G. Powles, Repts. Prog. Phys., 1959, 22, 433.
6. P.L. Corio, Chem. Rev., 1960, 60, 363.
7. H.S. Gutowsky, D.W. M^cCall, C.P. Schlichter, J. Chem. Phys., 1953, 21, 279.
8. E.L. Hahn, D.E. Maxwell, Phys. Rev., 1952, 88, 1070.
9. H.M. M^cConnell, A.D. M^cLean, C.A. Reilly, J.Chem.Phys., 1955, 23, 1152.
10. H.J. Bernstein, J.A. Pople, W.G. Schneider, Can.J.Phys., 1957, 35, 65.
11. C.A. Reilly, J.D. Swalen, J.Chem.Phys., 1960, 32, 1378.
12. E.E. Wilson, J.Chem.Phys., 1957, 27, 60.
13. J.A. Pople, T. Schaefer, Mol.Phys., 1960, 3, 547.
14. P. Diehl, J.A. Pople, Mol.Phys., 1960, 3, 557.
15. J.D. Swalen, C.A. Reilly, J.Chem.Phys., 1962, 37, 21.
16. A.L. Bloom, J.N. Shoolery, Phys.Rev., 1953, 97, 1261.
17. F. Bloch, Phys. Rev., 1956, 102, 104.
18. W.A. Anderson, Phys. Rev., 1961, 102, 151.
19. D.E. Whitman, J.Chem.Phys., 1962, 36, 2085.
20. N.F. Ramsey, Phys. Rev., 1953, 91, 303.
21. A. Abragam, "The Principles of Nuclear Magnetism, Oxford Univ. Press, 1961.
22. Milne, "Vectorial Mechanics", London 1948.
23. N.F. Ramsey, E.M. Purcell, Phys. Rev., 1952, 85, 143.
24. J.A. Pople, Mol. Phys., 1963-64, 7, 301.
25. J.A. Pople, D.P. Santry, Mol. Phys., 1964, 8, 1.
26. H.S. Gutowsky, J.Chem.Phys., 1959, 31, 1683.
27. H.S. Gutowsky, 1959, Technical Report No. 18, Office of Naval Research, Task No. NR-051-215.
28. T.F. Wilmott, Phys.Rev., 1953, 91, 476.
29. E.P. Stoicheff, Can.J.Phys., 1957, 35, 730.
30. (a) A. Nordseick, Phys.Rev., 1940, 58, 310.
(b) S.C. Wang, Phys.Rev., 1928, 31, 579.
31. T.W. Marshall, J.A. Pople, Mol.Phys., 1958, 1, 199.
32. N.F. Ramsey, et al., Phys. Rev., 1958, 112, 1929.
33. (a) G. Herzberg, Can.J.Research, A, 1950, 28, 144.
(b) E.P. Stoicheff, Can.J.Phys., 1957, 35, 730.
34. T.W. Marshall, Mol.Phys., 1961, 4, 61.
35. Das and Hahn, "N.Q.R. Spectroscopy", Academic Press 1958.
36. E.I. Fedin, G.K. Semin, Zhurnal Strukturnoi Khimii, 1960, 1, 252, 1960, 1, 464.

37. C. Dean, Rev.Sci.Inst., 1960, 31, 934.
38. Whitehead, "Super Regenerative Receivers", Cambridge Univ. Press, 1950.
39. Barnes and Segel, Phys.Rev.Letters, 1959, 3, 462.
40. Ito, Nakamura, Ito, and Kubo, Inorg. Chem., 1963, 3, 690.
41. L.F. Dahl, R.E. Rundle, Acta Cryst., 1963, 16, 419.
42. A.D. Buckingham, Trans.Faraday Soc., 1962, 58, 1277.
43. R.M. Sternheimer, Phys. Rev., 1951, 84, 244.
44. " " " " 1952, 86, 316.
45. " " " " 1954, 95, 736
46. R.M. Sternheimer, H.M. Foley, Phys Rev., 1956, 102, 731.
47. " " " " " " " "
48. H.M. M^cConnell, J. Strathdee, J.Mol.Phys., 1959, 2, 129.
49. E. Scrocco, Advances in Chemical Physics, 1963, 5, 319.
50. P.O.Lowdin, Phys.Rev., 1955, 97, 1474-1520.
51. M.P. Barnett, C.A. Coulson, Phil.Trans.Roy.Soc.(London) A, 1951, 243,
52. M.P. Barnett, C.A. Coulson, "Quantum Mechanical Methods in Valence Theory". 8-10 Sept. 1951. U.S. Office of Naval Research.
53. R.M. Pitzer, C.W. Kern, W.N. Lipscomb, J.Chem.Phys., 1962, 37, 267.
54. L.I. Schiff, "Quantum Mechanics", M^cGraw- Hill, 1955.
55. A.R. Edmonds, "Angular Momentum in Quantum Mechanics", Princeton University Press, 1957.
56. Fano and Racah, "Irreducible Tensorial Sets", Academic Press 1959.
57. Rotenberg, Bivins, Metropolis, Wooten, "The 3-j and 6-j Symbols", Technology Press, M.I.T., 1961.
58. Hobson, "Theory of Spherical and Elipsoidal Harmonics". Cambridge University Press, 1931.

Bibliography.

(A) Nuclear Magnetic Resonance Spectroscopy.

- (1) "High Resolution Nuclear Magnetic Resonance".
by Pople, Schneider, and Bernstein.
pub. M^CGraw-Hill 1959.
- (2) "The Principles of Nuclear Magnetism".
by A. Abragam.
pub. Oxford University Press. 1961.
- (3) "Principles of Magnetic Resonance".
by C. P. Schlichter.
pub. Harper and Row 1963.
- (4) "Nuclear Magnetic Resonance".
by E. R. Andrew.
pub. Cambridge University Press 1956.
- (5) "An Introduction to the Analysis of Spin-spin Splitting
in Nuclear Magnetic Resonance".
by J.D. Roberts.
pub. W.A. Benjamin 1961.
- (6) "Interpretation of N.M.R. Spectra".
by Wiberg and Nist.
pub. W.A. Benjamin 1962.

(B) Quantum Theory and Angular Momentum.

- (1) "Quantum Mechanics".
by L.I. Schiff.
pub. M^CGraw-Hill. 1955.
- (2) "Angular Momentum in Quantum Mechanics".
by A.R. Edmonds.
pub. Princeton University Press. 1957.

(3) "Irreducible Tensorial Sets".

by Fano and Racah.

pub. Academic Press 1959.

(3) Nuclear Quadrupole Resonance Spectroscopy

(1) "Nuclear Quadrupole Resonance Spectroscopy".

by Das and Hahn.

pub. Academic Press 1958.

(2a) E.I. Fedin, G.K. Semin, Zhurnal Strukturnoi Khimii,
1960, 1, 252.

(2b) E.I. Fedin, G.K. Semin, Zhurnal Strukturnoi Khimii,
1960, 1, 464.